PB-230 143

THEORETICAL AND EXPERIMENTAL INVESTIGATION OF TEMPERATURE AND COMPOSITION DURING COMBUSTION IN A CLOSED SYSTEM

Lawrence Joseph Muzio

California University
Berkeley, California

July 1970

DISTRIBUTED BY:

NTIS
National Technical Information Service
U. S. DEPARTMENT OF COMMERCE
5285 Port Royal Road, Springfield Va. 22151

PB 230 143

Theoretical and Experimental Investigation of Temperature and Composition during Combustion in a Closed System

By

Lawrence Joseph Muzio
B.S. (University of California) 1966
M.S. (University of California) 1968

DISSERTATION

Submitted in partial satisfaction of the requirements for the degree of

DOCTOR OF PHILOSOPHY

in

Engineering

in the

GRADUATE DIVISION

of the

UNIVERSITY OF CALIFORNIA, BERKELEY

Approved: Ernest Starkman
Lawrence S. Caretto
C. Bradley Moore

Committee in Charge

Reproduced by
NATIONAL TECHNICAL
INFORMATION SERVICE
U S Department of Commerce
Springfield VA 22151

....

THEORETICAL AND EXPERIMENTAL INVESTIGATION OF TEMPERATURE AND COMPOSITION DURING COMBUSTION IN A CLOSED SYSTEM

By

Lawrence Joseph Muzio

ABSTRACT

An analytical model of the combustion process in a closed system is developed. The model utilizes real gas properties and assumes the burned gas region to be non-uniform. Numerical calculations using this model predict a 600°K temperature difference across the combustion chamber with the high temperature region adjacent to the point of ignition. Chemical kinetic calculations show that the formation of nitric oxide is greatly influenced by the temperature gradient. Experimentally infrared spectroscopic measurements were made to substantiate the existance of this temperature gradient.

Experimentally an infrared polychromator and a single cylinder CFR engine equipped with quartz windows in the combustion chamber and run on a premixed propane/air mixture were used to determine the temperature and temperature gradient in the combustion products during the expansion process. Selected spectral regions of the 1.8 and 2.7 micron water vapor bands were monitored simultaneously during a single engine cycle and the temperatures determined using the emission-absorption technique. Results showed that the spectroscopic temperatures were within 100°K of the ideal bulk gas temperature which was inferred from the combustion chamber pressure and volume.

A multiple wavelength, single line of sight technique was employed to measure the temperature gradient along the path of flame travel. This technique was chosen in order to obtain all necessary experimental data during a single engine cycle and avoid averaging due to cycle to cycle variations. Results of a two wavelength two zone formulation yielded a temperature difference on the order of 750°K across the combustion chamber. Considering the probable experimental uncertainty this result is shown to be in agreement with the analytical predictions.

approved E. Starkman
E. S. Starkman
Chairman, Thesis Committee

ACKNOWLEDGEMENTS

The author wishes to express his sincerest thanks to the many persons who have made this work possible.

Special thanks are due to the author's advisor, Professor Ernest S. Starkman for his encouragement and advice throughout the author's graduate studies.

The advice and discussions with Dr. L. S. Caretto and Professor R. F. Sawyer are gratefully acknowledged.

Without the skilled help of J. De Costa, H. Stewart and R. Jensen of the Thermal Systems Laboratories the experimental phase of the work would have been put in jeopardy.

The typing done by Mrs. Diana Muzio, Mrs. Lidia Chiappari, and Miss Bonnie Hutchings is greatly appreciated.

Sincerest thanks to my family, Diana, Diva and Gina for their perseverence throughout these years.

This work was supported in part by the U.S. Public Health Service through fellowships and research grants.

TABLE OF CONTENTS

Page

Chapter I - Introduction.. 1

Chapter II - Analytical Combustion Model.......................... 5
  2.1 Fundamental Thermodynamic Observation...................... 5
  2.2 Detailed Model of the Combustion Process................... 7
  2.3 Chemical Kinetics of Nitric Oxide.......................... 14

Chapter III - Experimental Approach............................... 31
  3.0 General Approach... 31
  3.1 Equation of Radiative Transfer............................. 32
  3.2 Infrared Spectrum of Combustion Products................... 36
  3.3 Radiation Properties of Water Vapor........................ 38
  3.4 Vibrational Relaxation of Water Vapor...................... 44
  3.5 Optical System Calibration................................. 45
  3.6 Experimentally Measured Quantities......................... 47

Chapter IV - Experimental Procedure and Apparatus................. 57
  4.0 Overall Experiment... 57
  4.1 Experimental Apparatus..................................... 57
    4.1-1 Engine and Instrumentation............................. 57
    4.1-2 Optical System... 58
  4.2 Experimental Procedure..................................... 62

Chapter V - Experimental Results.................................. 74
  5.1 Emission Absorption Temperature Measurements............... 75
  5.2 Absorptivities of Water Vapor.............................. 78
  5.3 Emission Absorption Temperatures Along a Non Isothermal Path... 79
  5.4 Temperature Gradient Data Reduction........................ 81
  5.5 Conclusions.. 85

References.. 108

Appendix I Sample Data Reductions................................. 112

Appendix II Error Analysis.. 124

Appendix III Solution of Non Linear Algebraic Equations........... 131

Appendix IV Fortran Listing - Analytical Combustion Model......... 133

Appendix V Fortran Listing - Data Reduction....................... 155

LIST OF ILLUSTRATIONS

Figure	Title
2-1	T-S Diagram of Idealized Processes of First and LastGas Elements
2-2	Schematic Diagram of Cylindrical Flame Propagation
2-3	T-S Diagram of General Non-Uniform Combustion Model
2-4	Calculated and Experimental Pressure History
2-5	Temperature Map at the End of Flame Travel
2-6	Temperature Distribution During Flame Travel
2-7	Temperature Distribution During Isentropic Expansion
2-8	Component of the Flame Velocity
2-9	Degree of Mixture Motion
2-10	Equilibrium Distribution of Nitric Oxide at the End of Flame Travel
2-11	Calculated Kinetic Formation of Nitric Oxide
3-1	Infrared Spectrum of Hydrocarbon Combustion Products
3-2	s/d for Selected Spectral Regions of Water Vapor
3-3	Transmittance of Water Vapor at 2.5 microns
3-4	Transmittance of Water Vapor at 2.0 microns
3-5	Transmittance of Water Vapor at 1.8 microns
4-1	Photograph of Optical System and Instrumentation
4-2	Schematic of Experimental Apparatus
4-3	Tracing of Oscilloscope Picture
4-4	Photograph of Engine and Propane System
4-5	Schematic Diagram of Fuel-Air System
4-6	Modified Detector Section of the Polychromator
4-7	Spectral Transmission of the Corning 7-86 Filter
4-8	Spectral Characteristics of Quartz Windows

Figure	Title
4-9	Spectral Characteristics of the IR Detectors
4-10	Intensity of Radiance Standard
5-1	"Isothermal" Spark Plug Configuration
5-2	"Gradient" Spark Plug Configuration
5-3	Cycle I-1 Emission-Absorption Temperature History
5-4	Cycle I-2 Emission-Absorption Temperature History
5-5	Cycle I-3 Emission-Absorption Temperature History
5-6	Cycle I-4 Emission-Absorption Temperature History
5-7	Experimental Absorptivity of Water Vapor at 1.8 microns
5-8	Experimental Absorptivity of Water Vapor at 2.0 microns
5-9	Experimental Absorptivity of Water Vapor at 2.5 microns
5-10	Cycle G-1 Average Emission-Absorption Temperature History
5-11	Cycle G-2 Average Emission-Absorption Temperature History
5-12	Cycle G-3 Average Emission-Absorption Temperature History
5-13	Cycle G-4 Average Emission-Absorption Temperature History
5-14	Average 2.5μ Temperature Histories for the "Isothermal" and "Gradient" Configurations
5-15	Schematic of Zonal Temperature Distribution Data Reduction
5-16	Two Zone Temperature Distribution
5-17	Normalized Two Zone Temperature Distribution

LIST OF TABLES

Table	Title
2-1	Reaction Rate Constant for Nitric Oxide Reactions
3-1	Infrared Properties of Combustion Products
4-1	Polychromator Data
5-1	CFR Engine Conditions
5-2	Two Zone Data Reduction
5-3	Three Zone Data Reduction

CHAPTER I

INTRODUCTION

As atmospheric pollution increases the spark ignition engine continues to be one of the major contributors. In halting the increase in atmospheric pollution from spark ignition engines two fundamental approaches are available. First is to prevent the formation of the pollutants during the combustion process. This can be accomplished by varying engine parameters fuel/air mixtures, and combustion chamber design. The second approach to the reduction of exhaust omissions is to prevent the pollutants from entering the atmosphere after they have been formed during the combustion process. This approach utilizes devices such as thermal exhaust reactors and catalytic mufflers. Obviously the optimum approach would employ both of the approaches outlined above.

The work presented here is principally aligned with the first approach described above by presenting a better understanding of the combustion process in the cylinder of a spark ignition engine and the subsequent effects on atmospheric pollutants. As early as 1906 Hopkinson[1] showed that combustion in a closed system resulted in a substantial temperature gradient within the chamber. Later, Lewis and von Elbe[2] developed a theory of centrally ignited explosions in spherical vessels which explained the origin of this temperature gradient. Centrally ignited combustion in spherical vessels encompasses a great simplification over the general shape in that mixture motion is everywhere normal to the surface and spherically symmetric The other extreme would be represented by combustion in long cylindrical tubes. In this case two major interactions occur: 1) there is significant boundary layer formation which will distort the shape of the flame front, and 2) reflected compression waves formed from the mixture motion will interact with the flame causing significant distortion of the flame shape. In the extreme case the flame front will become concave.[3] It is to be expected that combustion in a spark ignition engine is an intermediate case between the two extremes alluded to above.

In 1935, Rassweiler and Withrow[4] employed an L-head engine along with a stroboscopic sodium D-line technique to determine the temperatures in an engine cylinder. These results, which represent observations over many engine cycles, showed a temperature difference of the order of 200°K to exist at the end of the combustion process; the hottest region being that around the spark plug.

Recently, Starkman, et al[5] utilized a hydraulically actuated sampling valve to sample the combustion gases of a CFR engine as a function of crankshaft angle. The sampling was performed at two locations relative to the point of ignition. The first sampling location was at a location of approximately 25% flame travel while the second was at a point of 50% of flame travel. Their results showed that the nitric oxide levels at the point closer to the spark plug were about 1000 ppm higher than those values obtained from the second location at the end of flame travel. For the engine condition at hand and from chemical equilibrium considerations this 1000 ppm difference corresponds to a temperature difference on the order of 500°K.

Lavoie et al[6] have recently measured the spatial variation of nitric oxide in a single cylinder L-head engine by monitoring the light emitted from the $NO + O \rightarrow NO_2$ recombination continuum. Their results showed nitric oxide variations on the order of 0.5 mole %, thus lending support to previous findings of non uniformity in the engine cylinder.

In previous years a concept that has hindered the development of a non-uniform model is tubulence. An observation that is made during the combustion process in a spark ignition engine is that the flame speed increases with engine speed. Hence regardless of the engine speed flame travel occurs during the same crankshaft angle increment [7]. This increase in flame speed is attributed to turbulence in the combustion gases,with a scale of turbulence such that the burned gases are well mixed. To date no definitive work has been done to determine the scale of turbulence in the engine cylinder. The indirect evidence described above seems to indicate a small scale of turbulence at the flame front as opposed to large scale turbulence with mixing.

Another aspect of combustion engine research which to a limited extent is as yet undefined is the measurement of combustion gas temperatures. A number of workers have delt with the temperature of the end gas in an attempt to unravel the complicated problem of knock [8]. Recently, Smith [9] utilized the ultraviolet radiation of the $A^2\Sigma^+ \rightarrow X^2\Pi$ transition of OH along with the emission - absorption technique to determine the temperature of the combustion products during the expansion process. Spurious results were obtained due to the nature of the radiation that was observed at 3064 A^o.

In view of the above work it was decided to take a further look into the state of the combustion gases in the cylinder of a spark ignition engine.

Analytically this work includes the development of a non-uniform model of the combustion process in the cylinder of a spark ignition engine. The model takes into account real gas properties and includes the chemical kinetics of nitric oxide formation.

Experimentally this work utilizes the infared radiation of water vapor to determine the temperature of the combustion products. Temperatures are simultaneously determined at three wavelengths for comparison purposes along with the ideal bulk gas temperature inferred from the pressure and volume. Measurements are also made looking along the path of flame travel and the temperature distribution is inferred from the equation of radiative transfer. In order to further study in situ methods of combustion processes at high pressure the measured absorptivities of water vapor are compared with theoretical predictions employing a statistical narrow band model.

CHAPTER II

ANALYTICAL COMBUSTION MODEL

2.1 Fundamental Thermodynamic Observation

There are basically three approaches to modeling the combustion process in a closed system. The first considers the combustion to occur instantaneously and homogeneously throughout the volume.[7,10] The next approach considers a finite flame propagation rate and considers the mass in the volume to be divided into two zones: an unburned gas zone and a uniform burned gas region.[11] Yet a third approach is to consider an unburned gas region and a non-uniform or unmixed burned gas region whereby each element which burns maintains its identity. Lavoie et al[6] recently published a model of this nature, with constant specific heats and the assumption that each zone burned at constant pressure. Obviously, the actual combustion process approaches a combination of the second and third idealizations. In this chapter, a general model utilizing a non-uniform burned gas region and real gas properties will be developed and the effects of this non uniformity will be investigated.

Before proceeding with the general model of the combustion process it is of value to look at the processes which occur in a closed constant volume system from an elementary thermodynamic point of view. This can be accomplished by considering the thermodynamic processes which the first increment of mass and the last increment of mass undergo during combustion in a constant volume system. In order to develop this simplified model the following idealizations and assumptions will be made:

a) constant specific Cp

b) the gas is homogeneous

c) $pv = NRT$

d) since the pressure drop across a deflagration is negligible [3] each element burns at constant pressure

e) the entire system is adiabatic

f) the thermoconductivity of the gas is zero and there is no radiant transfer within the cylinder

g) the gas is non-reacting and the combustion process can be modeled as a heat addition, ΔH_R .

With the above assumptions, the processes which the first element of gas undergo can be idealized as: 1) a constant pressure heat addition at the initial pressure P_o followed by 2) an isentropic compression to the final pressure P_f. These are shown in figure 2-1. If ΔH_R is the enthalpy per unit mass released during the combustion process, then the temperature of the first element after the constant pressure heat addition is given by

$$T_1 = T_0 + \Delta H_R / C_p \qquad (2.1\text{-}1)$$

The final temperature attained by the first element of mass to burn after isentropic compression by the remainder of the combustion process is given by

$$T_{f_1} = [T_o + \Delta H_R / C_p] \, (P_o/P_f)^{(1-\gamma)/\gamma} \qquad (2.1\text{-}2)$$

On the other hand, the last element of gas to burn undergoes a different sequence of thermodynamic processes. First, an isentropic compression by the ensuing flame front from the initial pressure of P_o and temperature to the final pressure P_f, followed by a constant pressure heat addition of an amount ΔH_R per unit mass at the final pressure, P_f. The temperature at the end of the isentropic compression is given by

$$T_2 = T_o(P_o/P_f)^{(1-\gamma)/\gamma} \qquad (2.1\text{-}3)$$

and the final temperature attained by the last element of gas to burn is

$$T_{f_2} = T_o(P_o/P_f)^{(1-\gamma)/\gamma} + \Delta H_R/C_p \qquad (2.1\text{-}4)$$

Comparing the final temperatures reached by the first and last elements to burn ΔT_{f_1} and T_{F_2} respectively we see that

$$T_{f_1} - T_{f_2} = (\Delta H_r/C_p)[(P_o/P_f)^{(1-\gamma)/\gamma} - 1] \qquad (2.1\text{-}5)$$

since H_r has been defined to be positive and since $\gamma > 1$ it is observed that

$$T_{f_1} > T_{f_2}$$

since $P_f > P_o$.

Hence, in the absence of heat transfer and mixing, the first element of mass to burn in a constant volume closed system will achieve a higher temperature than the last element to burn.

Therefore, even very elementary thermodynamics predicts that during combustion in a closed system a temperature gradient will be formed due to the fact that each successive element of mass to burn undergoes a different sequence of thermodynamic processes.

2.2 Detailed Model of the Combustion Process

In this section a more detailed and general model of the combustion process is developed in order to quantitatively assess the effect of finite combustion time on the temperature distribution in time and space within the combustion chamber. Ultimately, it is of interest to investigate the effects on the chemical process which take place both from an equilibrium and a non-equilibrium point of view.

Ultimately, the ideal model of the combustion process would consist of a complete and continuous numerical integration of all the kinetic processes occurring in the combustion chamber. In this model the heat release rate and hence the flame speed would be calculated from the numerical integration of the kinetics. At this time a model of this detail and complexity is beyond the scope of technology due to the inability to specify each kinetic step along with the uncertainty in the kinetic data for the individual process. Thus in order to overcome the lack of knowledge of the individual kinetic steps, experimental pressure time histories or flame speed histories can be utilized along with a finite difference model in lieu of the detailed kinetics. This approach is utilized in the following analysis.

Basically the model is the same as that considered in the previous section, a homogeneous unburned region and an unmixed, nonuniform burned region. Since the model was developed for solution on a digital computer it will be presented in a finite difference form. Flame propagation will be assumed one-dimensional and cylindrical in geometry as opposed to spherical as in the real problem (i.e. an ignition wire as opposed to an ignition point). This geometrical assumption is valid due to the small height to diameter ratio of the combustion chamber during the time of flame travel.

As the flame propagates an increment Δr into the unburned gas region consuming an increment of mass Δm during a piston travel of $\Delta\theta$ crank angle degrees, the cylinder pressure increases by an amount Δp. The limiting case of no mixing is considered so that each of these elements of mass, Δm, maintains its identity throughout the system is uniform and since each element is adiabatic, as the cylinder pressure increases by an amount, Δp_j due to the combustion of mass Δm_j and piston travel $\Delta\theta_j$ the other burned gas zones $\Delta m_i (i \neq j)$ along with the unburned gas m_{ub} are being isentropically compressed. The final state of the gas can be determined from a first law analysis of the system and does not require the assumption of isobaric combustion. The geometrical arrangement of the system is shown in figure 2-2 and the thermodynamic processes are shown diagramatically on a T-S diagram in figure 2-3.

With regard to the description of the gas, the unburned gas is assumed to be a non-reacting ideal gas mixture of propane and air with variable specific heats. The burned gas zones are assumed to be an equilibrium mixture of combustion products: CO_2, CO, N_2, O_2, H_2O, O, N, H, H_2, OH, NO. It should be pointed out that all thermodynamic properties data, with the exception of propane, were obtained from the JANAF Tables.[2]

In developing an algorithm to solve the flame propagation problem one may input either the pressure-time history or the flame speed. The algorithm that is developed here uses the flame speed as input as this was found to simplify the numerical analysis. The computer pressure-time history could then be compared to experimental pressure data in order to verify the form of the flame speed function. In choosing a flame speed one must be careful in the definition of flame speed in a confined system. Since the unburned gases are being compressed by the oncoming flame front the burned gases move relative to the combustion chamber with a velocity U_T. Hence, the observed flame moves across the combustion chamber at a rate given by [10]

$$U_f = U_T + U_b$$

where U_b is the rate of flame propagation into the unburned gas region. This quantity is commonly called the flame speed. In terms of the combustion model it is U_b which is input to the algorithm.

The algorithm can best be presented in the following outline:

a. increment the crank shaft angle $\Delta\theta$ and compute the flame travel Δr and the mass of unburned gas consumed Δm

b. assume the incremental pressure rise Δp

c. the state of the unburned gas after isentropic compression through Δp can be determined

$$[\int ds] = 0 = \left[\int_{T'}^{T''} (\bar{C}_p(T)/T)\,dT - R\ln\,(1+\Delta P/P)\right]_{\text{unburned gas}} \qquad (2.2\text{-}1)$$

where

$\bar{C}_p(T)$ = specific heat of the unburned fuel/air

d. the state of each element of burned Δm_j after isentropic compression is determined from

$$[\int ds_j] = 0 = [(\Sigma n_{ij} s_{ij})'' - (\Sigma n_{ij}\, s_{ij})']_{\text{burned zone } j} \qquad (2.2\text{-}2)$$

where

superscript: (') = initial state with pressure, p

(") = final state with pressure, p + Δp

n_{ij} = number of moles of specie i in the j^{th} burned gas region

s_{ij} = entropy per mole of the i^{th} specie in the j^{th} element

e. the final state of the burning zone may be determined by performing a first law analysis on the total system

$$(U_f - U_i)_{system} = Q_{system} + WK_{system} \qquad (2.2\text{-}3)$$

since the system is assumed adiabatic

$Q_{system} = 0$

the total system work WK_{syst} is just

$$WK_{syst} = - pdV_{syst} \qquad (2.2\text{-}4)$$

and may be determined for the increment of interest by fitting a parabola through three local (p,v) points and integrating. The total change in internal energy of the system may be written in terms of the individual zones

$$(U_f - U_i)_{syst} = m_{ub}(u'' - u')_{\text{unburned gas}} + \{\Sigma\Sigma[(m_{ij}u_{ij})'' - (m_{ij}u_{ij})']\}_{\text{burned gas}}$$
$$+ m_b(u_b'' - u_b')_{\text{burning gas}} \qquad (2.2\text{-}5)$$

where

m_{ub} = mass of unburned gas

m_{ij} = mass of species i in burned zone j

m_b = mass burning

u_{ij} = total internal energy of the i^{th} species in the j^{th} zone

superscript: (') initial state with pressure = p

(") final state when pressure = p + Δp

hence equations (2.2-5), (2.2-4), (2.2-3) may be used to find the final internal energy of the burning zone and hence all of its thermodynamic properties.

f. since the state points of the gas in the cylinder have been determined for the assumed pressure rise Δp the total volume may be calculated from the known specific volumes of the zones and compared to the known physcial volume of the combustion chamber. If they do not match a new pressure rise is assumed $\Delta p'$ and the process repeated. The new pressure rise $\Delta p'$ is determined by assuming an overall isentropic expansion/compression through the volume defect calculated above.

These calculations were carried out on a CDC 6400 computer for the combustion of propane and air at a compression ratio of 7:1 for various fuel-air mixture ratios. A flame speed of the form

$$U_b = a+b\theta+c\theta^2$$

where θ is the crankshaft angle, was used and the resulting pressure-time history for a stoichiometric mixture is shown in figure 2-4 along with an experimental pressure trace. A fortran listing of the program appears in Appendix IV.

Just as the elementary model of section 2.1 qualitatively predicted the more detailed model predicts a temperature difference at the end of flame travel of approximately 600°K; the region of higher temperature being near the point of ignition as shown in Figure 2.5. Since no mixing was considered the difference exists throughout the combustion process and subsequent isentropic expansion as shown in Figures 2.6 and 2.7.

Another interesting result which is obtained from this model is the motion of the mixture. Since the flame front location in the cylinder is a function of two factors the burning rate and the transport due to the isentropic compression the transport velocity U_T can be obtained by determing the flame front velocity and subtracting the burning velocity U_b which was input to the solution, this is shown in Figure 2.7.

Since many workers have used sampling valves to sample the cases as a function of time[5, 13] in a reciprocating spark ignition engine it is of interest to point out that if this non homogeneous model is valid then the change in concentration as a function of time may not reflect a true situation since the sampling valve may be sampling a different portion of the gas from one point in the cycle to another. This is shown in Figure 2.8 where the outer boundary of the first element of mass to burn is plotted as a function of crankshaft angle.

By far the most profound affect that this temperature gradient has is its influence in the formation of air pollutant chemical species such as nitric oxide. The greatest influence will be with nitric oxide since chemical equilibrium calculations show that nitric oxide increases exponentially with temperature. It has been inferred from exhaust gas analysis and shown spectroscopically[14,6] that the nitric oxide concentration in the exhaust of a spark ignition engine is much greater than that predicted from chemical equilibrium at exhaust conditions, and that the nitric oxide level is on the order of that predicted at peak cycle temperature. As seen in Figure 2.9 the non homogeneous model predicts almost a factor of four variation in the equilibrium nitric oxide mole fraction across the cylinder.

As was noted above the nitric oxide concentration cannot be predicted from equilibrium considerations. In the next section the non-equilibrium formation of nitric oxide will be investigated with the non uniform model.

2.3 Chemical Kinetics of Nitric Oxide

Since it is generally agreed that history of nitric oxide in the engine cylinder is kinetically controlled it is of interest to look at the kinetic formation in the non uniform model.

It has been shown that the nitric oxide kinetics can be described by the following simple kinetic mechanism[15-16]

$$N_2 + O \rightarrow NO + N \qquad (1)$$

$$O_2 + N \rightarrow NO + O \qquad (2)$$

$$NO + N \rightarrow N_2 + O \qquad (3)$$

$$NO + O \rightarrow O_2 + N \qquad (4)$$

where the rate constants for the kinetic steps (1)-(4) above are given in table 2.1

The nitric oxide kinetics are sufficiently slow with respect to the C-H-O kinetics that the majority of nitric oxide formation occurs in the post flame region[6,15]. Hence, a reasonable assumption is that the C-H-O system is in equilibrium and that the N-O system can be decoupled and integrated separately.

From the above mechanism the time rate of change of nitric oxide in the j^{th} zone is given by

$$\frac{1}{V}\frac{dN_{NO}}{dt} = \{K_1[N_2][O] + K_2[O_2][N] - K_3[NO][N] - K_4[NO][O]\}_j \quad (2.3\text{-}1)$$

Formal integration of the above equation requires the complete specification of the time histories of each term on the right hand side.

Since the object of this section is to infer the effects of the chemical kinetics and the non uniform model on the formation of nitric oxide the following assumptions will be made. First, the temperature and volume time histories will be assumed to be made up of a series of isothermal and isochoric increments. Secondly, it will be assumed that the concentration of nitrogen atoms and oxygen atoms is given by the equilibrium values and remain constant during each isothermal time increment. Since the nitrogen and oxygen atoms are involved in a chain mechanism this second assumption should prove valid. Thirdly, it will be assumed that the concentration of diatomic nitrogen and oxygen at the beginning of each isothermal step is given by the equilibrium value.

Defining a new variable β_i, where

$$\beta_i = n_i/m = x_i/\overline{MW} = [i]/\rho$$

where

x_i = mole fraction of specie i

n_i = moles of specie i

$[i]$ = concentration of specie i

ρ = density

$\overline{MW}$ = mixture molecular weight

Substituting into equation (2.3-1)

$$\frac{d\beta_{NO}}{dt} = \rho[K_1\beta_{N_2}\beta_O + K_2\beta_{O_2}\beta_N - K_3\beta_{NO}\beta_N - k_4\beta_{NO}\beta_O] \quad (2.3\text{-}4)$$

Since the molecular weight of each zone changes only slightly during each time increment it may be assumed constant. Therefore, equation (2.3-4) may be put in terms of the mole fractions of each specie,

$$\frac{dx_{NO}}{dt} = (\rho/\overline{MW})[K_1x_{N_2}x_O + K_2x_{O_2}x_N - K_3x_{NO}x_N - K_4x_{NO}x_O] \quad (2.3\text{-}5)$$

utilizing another change of variable,

$$\alpha = x_{NO} - x^o_{NO}.$$

the mole fraction of each specie may then be described as

$$x_{O_2} = x^o_{O_2} - \alpha/2$$
$$x_{N_2} = x^o_{N_2} - \alpha/2$$
$$x_O = x^o_O$$
$$x_N = x^o_N$$

where x^o_{NO}, $x^o_{N_2}$, $x^o_{O_2}$, x^o_N, x^o_O, are the values at the beginning of the time increment under consideration. In each instance it is assumed that they are given by their equilibrium values except for x^o_{NO}, which assumes the value from the kinetic solution at the end of the previous step. With these substitutions, the following equation is obtained

$$\frac{d\alpha}{dt} = \Gamma[\eta - \xi\alpha] \quad (2.3\text{-}6)$$

where

$$\Gamma = \rho/\overline{MW}$$
$$\eta = [K_1x^o_{N_2}x^o_O + K_2x^o_{O_2}x^o_N - K_3x^o_{NO}x^o_N - K_4x^o_{NO}x^o_O]$$
$$\xi = 1/2[K_1x^o_O + K_2x^o_N] + k_3x^o_N + K_4x^o_O$$

Integrating equation (2.3-6) over the time increment Δt

$$\Gamma\Delta t = \int_0^\alpha \frac{d\alpha}{\eta - \xi\alpha}$$

or

$$\alpha = (\eta/\xi)(1 - e^{-\xi\Gamma\Delta t}) \qquad (2.3\text{-}7)$$

where $\alpha = x_{NO} - x_{NO}^o$ and represents the change in nitric oxide during the particular time step. Hence, the mole fraction of nitric oxide which exists after k kinetic steps is given by

$$(x_{NO})_k = (x_{NO})_{k-1} + \alpha_k \qquad (2.3\text{-}8)$$

Since the initial amount of nitric oxide is zero prior to the arrival of the flame at each zone equation (2.3-8) reduces to

$$(x_{NO})_k = \sum_{i=1}^{k} \alpha_i \qquad (2.3\text{-}9)$$

This scheme was programed on the CDC 6400 computer to calculate the kinetic history of nitric oxide in each of the zones of the non uniform model considered in section 2.2.

As seen in Figure 2-11 some rather interesting results were obtained. Since the temperature in the first zone is the hottest and since the residence time for this zone is longest the nitric oxide reaches its peak value here. It does not quite reach the peak equilibrium value when it begins to disappear due to the quenching during the expansion. This disappearance continues until the temperature decreases to a crankshaft angle of approximately 90° after top center where the reactions slow down and the nitric oxide freezes. Similar trends are exhibited for the other zones except their peak temperatures are lower and residence times shorter so that less nitric oxide is formed and freezing occurs at an earlier point.

The spectroscopic measurements by Newhall and Starkman[14] of nitric oxide in an engine cylinder showed no change with time during the expansion process. These results are in agreement with the model presented in this section since their experiment utilized a dual ignition system with the spectrometer observing the last mass to burn.

In order to assess the amount of nitric oxide that would be formed in an engine a value that is frequently used is the equilibrium amount for peak cycle temperature,[17] where the peak cycle temperature is inferred from the pressure and volume. This value was calculated from the model in section 2.2 and found to be 0.39 mole percent nitric oxide. From the kinetic calculations it is found that the average nitric oxide mole fraction after freezing has occurred is approximately 0.34 mole percent.

TABLE 2-1

Reaction Rate Constants

Reaction	Rate Constant - $\frac{\text{mole}}{\text{cm}^3\text{-sec}}$	Reference
$N_2+O \xrightarrow{k_1} NO+N$	$7\times10^{13}\ \exp(-75{,}500/RT)$	15,18
$O_2+N \xrightarrow{k_2} NO+O$	$13.3\times10^{9}\ T\ \exp(-7080/RT)$	
$NO+N \xrightarrow{k_3} N_2+O$	1.55×10^{13}	
$NO+O \xrightarrow{k_4} O_2+N$	$3.2\times10^{9}\ T\ \exp(-39{,}100/RT)$	

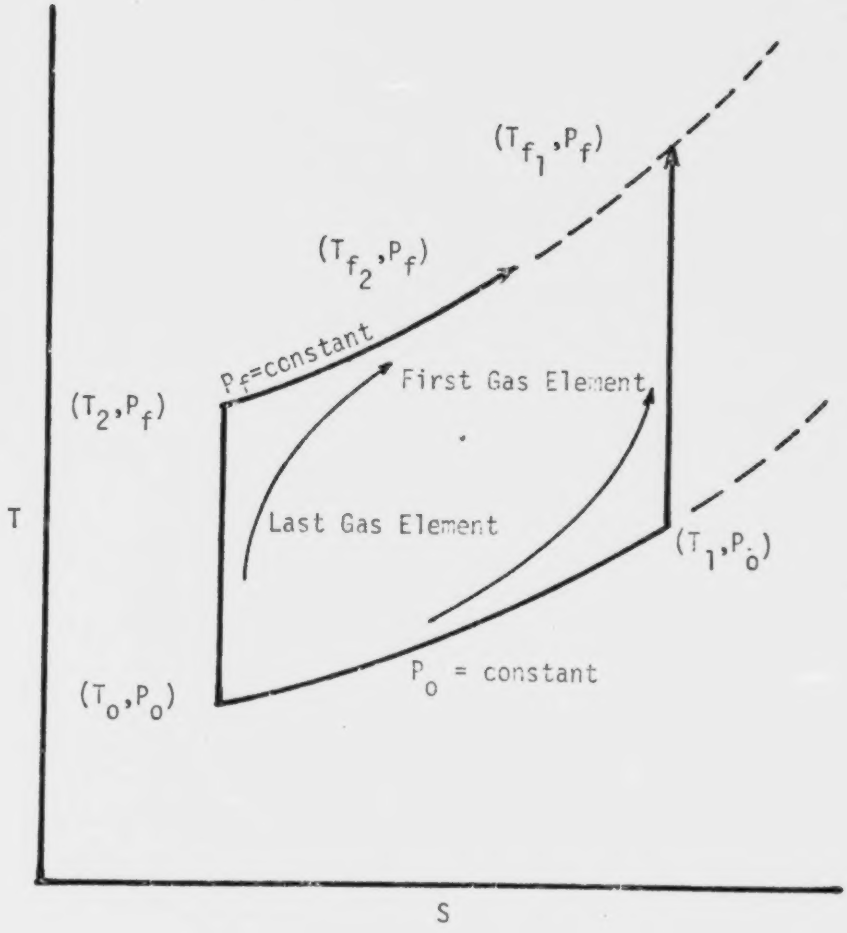

(T_{f_1},P_f)
(T_{f_2},P_f)
P_f=constant
First Gas Element
(T_2,P_f)
T
Last Gas Element
(T_1,P_o)
(T_o,P_o)
P_o = constant
S

Figure 2-1

IDEALIZED PROCESSES OF FIRST AND
LAST GAS ELEMENTS

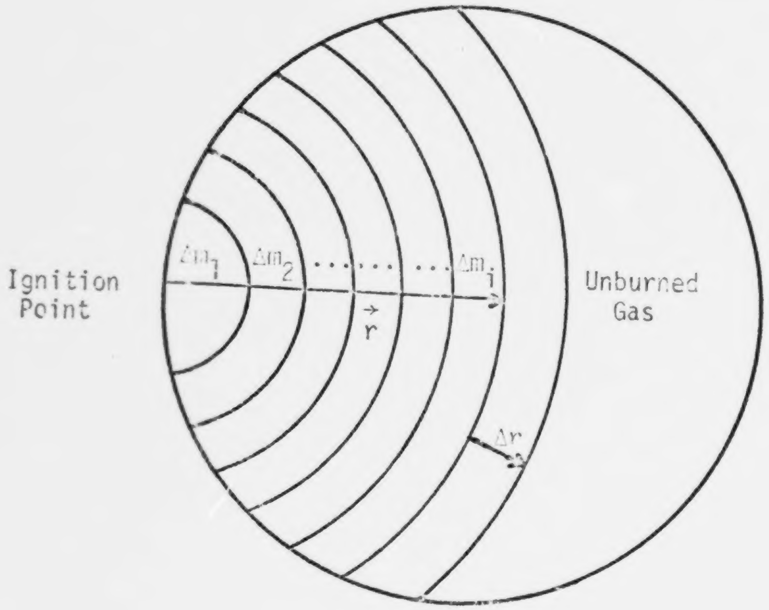
Ignition Point
Δm_1
Δm_2
Δm_i
$\vec{r}$
Unburned Gas
Δr

Figure 2-2

SCHEMATIC DIAGRAM OF CYLINDRICAL FLAME PROPAGATION

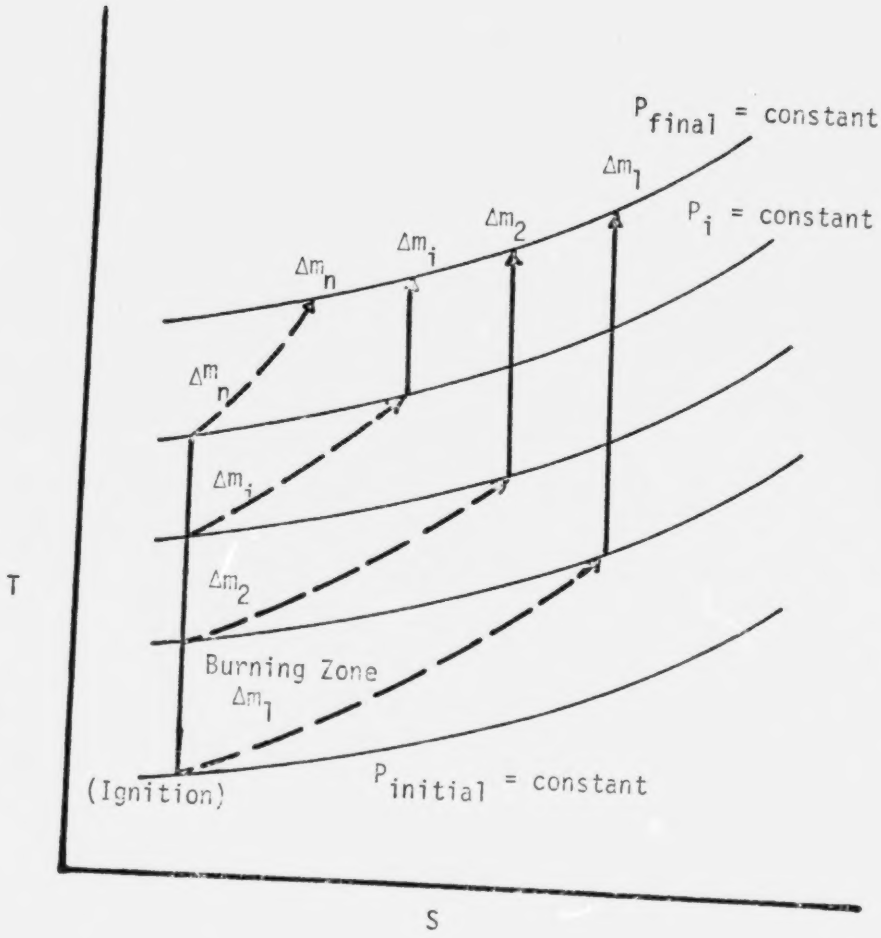
P_{final} = constant
Δm_1
P_i = constant
Δm_2
Δm_i
Δm_n
Δm_n
Δm_i
T
Δm_2
Burning Zone
Δm_1
(Ignition)
$P_{initial}$ = constant
S

Figure 2-3

T-S DIAGRAM OF GENERAL
NON UNIFORM COMBUSTION MODEL

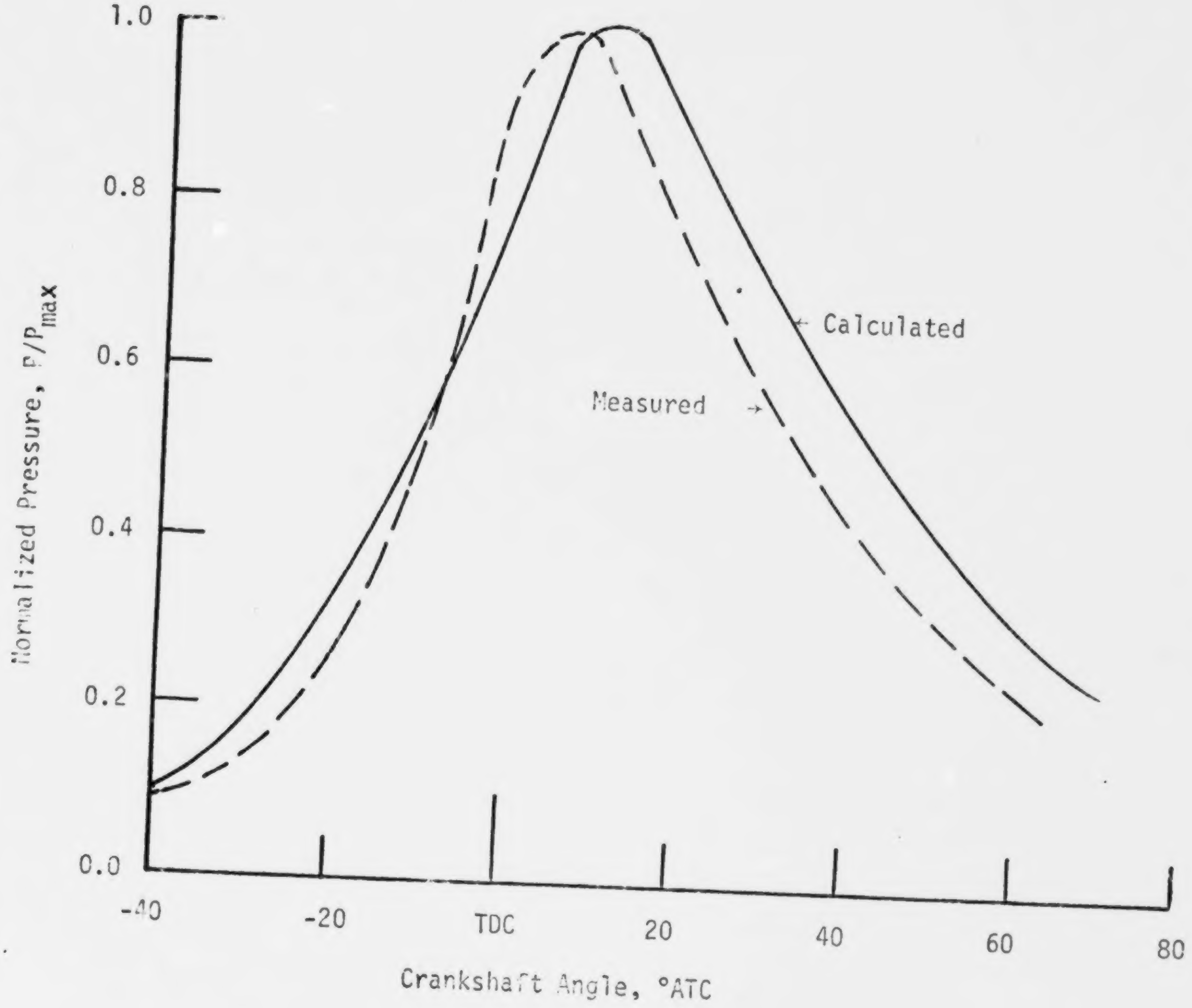

Figure 2-4

CALCULATED AND EXPERIMENTAL PRESSURE HISTORY

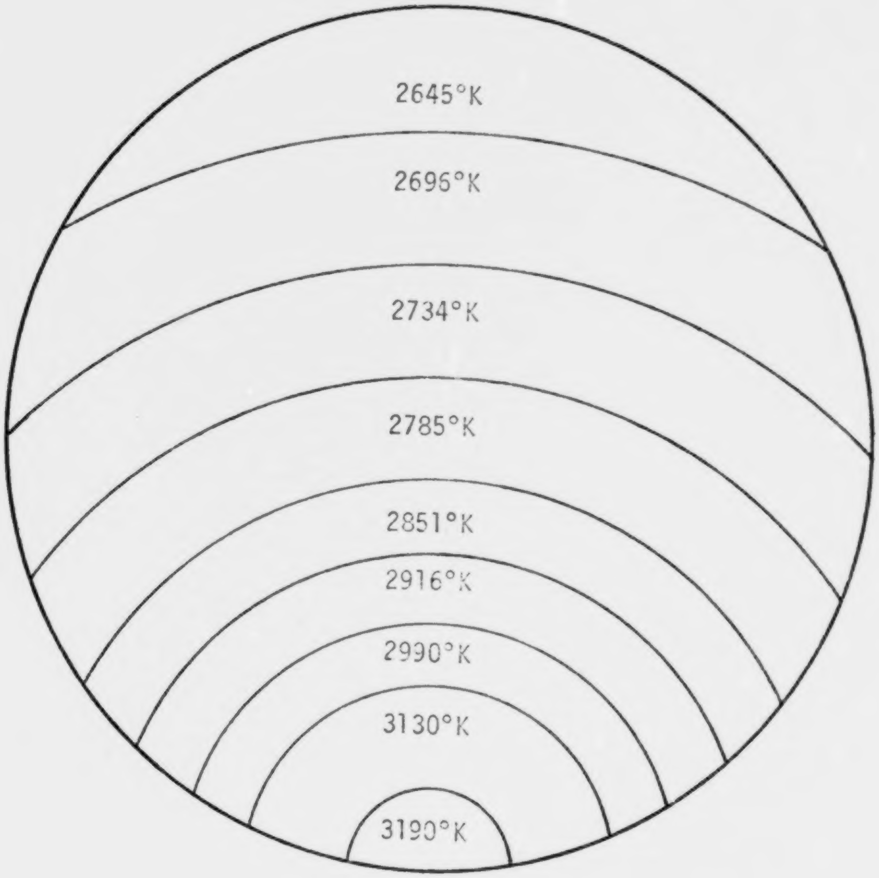
2645°K
2696°K
2734°K
2785°K
2851°K
2916°K
2990°K
3130°K
3190°K

Figure 2-5

TEMPERATURE MAP AT THE END OF FLAME TRAVEL, PROPANE/AIR $\phi = 1.0$

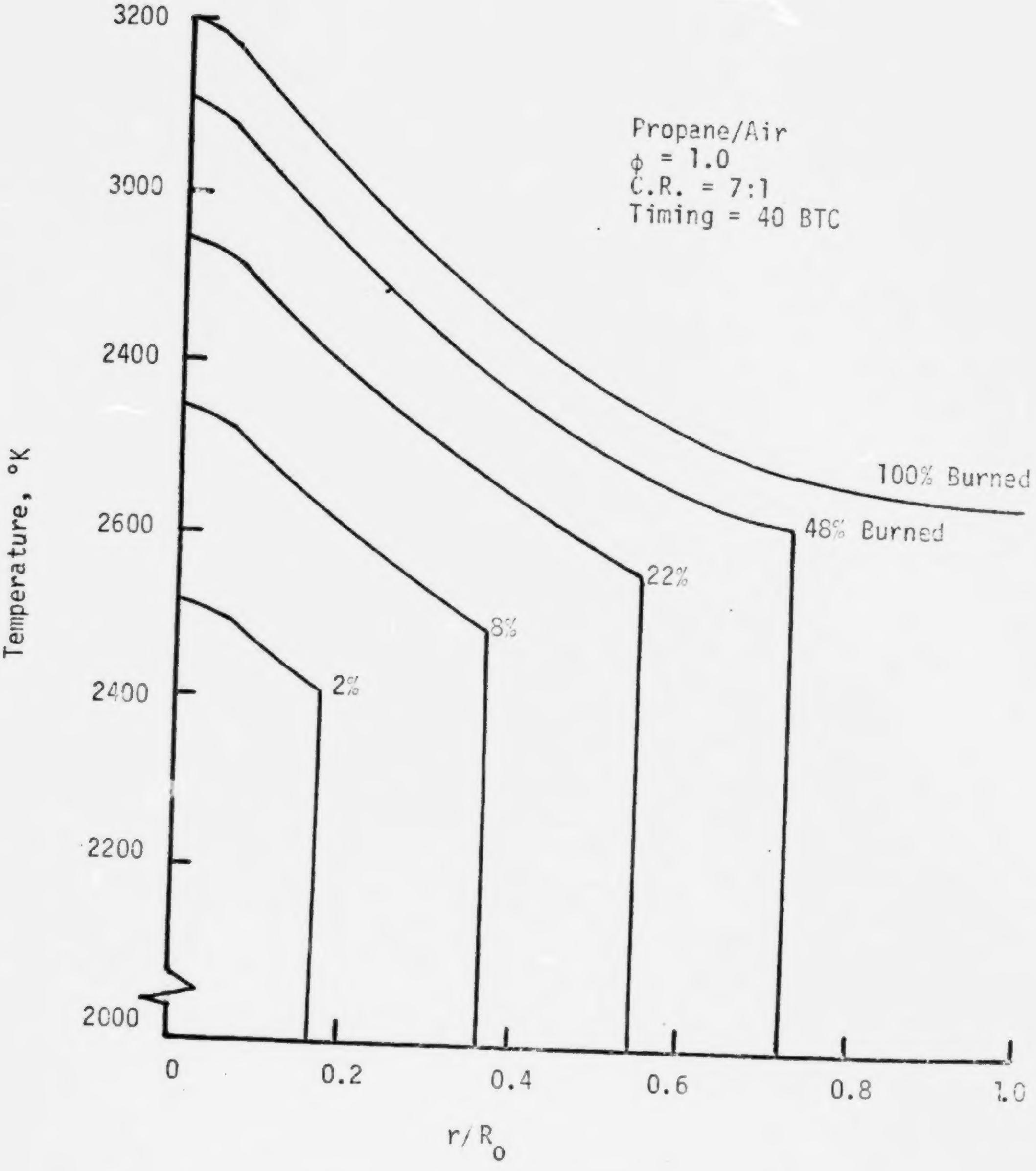

Figure 2-6

TEMPERATURE DISTRIBUTION DURING THE COMBUSTION PROCESS

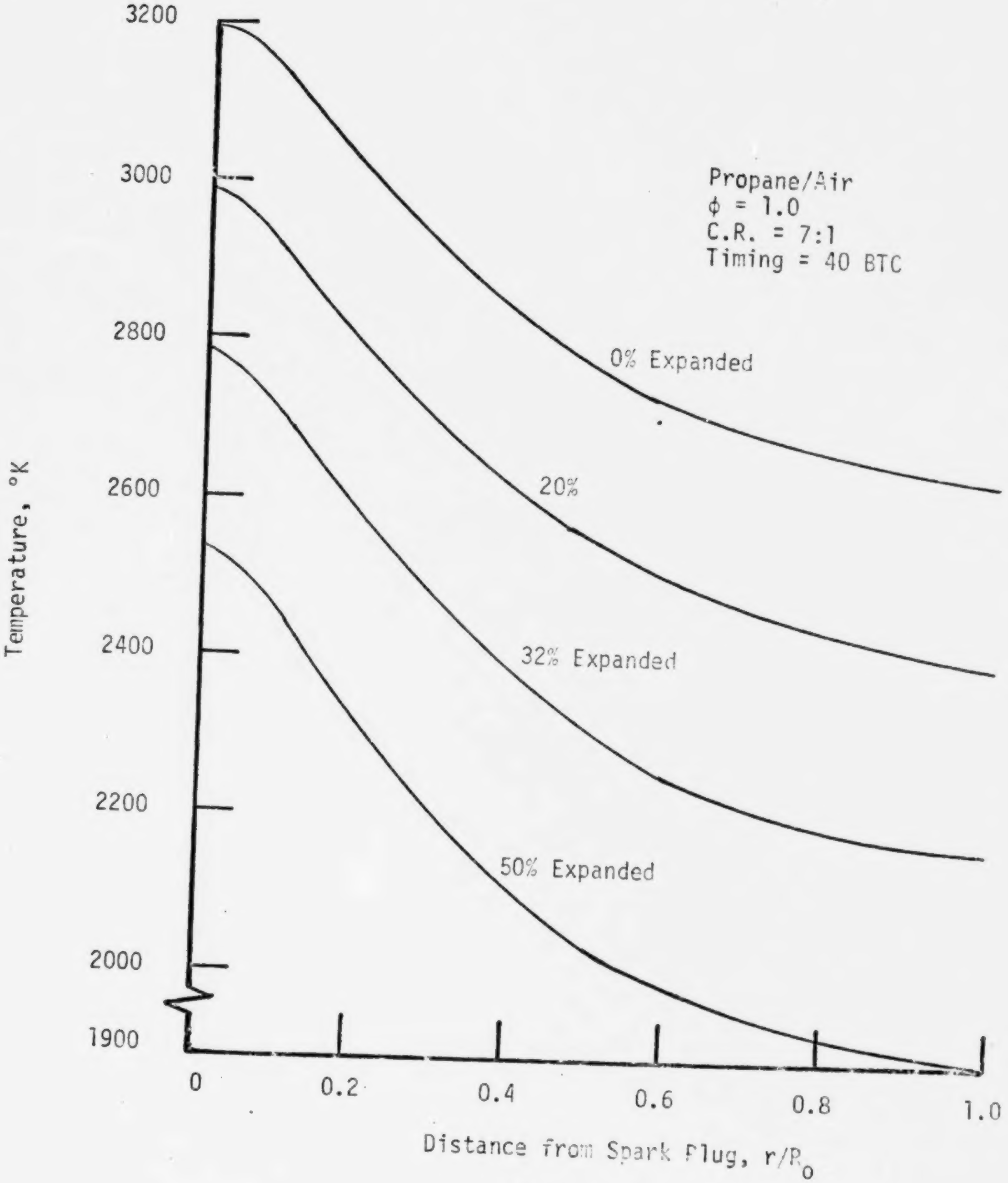

Figure 2-7

TEMPERATURE DISTRIBUTION DURING ISENTROPIC EXPANSION

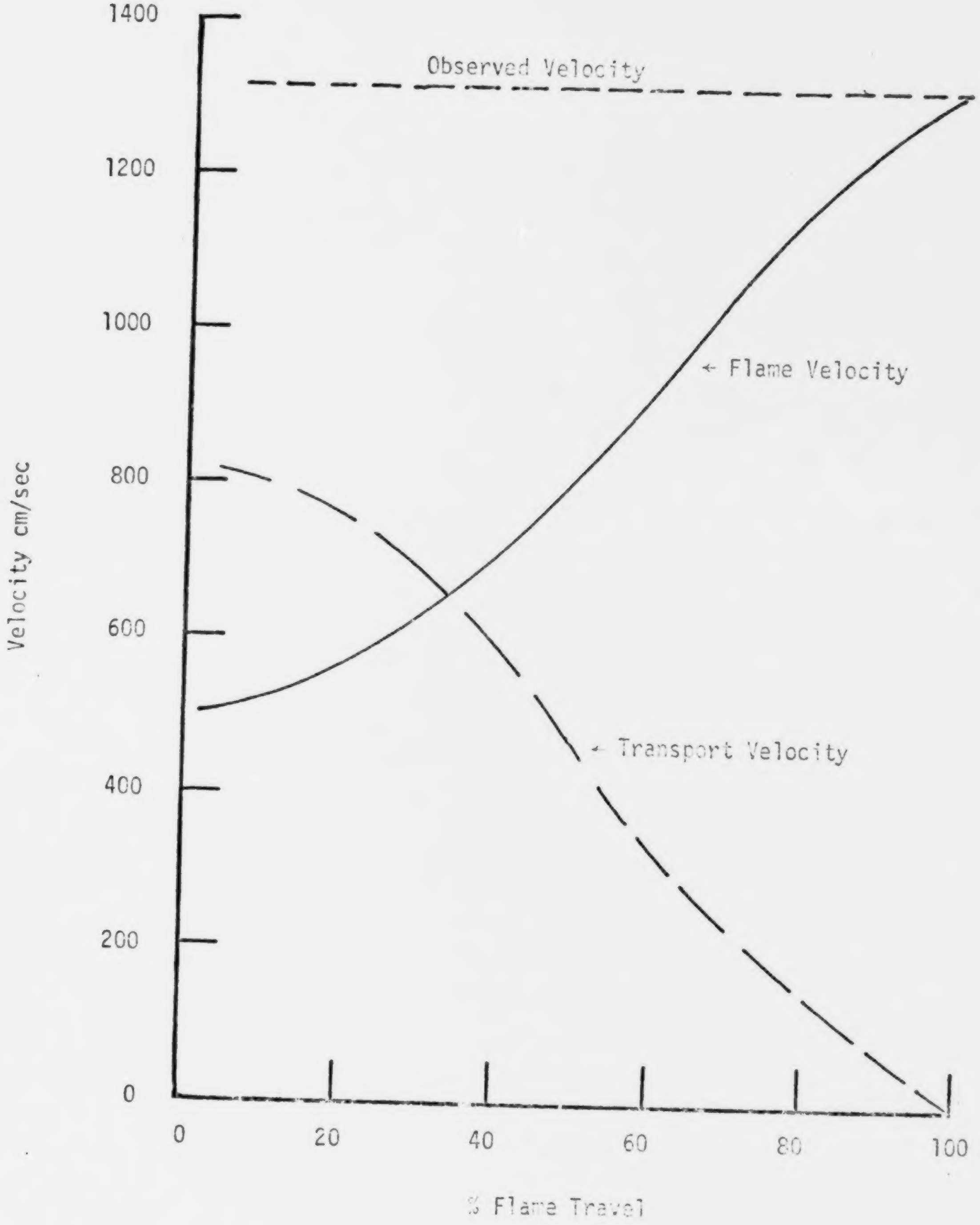

Figure 2-8

COMPONENT OF FLAME VELOCITY

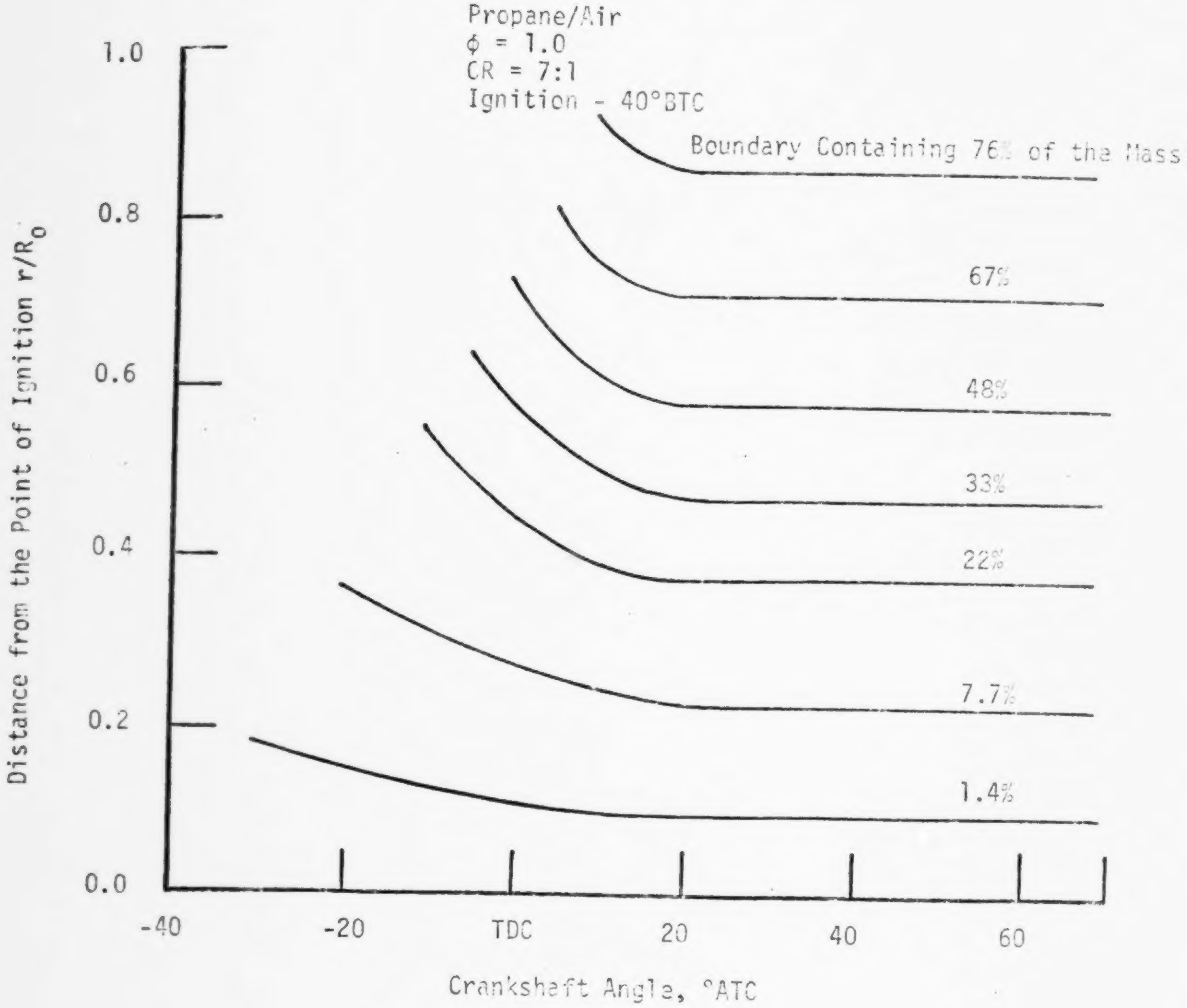

Figure 2-9

DEGREE OF MIXTURE MOTION

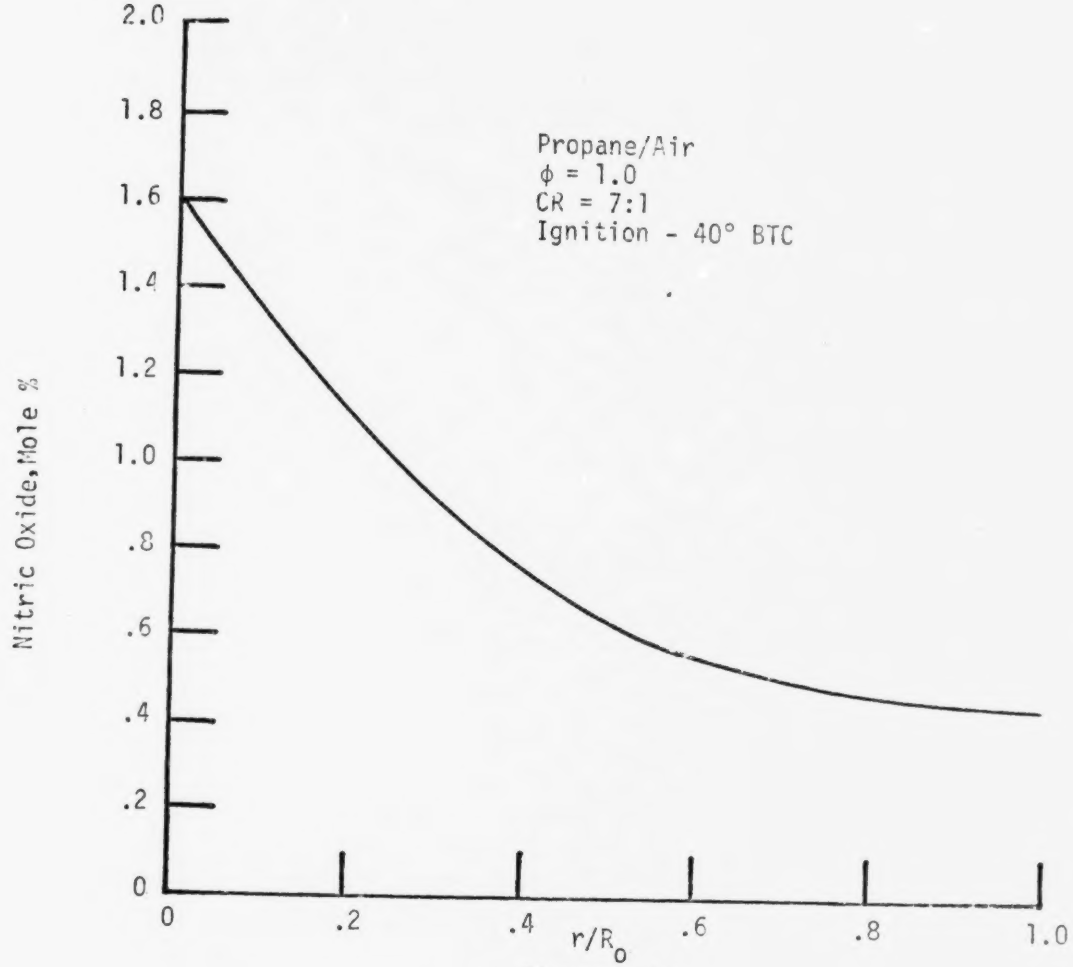

Figure 2-10

EQUILIBRIUM DISTRIBUTION OF NITRIC OXIDE
AT THE END OF FLAME TRAVEL

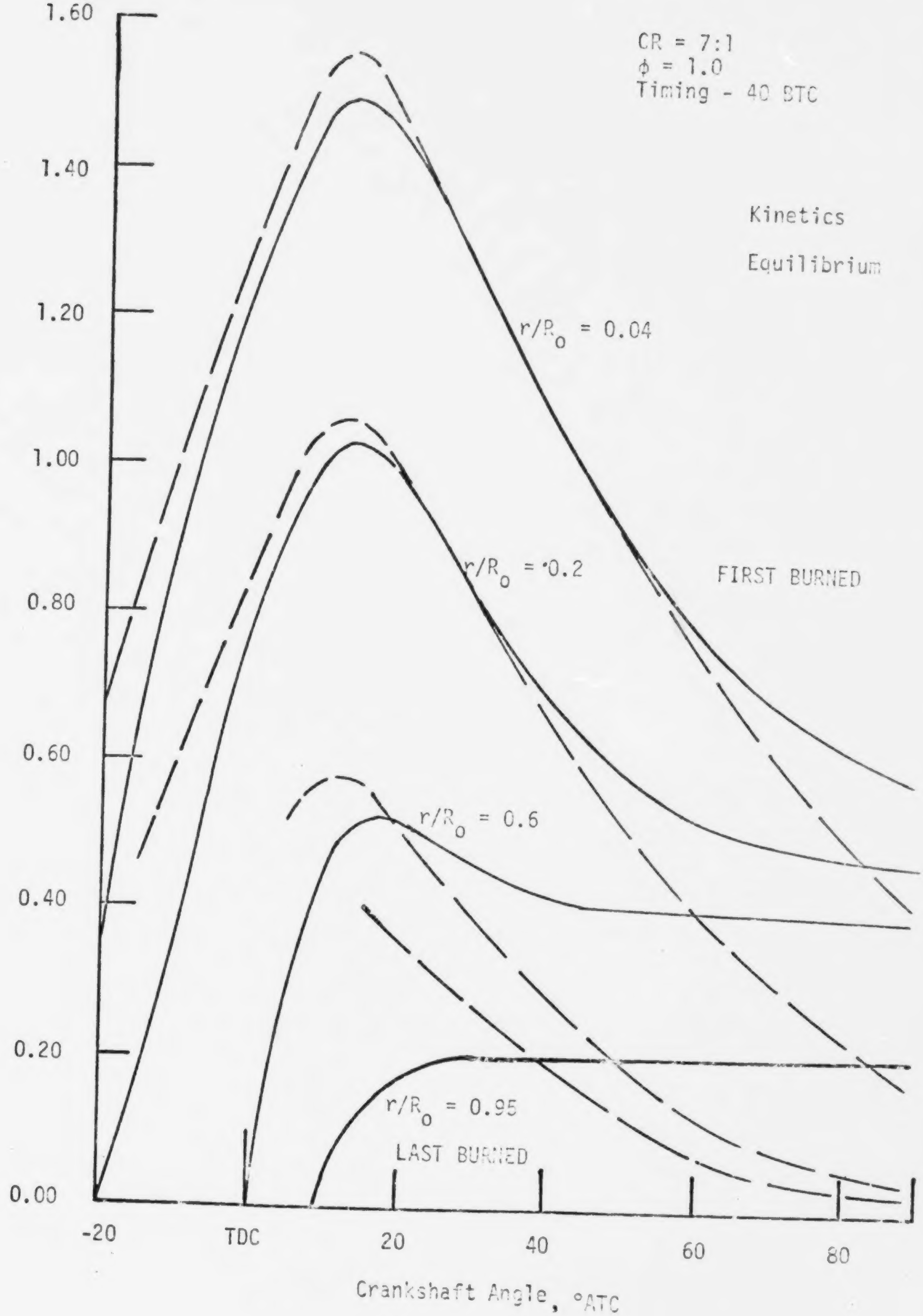

Figure 2-11

KINETIC FORMATION OF NITRIC OXIDE

CHAPTER III

EXPERIMENTAL APPROACH

3.0 GENERAL APPROACH

Before developing an experimental technique for the in situ analysis of the state of the gas in the cylinder consideration should first be given to the requirements of a measuring system. First, sufficient time response must be exhibited in order to follow the processes occuring in the engine. This characteristic time is of the order of 10^{-4} seconds. Secondly, a spark ignition engine has the characteristic of exhibiting cycle to cycle variation. This cycle to cycle variation results in random fluctuations in the peak cycle pressure of the order of 25-30%. Due to this cycle to cycle variation each spark plug firing should be treated as an individual experiment. Hence, all pertinent data must be collected during one engine cycle. It is this second constraint which puts severe limitations on the measurement technique. Given the two constraints described above the only experimental methods of temperature measurement which are feasible are optical techniques.

A number of techniques have been developed to determine chemical species in an engine cylinder [6,9,14]. Also, Smith [9] attempted to use the emission - absorption technique to determine the combustion gas temperature during the expansion stroke of a spark ignition engine. The radiation at 3064 A^o from the OH radical was used by Smith. Due to possible interference from the $CO+O \rightarrow CO_2^*$ continuum and/or non-equilibrium radiation from the OH species, Smith, obtained anomolous results for the combustion gas temperature. One of the objectives of this study was to use the emission - absorption technique in a region of the spectrum where interference will not be a hindrance and check these results.

With regards spatial temperature gradients there are basically two optical methods available: 1) single wavelength observations along various geometrical lines of sight[19,20,21] and 2) multiple wavelength observations along a single line of sight. Due to the restrictions imposed by cycle to cycle variations it was decided to develop a multiple wavelength single line of sight technique to determine the temperature distribution along the path of flame travel.

3.1 EQUATION OF RADIATIVE TRANSFER

It has been shown by Newhall [27] that scattering of light in the engine cylinder is negligible. Hence, in the absence of scattering the monochromatic equation of radiative transfer along a direction $\vec{r}$ takes the form, [19,28,29]

$$\frac{dI(\lambda,\vec{r})}{d\vec{r}} = -kI(\lambda,\vec{r}) + E \tag{3.1-1}$$

where the terms have the following meaning

$I(\lambda,\vec{r})$ = radiation intensity

$k = k(T,\lambda)$ = absorption coefficient

$E = E(T,\lambda)$ = emission coefficient

$\vec{r}$ = direction vector

$T = T(\vec{r})$ = temperature

λ = wavelength

If the gas is in local thermodynamic equilibrium, then Kirchoff's law is valid and the emission coefficient is given in terms of the absorbtion coefficient and the Planck blackbody function[28,29] as

$$E(\lambda,T) = k(\lambda,T)I_b(\lambda,T) \qquad (3.1\text{-}2)$$

where,

$$I_b(\lambda,T) = \frac{2hc^2}{\lambda^5[e^{hc/\lambda kT}-1]}$$

$$h = 6.62 \times 10^{-27} \text{ erg-sec}$$

$$c = 3.00 \times 10^{10} \text{ cm/sec}$$

$$k = 1.38 \times 10^{-16} \text{ erg/}^\circ\text{K}$$

Substituting equation (3.1-2) into (3.1-1) the equation of radiative transfer becomes

$$\frac{dI(\vec{r},\lambda)}{d\vec{r}} = -k(\lambda,T)[I(\lambda,\vec{r})- I_b(\lambda,T)] \qquad (3.1\text{-}3)$$

Equation (3.1-3) may be integrated from r=0 to r=L along a pencil of radiation contained in the differential solid angle dΩ, such that at r=0 there is an external source of radiation $I_o(0,\lambda)$. Performing this integration, the intensity of radiation which emerges at r=L is given by

$$I(L,\lambda) = e^{-\int_0^L k(\lambda,T)dr}\left[\int_0^L k(\vec{r},T)I_b(\lambda,T)e^{-\int_0^r k(\lambda,T)dr'} dr + I_o(0,\lambda)\right] \qquad (3.1\text{-}4)$$

For the condition where the intensity of radiation at r=0 is zero, equation (3.1-4) takes the form

$$I(L,\lambda) = e^{-\int_0^L k(\lambda,T)dr}\left[\int_0^L k(\lambda,T)I_b(\lambda,T)e^{-\int_0^r k(\lambda,T)dr'} dr\right] \qquad (3.1\text{-}5)$$

At this point it is of interest to look at a special case of equation (3.1-4). If the path between r=0 and r=L is isothermal, then the integrals in equation (3.1-4) can be evaluated and the equation becomes

$$I(\lambda,L) = e^{-kL}I_o(0,\lambda) + (1-e^{-kL})I_b(T,\lambda) \qquad (3.1\text{-}6)$$

which may also be written as

$$I(\lambda,L) = \tau_\lambda I_o(0,\lambda) + (1-\tau_\lambda)I_b(T,\lambda) \qquad (3.1\text{-}6a)$$

where τ_λ is the transmittance of the gas at wavelength λ between r=o and r=L. This equation is essentially the one used in the emission - absorption temperature measurement technique in that τ_λ is measured along with $I(\lambda,L)$ with $I_o(0,\lambda) = 0$. The value of the Planck function, $I_b(T,\lambda)$ is found and may be inverted to find the temperature along the isothermal path.

As seen by equation (3.1-6a) the radiant intensity emerging from an isothermal radiating gas is described by a fairly simple equation. However, for the case of a non-isothermal layer of radiating gas the integrals in equation (3.1-4) or (3.1-5) cannot in general be evaluated in such a simple fashion since $k(T,\lambda)$ cannot be removed from under the integral. Thus in order to utilize equation (3.1-4) suitable approximations must be made.

The simplifications that will be utilized here were first suggested by Tourin and Krakow.[23,24] The simplification assumes that the non-isothermal path can be divided into n isolated isothermal regions such that in each isothermal zone equation (3.1-6a) is valid. To this approximation the emergent monochromatic radiation at position L is given by

$$I(\lambda,L) = I_0(0,\lambda)\Pi_i^n\tau_i(\lambda,T_i) + \sum_{i=1}^{n} I_b(\lambda,T_i)[1-\tau(\lambda,T_i)]\Pi_{j=i+1}^{n}\tau_j(\lambda,T_j) \qquad (3.1\text{-}7)$$

Thus, we see that if one can make measurements of $I(\lambda,L)$ at n wavelengths and if a priori knowledge is available for the transmittance then the n temperatures can be found from the solution of the set of n by n non linear algebraic equations (3.1-7).

In any real situation consideration must be given to the fact that the radiation measured with an optical instrument is never truly monochramatic. An optical instrument has a finite resolution of $\Delta\lambda$ and a measurement represents an average over this finite spectral region. Hence the equation above (3.1-7) must be integrated over the spectral region $\Delta\lambda$ with the weighting function $g(\lambda,\Delta\lambda)$. Where $g(\lambda,\Delta\lambda)$ is the instrument function and is a measure of the systems response at wavelength λ' when the instrument is set to detect photons of wavelength λ.[30,31] When this integration is performed the transmittance from O-L will not in general be of the form.

$$\tau_0^L(\lambda) = \Pi_{i=1}^{n}\tau_i(\lambda,T_i) \qquad (3.1\text{-}8)$$

Hence, equation (3.1-7) should be written as

$$I(\lambda,L)' = \int_{\Delta\lambda} I_0(0,\lambda)\Pi_i^n\tau_i(\lambda,T_i)g(\lambda,\Delta\lambda)d\lambda$$

$$+ \sum_{i=1}^{n} \int_{\Delta\lambda} I_b(\lambda,T_i)[1-\tau(\lambda,T_i)]\Pi_{j=i+1}^{n}\tau_j(\lambda,T_j)g(\lambda,\Delta\lambda)d\lambda \qquad (3.1\text{-}9)$$

where, $I(\lambda,L)'$ is the measured intensity

$$I(\lambda,L)' = \int_{\Delta\lambda} I(\lambda,L)' g(\lambda,\Delta\lambda)d\lambda \qquad (3.1\text{-}10)$$

Now, the Planck function does not vary very much over the spectral width $\Delta\lambda$. Likewise for $I_o(0,\lambda)$. Thus these quantities may be removed from the integral signs and equation (3.1-9) becomes

$$I(\lambda,L)' = I_o(0,\bar{\lambda}) \int_{\Delta\lambda} \Pi_i^n \tau_i(\lambda,T_i) g(\lambda,\Delta\lambda)d\lambda$$

$$+ \sum_{i=1}^{n} I_b(\bar{\lambda},T_i) \int_{\Delta\lambda} [1-\tau(\lambda,T_i)] \prod_{j=i+1}^{n} \tau_j(\lambda,T_j) g(\lambda,\Delta\lambda)d\lambda \qquad (3.1\text{-}11)$$

The equation above (3.1-11) is the fundamental equation in determining a temperature gradient. Methods for predicting the transmittances and instrument function will be dealt with in subsequent sections.

3.2 INFRARED SPECTRUM OF COMBUSTION PRODUCTS

As discussed in the previous section the multiple wavelength line of sight technique requires a priori information regarding the transmittance of the radiating species. A number of alternatives are at ones disposal. A seeding material active in the spectral region of interest and whose radiation properties are known such as sodium, may be added to the combustion gas. On the other hand one of the combustion products which is active in an accessible region of the spectrum can be utilized.

Since the combustion products contain infrared active species which are in equilibrium with the bulk gas and whose radiation property data is known it was decided to use this radiation as the diagnostic tool.

Of the many products of combustion the two which are extremely infrared active and whose radiation properties are known are water vapor and carbon dioxide. Both have been studied extensively over many temperature and pressure ranges as they are extremely important in predicting radiation from rocket exhaust plumes and in predicting the transmission through the atmosphere.

If we consider the infrared spectrum of high temperature combustion products (a typical spectrum is shown in figure 3-1) the radiation originates from the following sources [32,33]

1.7 - 2.3μ region

The region between 1.7 - 2.3μ consists mainly of radiation from the ν_1 and $\nu_3$combination band of water vapor. There is also a small amount of radiation from the combination bands of carbon dioxide but the contribution is negligible [32]

2.3 - 2.6 region

The radiation in this region originates only from the R branch of the ν_3 branch of water vapor.

2.6 - 3.4 region

The radiation in this region is fairly complex in that it has contributions from the ν_1 and ν_3 H_2O bands along with the $\nu_1+\nu_3$ and $2\nu_2+\nu_3$ combination bands of carbon dioxide [32]

4.1 - 4.8μ region

The radiation in this region of the spectrum originates from the ν_3 carbon dioxide band with a slight contribution from the fundamental band of carbon monoxide.

Table 3-1 lists the fundamental radiation properties of the combustion gas molecules.

Based on the availability of spectral information and the degree to which the concentration of the radiating species can be predicted it was decided to utilize portions of the 1.8_μ and 2.7_μ bands of water vapor.

3.3 RADIATION PROPERTIES OF WATER VAPOR

As was seen in section 3.1 a priori information regarding the transmission of water vapor is required in order to carry out the measurements. Since it was not feasible to make experimental measurements of the water vapor transmittance under conditions found in the engine and since theoretical predictions have been made for only a limited number of molecules [34,35] this study utilized semiempirical relations.

These empirical relations are refered to as narrow band models and describe a spectrum of overlapping lines in terms of single line parameters. A number of band models have been developed. The two most widely used being the Elsasser and the statistical band model.[35]

The Elsasser band model considers the spectrum to consist of lines of equal intensity and spacing. Hence, the Elsasser model finds its greatest application in describing the vibration - rotation spectrum of diatomic molecules[30,33,36,37]

A model which has met with success in describing the spectrum of more complex molecules such as water vapor is the statistical model [38-41] The statistical model was first proposed by Goody [42] and considers the spectrum to consist of randomly spaced lines of random intensity. In the general case the absorptance over a spectral region $\Delta\lambda$ is given by

$$d = 1- \exp(-\overline{W}ld) \qquad (3.3\text{-}1)$$

where $\overline{W}$ is the average equivalent width of a single line over the wavelength interval $\Delta\lambda$. The equivalent width of a single spectral line is given by

$$W= \int_{\Delta\lambda}(1-e^{-k_\lambda x})d\lambda \qquad (3.3\text{-}2)$$

For conditions found in the engine cylinder the primary form of broadening will be Lorentz broadening and the spectral absorption coefficient of a Lorentz line is given by [33]

$$k_\lambda = \frac{S}{\pi}\frac{b}{(\lambda - \lambda_0)^2 + b} \qquad (3.3\text{-}4)$$

where S is the integrated line stregth

$$S = \int_{\Delta\lambda} k_\lambda d\lambda \qquad (3.3\text{-}5)$$

and b is the half width of the line.

With the above expression for the equivalent width of a line the average equivalent width over the spectral region is given by

$$\overline{W} = \int_0^\infty W(s)P(s)ds \qquad (3.3\text{-}6)$$

where P(s)ds is the probability of a line in the spectral region having a line strength between S and S+dS.

Many distribution functions have been suggested and utilized. However, it can be shown that the difference in predicted absorption using these different probability functions is small[35] A distribution function which results in a useable expression is an exponential distribution of line strengths[42]

$$P(s) = \frac{1}{S_0} e^{-S/S_0} \qquad (3.3\text{-}7)$$

Now substituting equation (3.3-7) into (3.3-6) along with (3.3-2) and (3.3-4) the absorptance is given by

$$\alpha = 1 - \exp\left[- \frac{\beta X}{\sqrt{1 + 2X}} \right] \qquad (3.3\text{-}8)$$

where

$$\beta = \frac{2\pi b}{d} \quad \text{and} \quad X = \frac{S/dx}{2\pi\gamma} \qquad (3.3\text{-}9)$$

b = average line half width

d = average line spacing

s = average line strength

γ = average line width to line spacing ratio

x = optical density.

Thus we see that the absorption over a narrow band is given in terms of two parameters S/d and γ

The water vapor molecule has been studied extensively under a wide variety of conditions and the parameters S/d and γ are fairly well known. An extensive review and summary of S/d valves for water vapor bands was performed by Ferriso, Ludwig and Thomson [38] over a temperature range from 300 to 3000°K. Valves used in this work were taken from the study by Ferriso, et. al. and S/d valves for the wavelength intervals around 1.8μ,2.0μ, and 2.5μ were curve fit with a nonlinear regression analysis and are plotted in figure 3-2.[43] The spectral width of the narrow band is approximately 25cm^{-1}.

The parameter γ is dependent on two quantities. The first is the average line spacing d. The line spacing, d, has been found to be primarily a function of temperature for the water vapor, a least square fit to the available data being given by [44]

$$d(T) = \exp(-0.0016T+1.21) \tag{3.3-10}$$

The line width parameter b is dependent primarily on the number of collisions the water vapor molecule experiences per unit time. Consideration must also be given to the collision partner, as example, another water vapor molecule should be expected to be more effective than a molecule of another species. Hence the line width is given by an equation of the form

$$b(\lambda) = b_{H_2O}P_{H_2O} + b_iP_i \tag{3.3-11}$$

where i stands for a species other than water. Ferriso[38] also suggests that at elevated temperatures the effects of interaction between resonating and non-resonating water molecules should be taken into account.

Hence the line width parameter takes on the form

$$b = P_{H_2O}[b^{o}_{H_2O}\frac{T_o}{T} + b^{o'}_{H_2O}(\frac{T_o}{T})^{0.5}] + P_i b^{o}_{i}(\frac{T_o}{T})^{0.5} \qquad (3.3\text{-}12)$$

where $b^{o'}_{H_2O}$ is the width due to non-resonating dipole interactions of H_2O at T_o. It is also assumed that the line width parameter is independent of wavelength and that the foreign gas can be considered nitrogen. Rearranging equation (3-12)

$$b = b^{o}_{H_2O}P_T[\frac{T_o}{T}]^{0.5}[x_{H_2O}(\frac{T_o}{T})^{0.5} + \sigma') + (1-x_{H_2O})\sigma_{N_2}] \qquad (3.3\text{-}13$$

where

$$\sigma' = \frac{b'^{o}_{H_2O}}{b^{o}_{H_2O}} = 0.1 \quad \text{(assumed)}$$

$$\sigma_{N_2} = \frac{b^{o}_{N_2}}{b^{o}_{H_2O}} = 0.18 \text{ (reference 44)}$$

$$T_o = 273\ ^{o}K$$

Thus equations (3.3-8) to (3.3-12) along with the curve fit function for S/d may be utilized in computing absorptance of water vapor as a function of wavelength, total pressure, and temperature.

In order to determine the transmittance the amount of water vapor in the optical path must be known. Since the pressure and equivalence ratio are known a functional relationship between the water vapor concentration and temperature can be obtained from chemical equilibrium considerations. Both "in situ" and exhaust studies in engines have shown that some of the combustion product species such as NO, CO, and OH are not in chemical equilibrium.[14,45,46] Hence, one must be cautious of using chemical equilibrium to predict combustion product concentrations, especially of radical and minor species such as H, N, and O. Since water vapor is a major species in the combustion products with a mole fraction of 15% non-equilibrium effects should not alter its absolute magnitude significantly. Even if the water vapor was out of equilibrium by as much as 15,000 ppm (10%) the transmittance would only be altered by 2.5% (see Appendix II). Since it is unlikely that the water vapor is 15,000 ppm from its equilibrium value chemical equilibrium should provide a reliable prediction in the transmittance calculations.

Since the geometrical path length is 8.25 cm we may utilize the model to predict the absorption of water vapor at the wavelengths of interest (1.8μ, 2.0μ, 2.5μ) as a function of temperature and total pressure. Results of these calculations are shown in figures 3-3, 3-4, and 3-5. The accuracy of the predictions remains to be seen and comparisons of measured and predicted values will be given in chapter 5. One observation that may be made a priori is that the prediction at 2.0μ will probably be fairly good due to the low temperature dependence.

3.4 VIBRATIONAL RELAXATION OF WATER VAPOR

Since the spectroscopically determined temperatures are representative of the water vapor vibrational temperature question arises as to the vibrational equilibrium of water vapor during the engine processes. In looking at the energy mode equilibrium two factors must be taken into consideration: 1) are the vibrational modes within the water vapor molecule in equilibrium with respect to one another? and 2) are the vibrational modes in equilibrium with the translational degrees of freedom? In assessing these questions the characterisitc relaxation times will be compared to the characteristic time for processes occurring in the engine. Times characteristic of engine processes are of the order of 10^{-4} seconds.

Vibrational relaxation times for vibration - translation interactions of diatomic gases at the temperatures and pressures of the combustion gases is of the order of 10^{-6} seconds.[3,47-49] For the case at hand it is expected that the relaxation of water vapor is much shorter due to vibrational exchange within the molecule and due to heteromolecular exchange of vibrational energy.[49] Measurements by Huber and Kantrowitz[50] indicate water vapor relaxation times of 2×10^{-8} seconds at 1 atmosphere pressure and a temperature of 706°K. Since the relaxation time should decrease at the elevated pressures and temperatures encountered in the engine cylinder there should be ample time for the vibrational modes to equilibrate.

3.5 OPTICAL SYSTEM CALIBRATION

In order to make abolute intensity measurements it is necessary to evaluate the instrument function $g(\lambda,\Delta\lambda)$ or as will be shown the integral of the instrument function over the spectral region of interest $\Delta\lambda$.

The instrument function is effected by many factors in the experimental equipment. Incorporated in the instrument function are all reflectances of the mirrors, the tramsmittances of all windows, response of the infrared detectors, slit function of the spectrometer, angle factors, etc. Since the calibration is performed for each condition it is not necessary to enumerate each contribution to the instrument function and hence, we may describe the response of the system with one function $g(\lambda,\Delta\lambda)$.

Calibration is performed in the following manner: At the entrance to the optical system, which for this purpose is considered to be the outer side of the window mounted in the engine, (see figure 5-3) is radiation of intensity $I(\lambda)$. In passing through the optical system, which is set to detect radiation of wavelength λ, the detector sees a quantity of radiation $I_m(\lambda,\Delta\lambda)$due to the finite resolution of the instrument. These two quantities are related through the relation [30,31]

$$I_m(\lambda,\Delta\lambda) = \int_{\Delta\lambda} g(\lambda,\Delta\lambda)I(\lambda)d\lambda \qquad (3.5\text{-}1)$$

The detector converts the radiation to an electrical signal and ultimately a voltage V_m is measured. The voltage V_m is related to the measured intensity by

$$V_m = CI_m(\lambda,\Delta\lambda)$$

$$V_m = C\int_{\Delta\lambda} g(\lambda,\Delta\lambda)I(\lambda)d\lambda \qquad (3.5\text{-}2)$$

or if we incorporate the constant C and the function $g(\lambda,\Delta\lambda)$ into a new function

$$V_m = \int_{\Delta\lambda} g'(\lambda,\Delta\lambda)I(\lambda)d\lambda \qquad (3.5\text{-}3)$$

Now the instrument constant is determined in the following manner: A standard source of known intensity is located at the entrance to the optical system, this study utilized a standard tungsten ribbon lamp and a blackbody cavity. Since the intensity from the standard source does not vary much over the spectral region of interest its band center value may be used and the quantity I^o_{std} removed from the integral of equation (3.5-3)

$$V^o_m = I^o_{std}(\bar{\lambda}) \int_{\Delta\lambda} g'(\lambda,\Delta\lambda)d\lambda \qquad (3.5\text{-}4)$$

Therefore the integral of the instrument function over the spectral band $\Delta\lambda$ is given by

$$\int_{\Delta\lambda} g'(\lambda,\Delta\lambda)d\lambda = V^o_m/I^o_{std}(\bar{\lambda}) \qquad (3.5\text{-}5)$$

3.6 EXPERIMENTALLY MEASURED QUANTITIES

At this point it is of interest to further investigate the quantities that will be measured experimentally. Of particular interest is the weighting effect of the instrument function.

The experiment is performed in the following manner: Radiation from an external source is directed through a radiating and absorbing gas. Measurements are made of the unabsorbed signal $I_o(\lambda)$, the radiation from the gas, $Ig(\lambda)$ and the combined emission from the gas and the unabsorbed portion of the external signal $I_o(\lambda)$. Due to the finite spectral resolution these quantities are weighted by the instrument function $g(\lambda,\Delta\lambda)$. Thus, the measured quantities are related to the actual quantities

$$I_{om}(\lambda) = \int_{\Delta\lambda} g(\lambda,\Delta\lambda) I_o(\lambda) d\lambda \qquad (3.6\text{-}1)$$

$$I_{gm}(\lambda) = \int_{\Delta\lambda} g(\lambda,\Delta\lambda) I_g(\lambda) d\lambda \qquad (3.6\text{-}2)$$

$$I_{bm}(\lambda) = \int_{\Delta\lambda} g(\lambda,\Delta\lambda) I_b(\lambda) d\lambda$$

$$= \int_{\Delta\lambda} g(\lambda,\Delta\lambda)[I_g(\lambda) + \tau(\lambda) I_o(\lambda)] d\lambda \qquad (3.6\text{-}3)$$

and the measured transmittance is given by

$$\tau_m(\lambda) = \frac{I_{bm} - I_{gm}}{I_{om}} \qquad (3.6\text{-}4)$$

$$\tau_m(\lambda) = \frac{\int_{\Delta\lambda}[I_g(\lambda) + \tau(\lambda)I_o(\lambda)]g(\lambda,\Delta\lambda)d\lambda - \int_{\Delta\lambda} I_g(\lambda)g(\lambda,\Delta\lambda)d\lambda}{\int_{\Delta\lambda} I_o(\lambda)g(\lambda,\Delta\lambda)d\lambda}$$

$$= \frac{\int_{\Delta\lambda}\tau(\lambda)I_o(\lambda)g(\lambda,\Delta\lambda)d\lambda}{\int_{\Delta\lambda} I_o(\lambda)g(\lambda,\Delta\lambda)d\lambda} \qquad (3.6\text{-}5)$$

Now the intensity of the external light source $I_o(\lambda)$ is essentially constant over the narrow spectral region of interest and may be removed from the integral sign. The relation between the measured and actual transmittance is then given by

$$\tau_m(\lambda) = \frac{\int_{\Delta\lambda}\tau(\lambda)g(\lambda,\Delta\lambda)d\lambda}{\int_{\Delta\lambda} g(\lambda,\Delta\lambda)d\lambda} \qquad (3.6\text{-}6)$$

A couple of observations can be made with respect to the measured and actual transmittance and equation (3.6-6). Taking a closer look at the instrument function $g(\lambda,\Delta\lambda)$ we see that it is essentially a product of two terms. The first term would include factors such as the window transmittances, mirror reflectances, detector response and is essentially a slowly varying function of wavelength. The second factor would primarily be a function of the spectral resolution $\Delta\lambda$ and effected mainly by the spectrometer slit width. Thus, the difference between the measured and actual transmittance is almost entirely dependent on the spectral bandpass $\Delta\lambda$.

A question which arises is which of the transmittances in equation (3.6-6) does the statistical band model predict? Since the statistical band model is a semi-empirical model with experimental data used to obtain the parameters it essentially predicts the measured transmittance. $\tau_m(\lambda)$. Hence in the conduct of the experiment a spectral bandpass of $25 cm^{-1}$ was used corresponding to that employed by Ferriso et. al. [38] in obtaining the band model parameters.

Also, as was shown in section 3.5 what is measured is not the intensity but a voltage output from the detector. Where the two are related by a constant valve. So the measurements which are made can be summarized as follows:

$$V_{om} = \int_{\Delta\lambda} g'(\lambda,\Delta\lambda) I_o(\lambda) d\lambda \qquad (3.6\text{-}7)$$

$$V_{gm} = \int_{\Delta\lambda} g'(\lambda,\Delta\lambda) I_g(\lambda) d\lambda \qquad (3.6\text{-}8)$$

$$V_{bm} = \int_{\Delta\lambda} g'(\lambda,\Delta\lambda)[I_g(\lambda) + \tau(\lambda) I_o(\lambda)] d\lambda \qquad (3.6\text{-}9)$$

$$\tau_m = \frac{\int_{\Delta\lambda} g'(\lambda,\Delta\lambda)\tau(\lambda)d\lambda}{\int_{\Delta\lambda} g'(\lambda,\Delta\lambda)d\lambda} = \frac{V_{bm} - V_{gm}}{V_{om}} \qquad (3.6\text{-}10)$$

Equation (3.6-8) may be expressed in a different form by noting that

$$I_g(\lambda) = \epsilon_\lambda I_b(\lambda, T_g) \qquad (3.6\text{-}11)$$

and since the gas is not-reflective and in equilibrium.

$$I_g(\lambda) = (1-\tau_\lambda) I_b(\lambda, T) \qquad (3.6\text{-}12)$$

Hence the right hand side of equation 3.6-8 may be expressed as:

$$\int_{\Delta\lambda} g'(\lambda,\Delta\lambda) I_g(\lambda) d\lambda = \int_{\Delta\lambda} g'(\lambda,\Delta\lambda)(1-\tau(\lambda)) I_b(\lambda,T) d\lambda$$

Since the Planck function is essentially constant over the spectral bandpass its band center value may be used

$$V_{gm} = I_b(\bar{\lambda},T)[\int_{\Delta\lambda} g'(\lambda,\Delta\lambda) d\lambda - \int_{\Delta\lambda} g'(\lambda,\Delta\lambda)\tau(\lambda) d\lambda] \qquad (3.6\text{-}13)$$

If we define

$$G' \equiv \int_{\Delta\lambda} g'(\lambda,\Delta\lambda) d\lambda \qquad . \ (3.6\text{-}14)$$

then equation (3.6-13) may be rearranged to give

$$I_b(\bar{\lambda},T) = \frac{V_{gm}/G'}{1-\tau_m(\lambda)} \qquad (3.6\text{-}15)$$

where the Planck function in equation (3.6-15) may be inverted in order to determine the temperature along an isothermal path.

The specific equations used in the reduction of experimental data will be summarized in chapter 5 after the experimental procedure is presented.

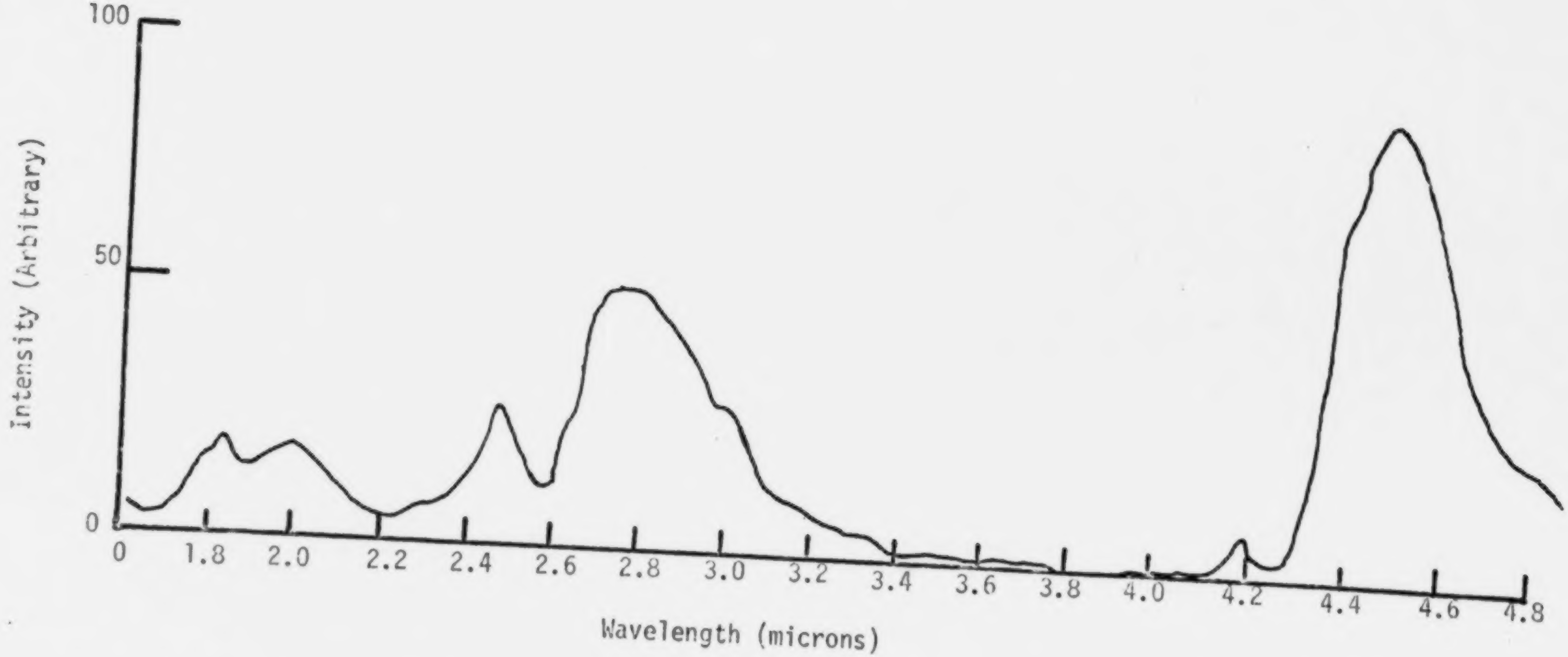

Figure 3-1

INFRARED SPECTRUM OF HOT
HYDROCARBON COMBUSTION PRODUCTS

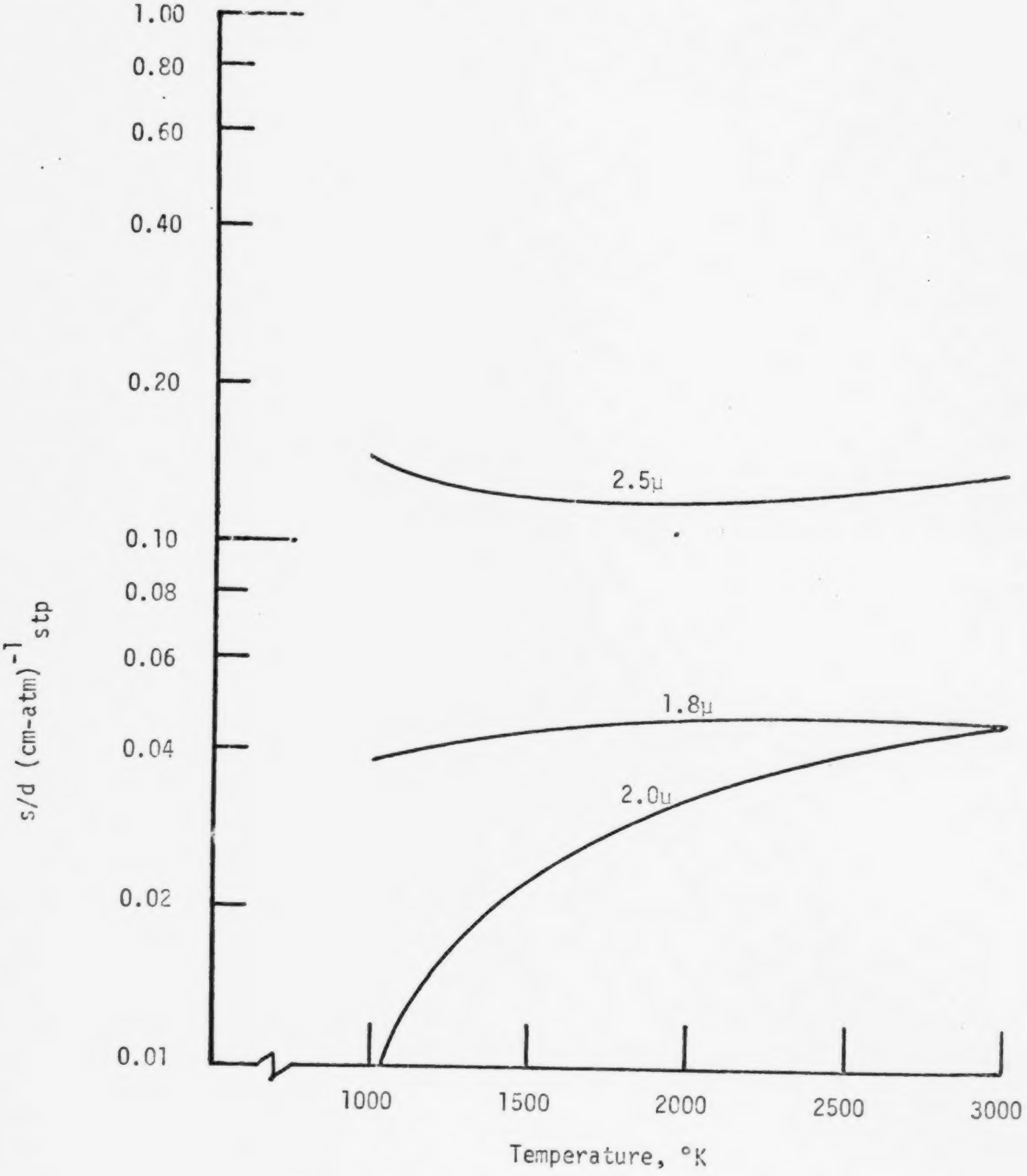

Figure 3-2

s/d VALUES FOR SELECTED
WATER VAPOR SPECTRAL REGIONS

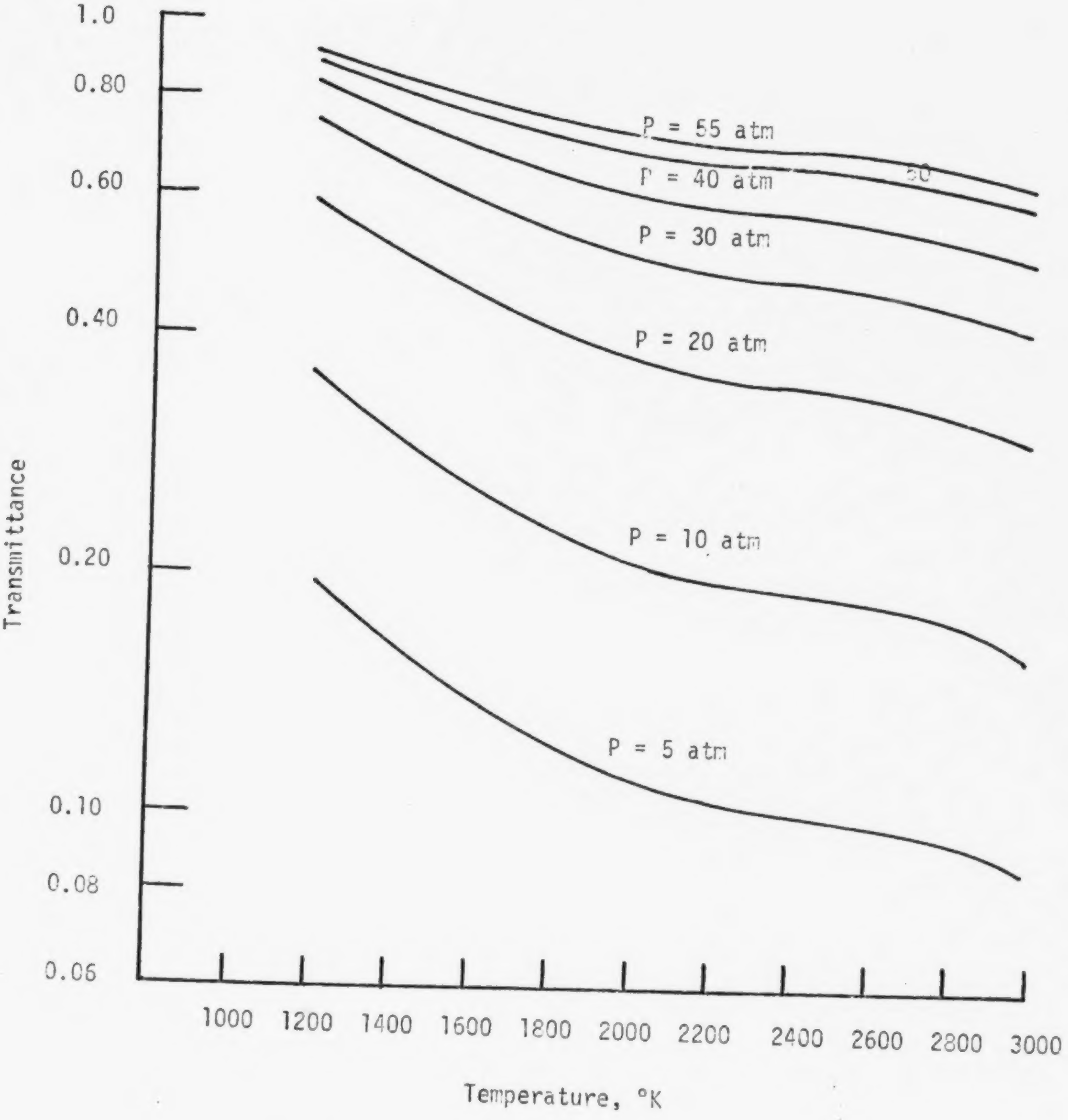

Figure 3-3

TRANSMITTANCE OF WATER VAPOR IN THE
COMBUSTION PRODUCTS AT 2.5 MICRONS
ϕ=1.0

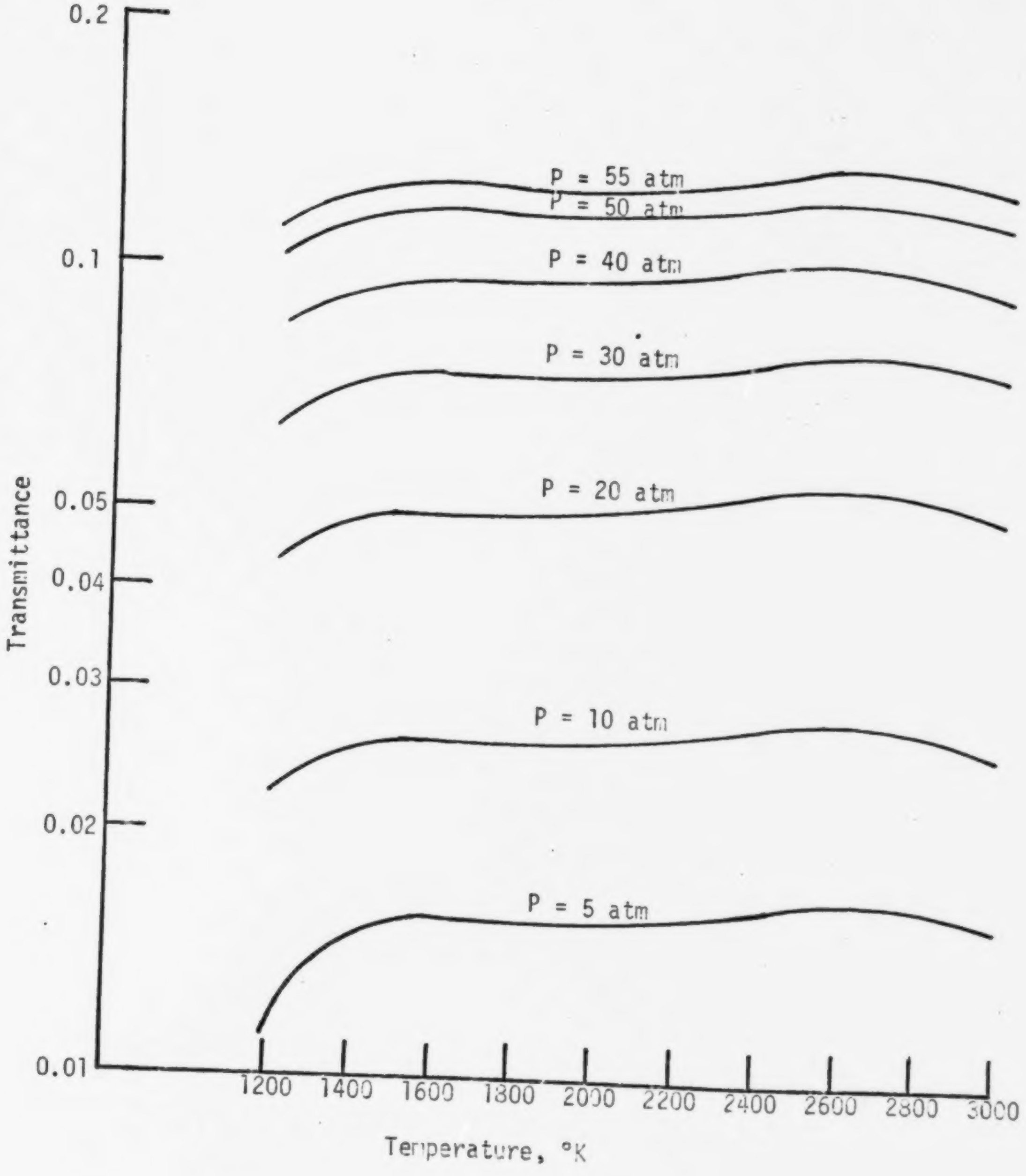

Figure 3-4

TRANSMITTANCE OF WATER VAPOR IN THE COMBUSTION PRODUCTS AT 2.0 MICRONS

$\phi=1.0$

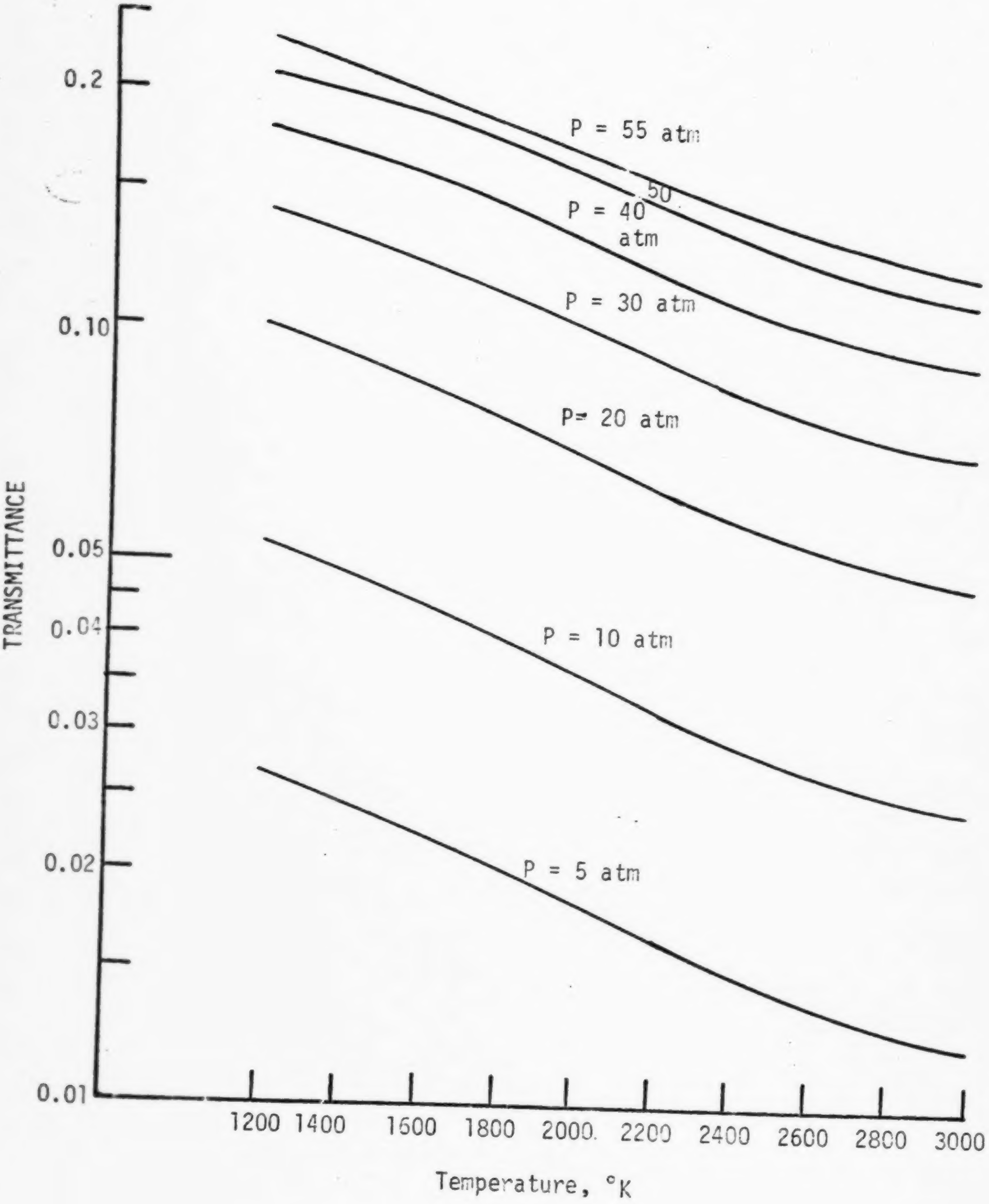

Figure 3-5

TRANSMITTANCE OF WATER VAPOR IN THE COMBUSTION PRODUCTS AT 1.8 MICRONS

$\phi=1.0$

CHAPTER IV

EXPERIMENTAL PROCEDURE AND APPARATUS

4.0 Overall Experiment

In order to accomplish the line of sight temperature measurements a single cylinder CFR engine[56] with appropriately mounted windows was utilized along with a polychromator and a modulated light source. A photograph of the system is shown in Figure 4-1 and a schematic in figure 4-2.

Hence, when the chopper was in front of the light source the detectors would only receive radiation emitted by the combustion gases in the cylinder of the engine. When the modulator was in the out position the detectors would receive the radiation from the combustion gases plus the fraction of the energy from the light source which was not absorbed by combustion gases. From this data it was possible to determine the intensity of emission and the transmittance of the gas at each of the monitored wavelengths. The cylinder pressure and crankshaft angle histories were also monitored along with the radiation data. Figure 4-3 shows a tracing of a typical oscilloscope picture.

4.1 Experimental Apparatus

4.1-1 Engine and Instrumentation

The engine used in this study was a single cylinder variable compression ratio CFR engine with a 3.25 inch bore and 4-1/2 in. stroke. The cylinder head had been modified to accommodate the optical windows and allow flexible location of spark plugs with respect to the optical axis. A Sprague electric dynamometer wasused to absorb the power developed by the engine.

In order to minimize the possibility of spatial non uniformity in the engine cylinder due to a non-uniform air-fuel mixture the engine was run on a premixed propane air mixture. Air was taken from the room and metered with a Meriam Laminar Flow Element model 50-MH10-2. The air meter was calibrated in the laboratory with a standard wet test meter.

The fuel was chemically pure grade propane obtained from the Matheson Company. Propane vapor was drawn from the bottle and metered with a Matheson #604 rotometer (see appendix VI for calibration). The propane vapor was injected into the airstream upstrean of a baffled mixing chamber. A photograph of the engine and propane mixing chamber is shown in Figure 4-4. The mixture was checked for uniformity by taking samples at various radial locations at the sampling port downstream of the mixing chamber. No distinguishable differences were found in the mixture ratio. Figure 4-5 shows the fuel system.

The crankshaft angle was monitored by displaying pulses from a magnetic pickup, which detected the presence of steel slugs located at 90^o intervals, on the oscilloscope.

The cylinder pressure was measured with a Kistler #621 piezoelectric device mounted in the cylinder wall. The output of the pressure transducer was amplified with a Kistler S/N/455 charge amplifier before the signal was input to the oscilloscope.

Engine speed was determined with a tachometer and from another magnetic pickup on the crankshaft. The pulse from this magnetic pickup was fed into a Hewlett Packard model 605A electronic counter.

4.1-2 Optical System

The main part of the optical system was a McPherson model 216.5 half meter grating spectrometer. The instrument contains Czery-Turner[57,58] type optics and is able to accommodate multiple exit slits. Modification to the detector section of the instrument was made in order to accept multiple cryogenically cooled infrared detectors. The original grating was replaced with a 150 line/mm grating blazed at 2μ in order to extend the spectral range of the instrument out to 8μ. Pertinent information concerning the instrument with the 150 line/mm grating is given in table 4-1. The modification to the detector section consisted of mounting plane mirrors on the photomultiplier rack to divert the radiation to the detectors which are held in a redesigned top. The modifications are shown in Figure 4-6.

The part of the optical system from the window in the cylinder up to and including the condensing optics (Figure 4-2) is basically the same as that described in reference (9,46). The radiation is contained in a half angle of 1 degree and hence the radiation field may be considered one dimensional.

The wavelengths of interest were selected by machining slits in bronze strips and mounting the strip across the exit slit. Correct location of the slits was checked by noting the known atmospheric absorption of water vapor and through the use of a mercury vapor lamp.

One of the characteristics of a grating spectrometer which inhibits its use in the infrared spectrum is the interference from higher orders. Hence, when the instrument is set to detect 2.0 micron radiation, 1.0 micron, 0.5 micron, etc. radiation is also passing through the exit slit. In order to exclude this interference in the 1.8μ to 2.5μ region used in this study a Corning #7-86 filter was mounted at the entrance slit to the polychromator. The spectral transmission of the filter is shown in Figure 4-7.

The light source used in the absorption work was an Oriel Coropration model 976-01 1000 watt xenon arc lamp. The lamp radiates an intense ultraviolet continuum and a sufficiently intense continuum of radiation in the infrared region of interest in this work.

Sufficient strength and transmission were obtained from General Electric type 102 discs which were utilized as engine cylinder windows. The front window was 11/4" in diameter and 3/8"thick while the rear window was 3/4" diameter and 1/4" thick. The spectral transmission characteristics of the quartz windows are shown in Figure 4-8.

In selecting the detectors to be used in this study the prime considerations were response time and sensitivity. The detectors that were selected were Philco-Ford model ISC-363 indium-antimonide photovoltaic detectors. The detectors are mounted in end-looking dewars and operate at liquid nitrogen temperature (77°K). The physical configuration along with the spectral characteristics are shown in Figure 4-9. The time response of the detectors is less than 1 microsecond which is on the order of two orders of magnitude faster than the characteristic time for events in the engine cylinder.

The output signals from the detectors were amplified with techronixs model 122 low level preamplifiers (2) and a Kiethley model 102B decade isolation amplifier. The amplified signals from the detectors along with the signal from the pressure transducer and crank angle indicator were displayed on a techtronixs model 565 dual beam oscilloscope. Utilized in the oscilloscope was a two channel # 3A72 and a four channel #3A74 plug in. The oscilloscope sweep was triggered by a wire wrapped around the spark plug wire so that the start of the sweep was coincident with the ignition of the propane air mixture.

The polychromator was calibrated with a standard General Electric 30/T24/17 tungsten ribbon lamp whose intensity characteristics are shown in Figure 4-10.[59] In conjunction with the tungsten ribbon lamp a standard water cooled blackbody cavity was utilized for calibration purposes.

The optical system was flushed with nitrogen to eliminate absorption by the CO_2 and H_2O in the ambient air.

4.2 Experimental Procedure

Since absolute intensities were being measured it was necessary to exercise extreme caution with regard to the cleanliness of the windows in the engine cylinder. Hence, the following procedure was followed in collecting data. First, the engine was warmed up without the windows mounted.

After warm-up the engine was shut down and the windows inserted. The transmission of the windows was then measured. The engine was then restarted and when stability at the desired operating conditions was attained data were obtained by taking a Polaroid picture of a single oscilloscope sweep. Upon completion of the data collection the engine was shut down and the transmission of the windows was measured again. If any change in the window transmission occured between the beginning and end of the run the data were discarded and the procedure repeated.

The engine operating conditions along with the data reduction and results are presented in the following chapter.

Table 4-1

Polychromator Data

Parameter	Value
Grating	150 line/mm
Blaze	2μ
Wavelength range	1050A°-8μ
Dispersion	133.3 A°/mm
First Order Resolution	3.2A
Focal Plane Span	1.36μ
Optics	f8.7

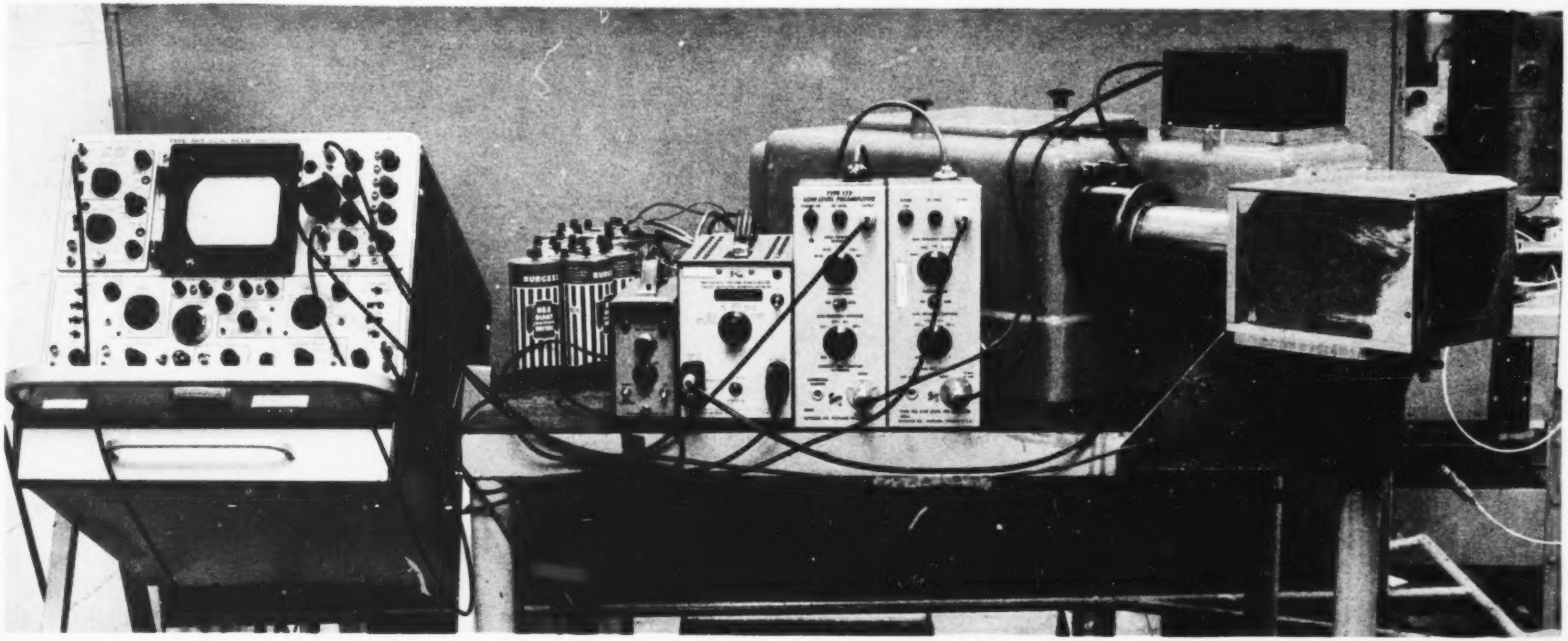

Figure 4-1

PHOTOGRAPH OF OPTICAL SYSTEM
AND INSTRUMENTATION

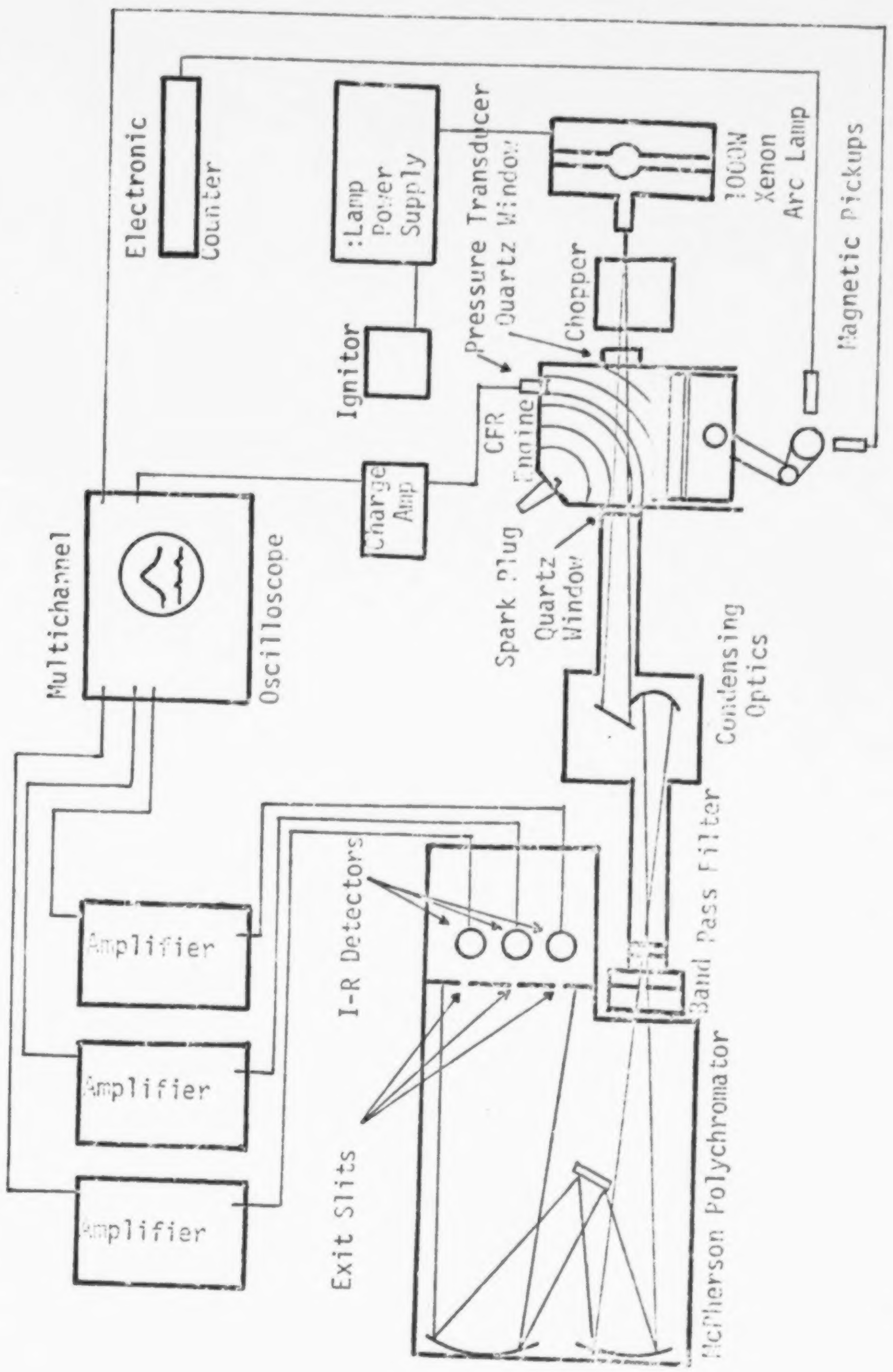
Electronic Counter
Lamp Power Supply
Pressure Transducer
Quartz Window
1000W Xenon Arc Lamp
Chopper
Magnetic Pickups
Ignitor
CFR Engine
Charge Amp
Spark Plug
Quartz Window
Multichannel Oscilloscope
Condensing Optics
Band Pass Filter
I-R Detectors
Amplifier
Amplifier
Amplifier
Exit Slits
McPherson Polychromator

Figure 4-2

SCHEMATIC OF EXPERIMENTAL APPARATUS

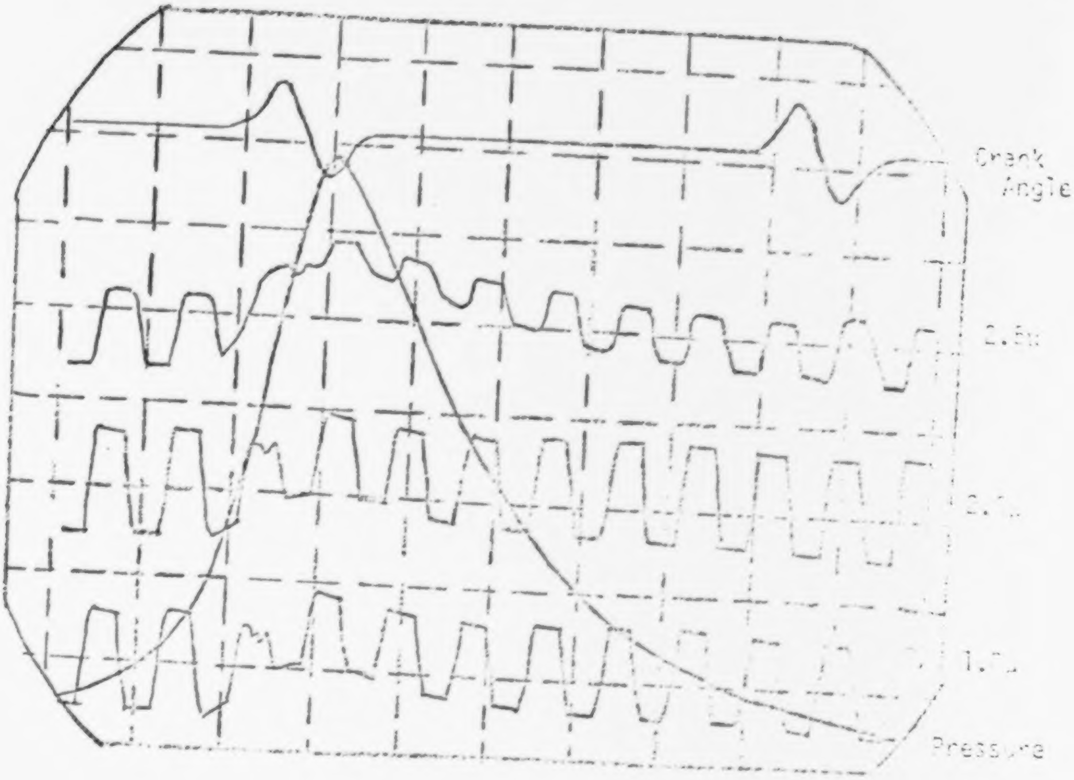

Figure 4-3

TRACING OF AN OSCILLOSCOPE PICTURE

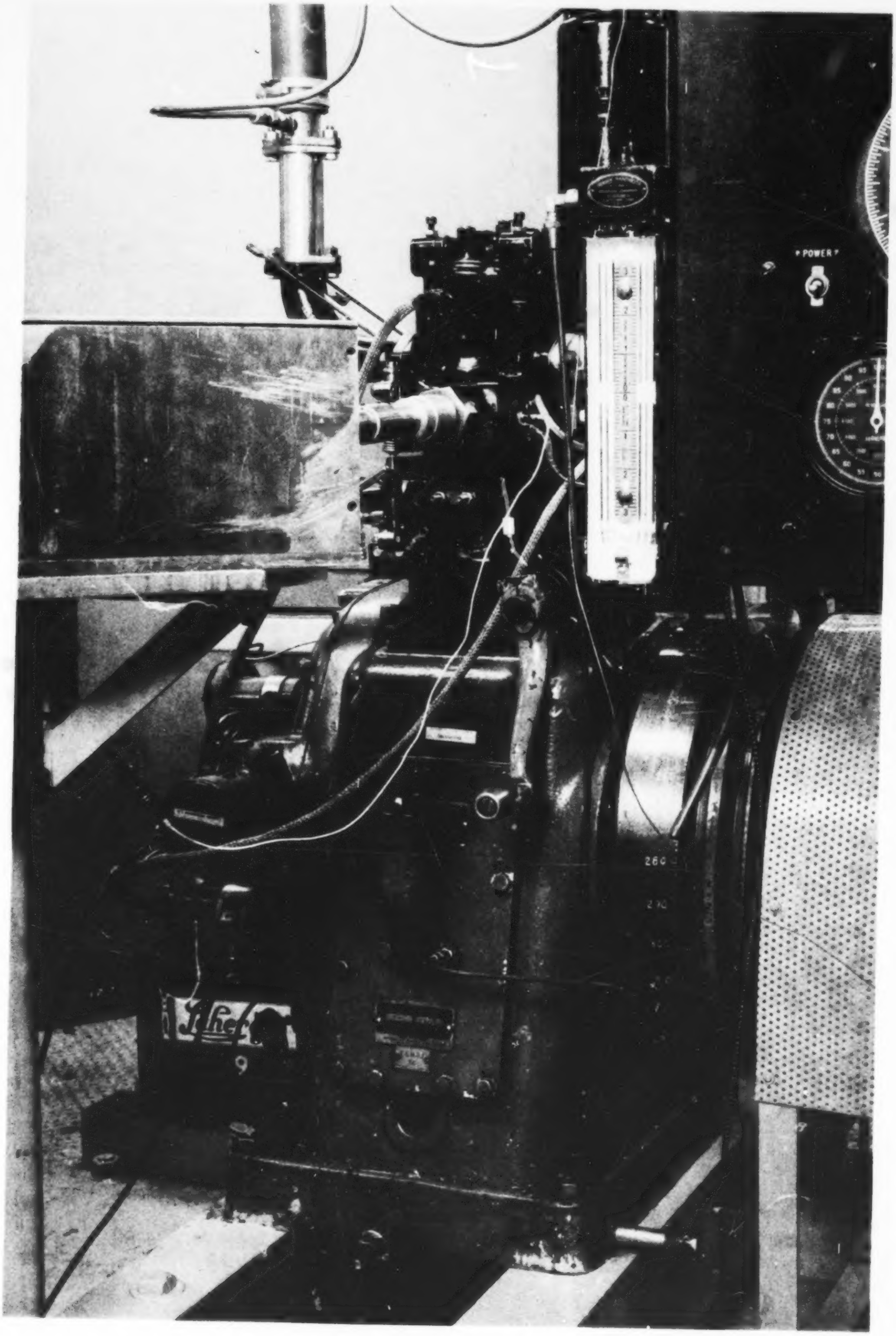

Figure 4-4

PHOTOGRAPH OF ENGINE AND
PROPANE SYSTEM

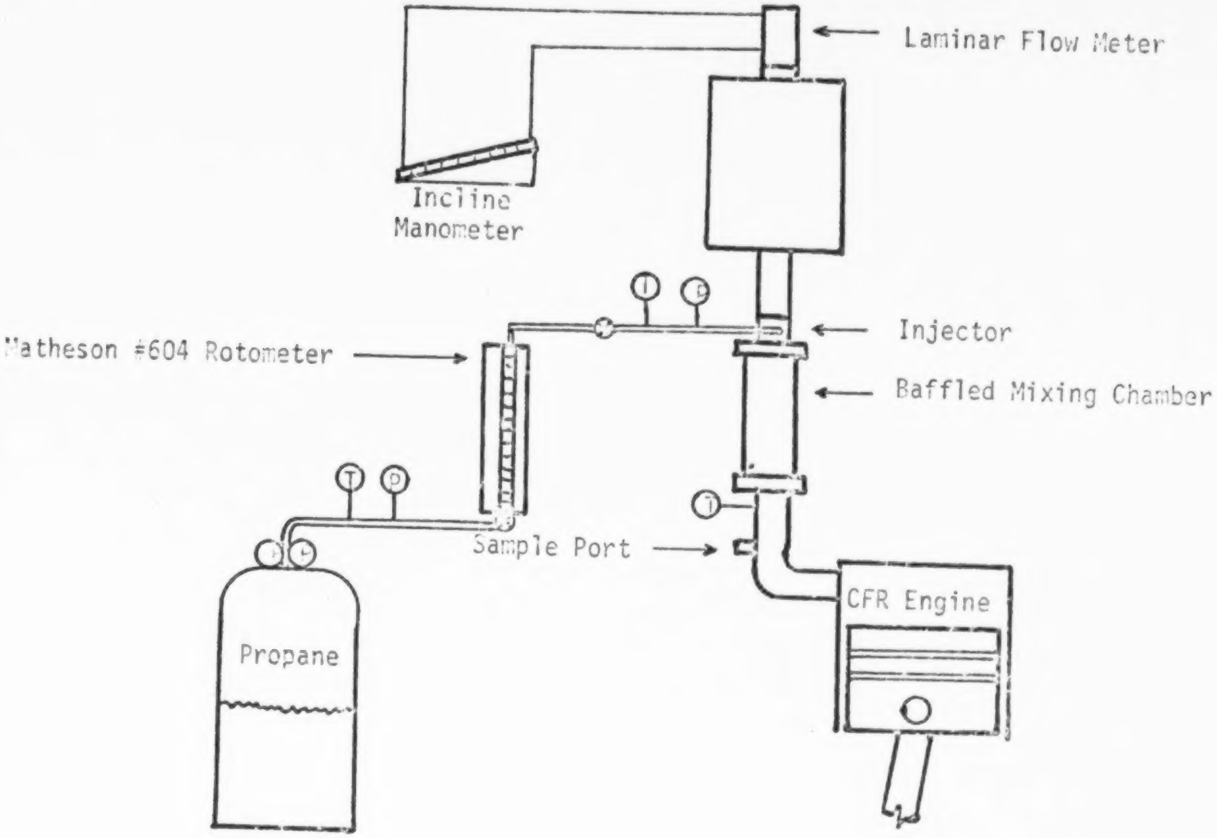
Laminar Flow Meter
Incline Manometer
Injector
Matheson #604 Rotometer
Baffled Mixing Chamber
T
P
T
P
T
Sample Port
CFR Engine
Propane

Figure 4-5

SCHEMATIC OF PROPANE-AIR SYSTEM

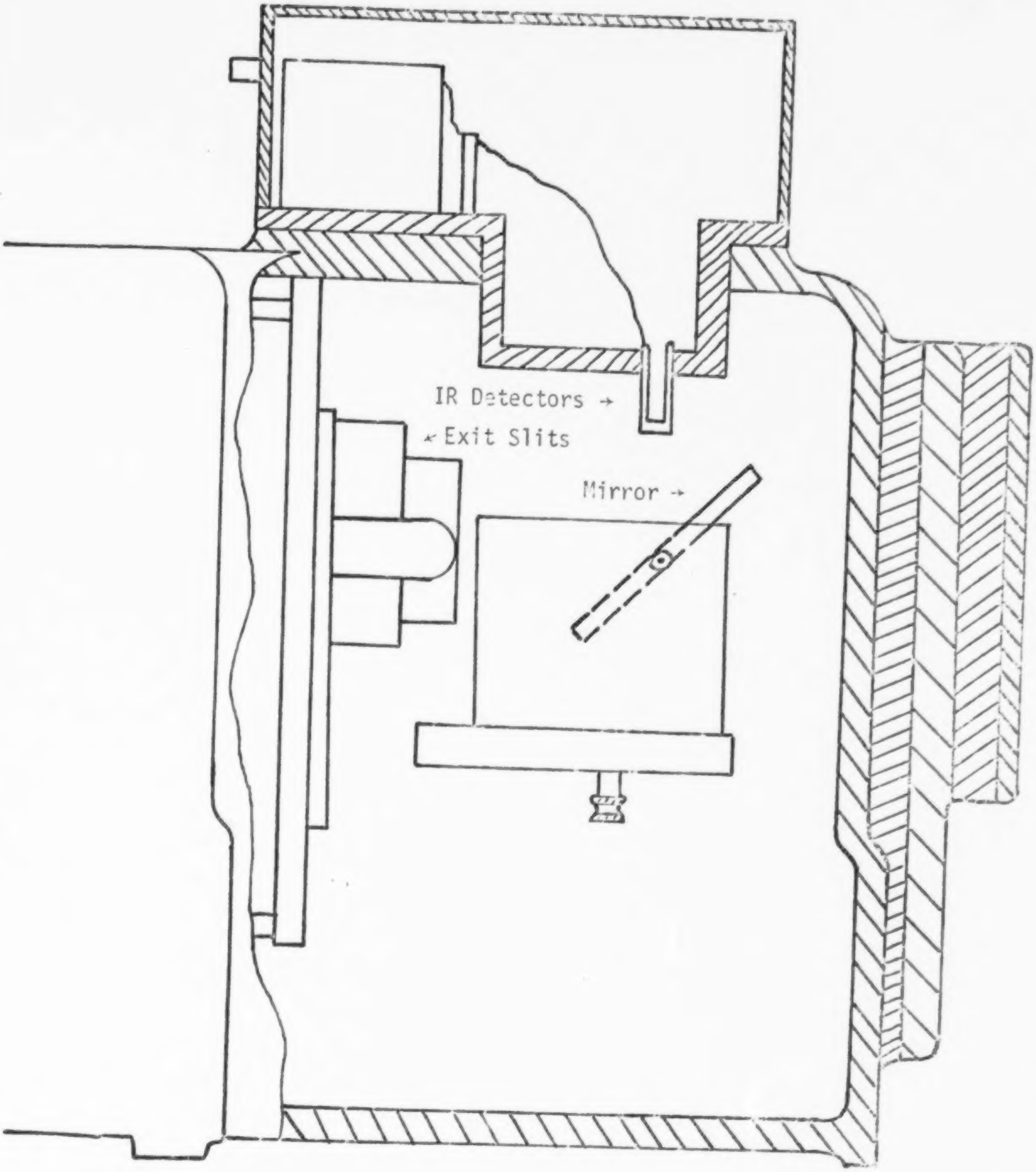
IR Detectors →
← Exit Slits
Mirror →

Figure 4-6

MODIFIED DETECTOR SECTION OF THE POLYCHROMATOR

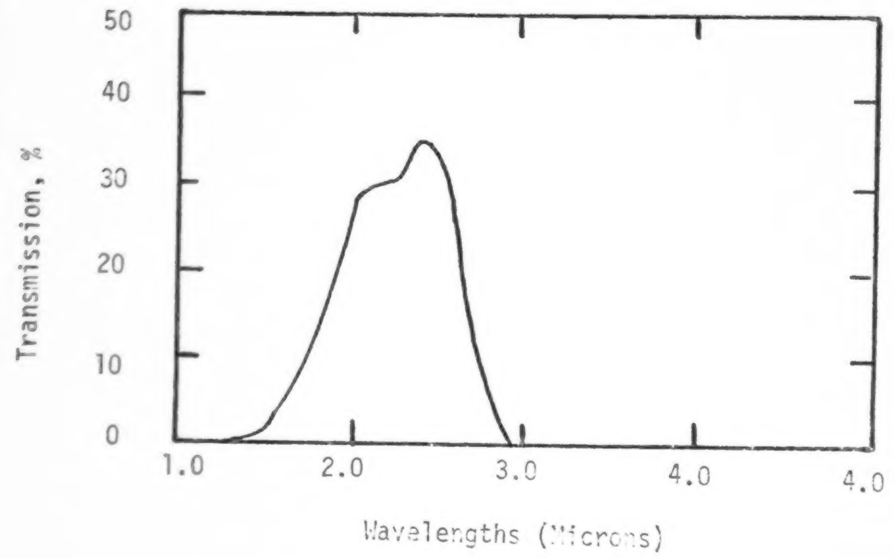

Figure 4-7

TRANSMISSION OF CORNING #7-86
BAND PASS FILTER

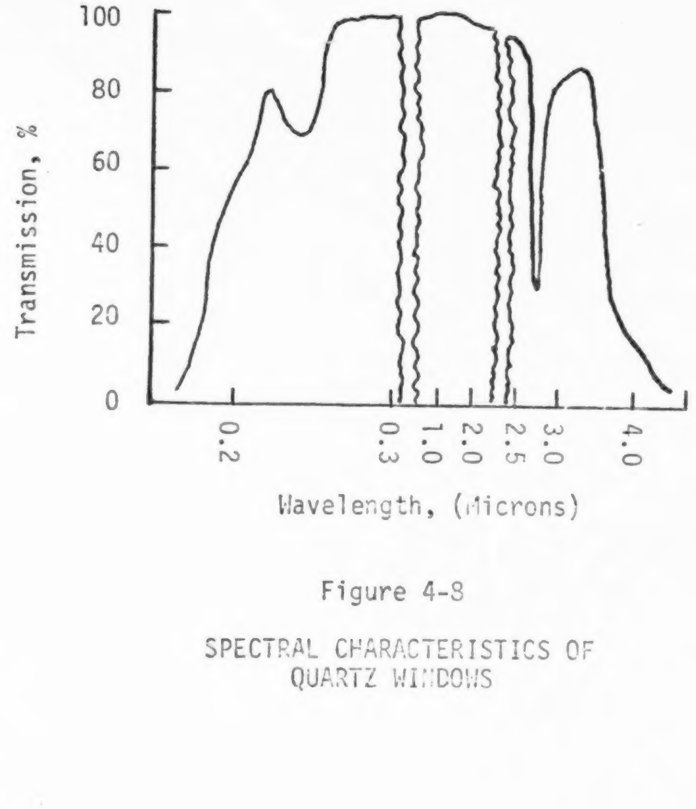

Figure 4-8

SPECTRAL CHARACTERISTICS OF
QUARTZ WINDOWS

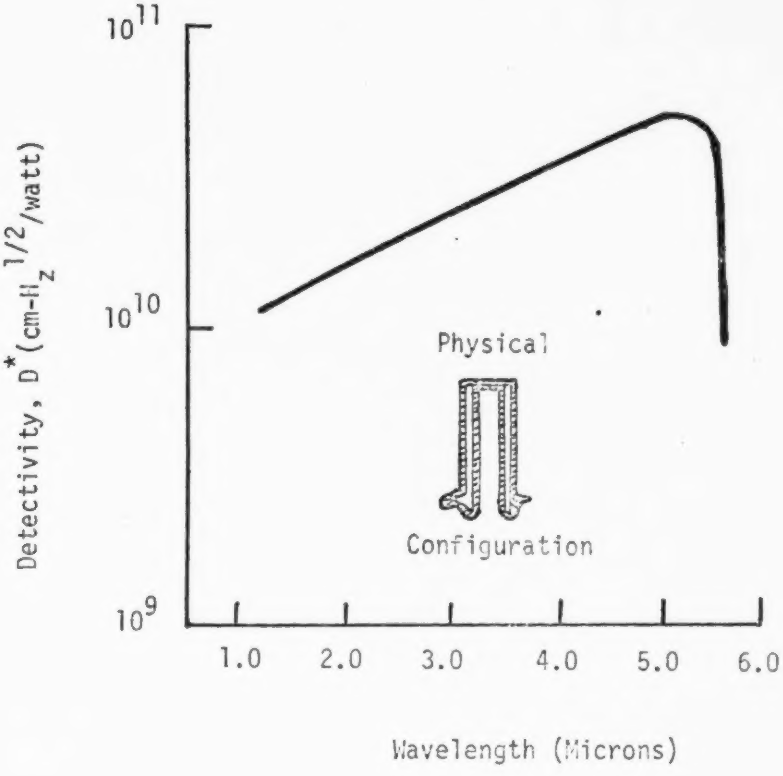

Figure 4-9

SPECTRAL CHARACTERISTICS OF
THE IR-DETECTORS

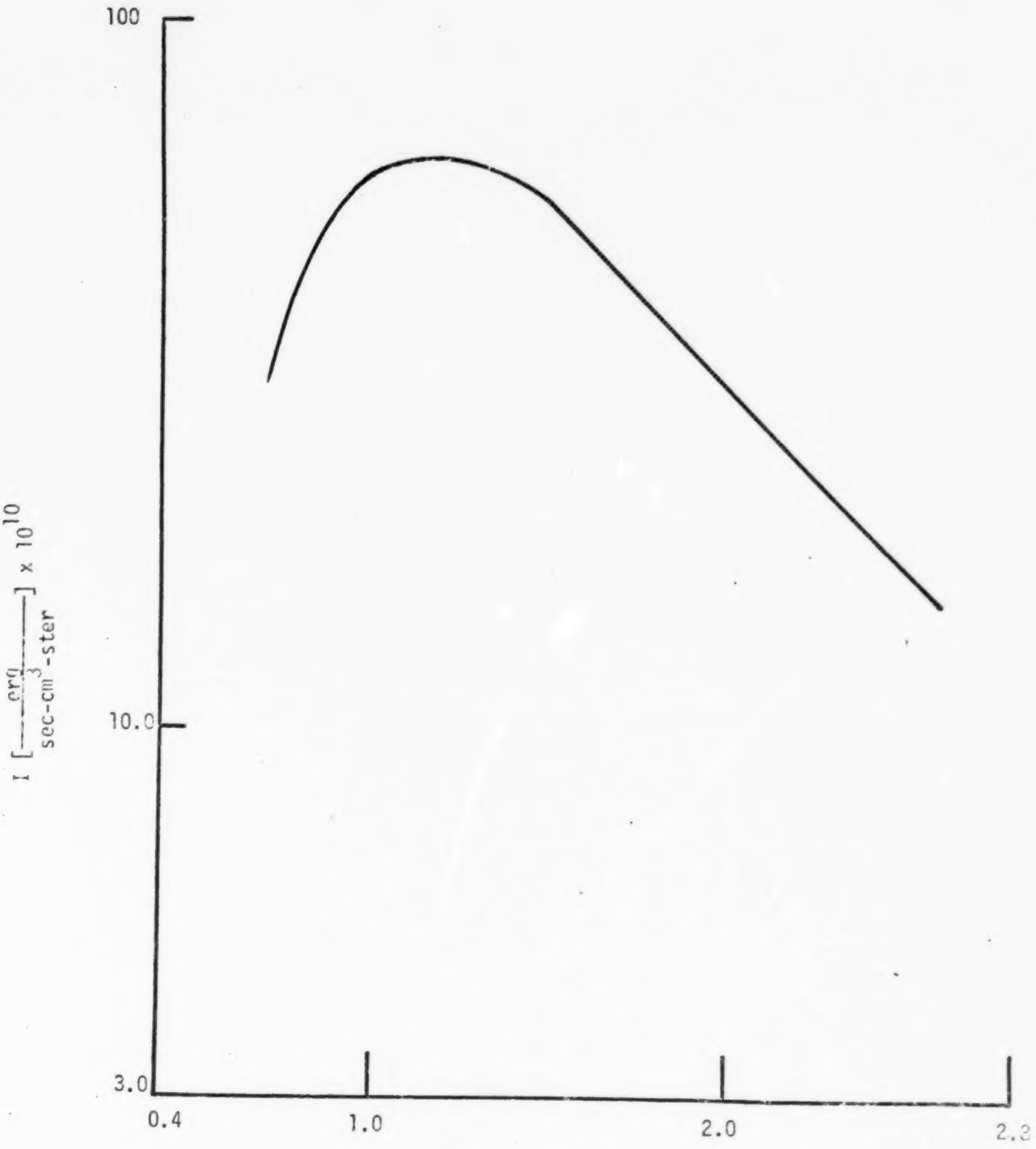

Figure 4-10

INTENSITY OF RADIANCE STANDARD

CHAPTER V

5.0 Scope of Experimental Work

In the course of the experimental work essentially three tasks were undertaken. The first effort entailed the utilization of the emission absorption technique in order to measure the temperature of the combustion products during the expansion process. In order to offer a comparison simultaneous measurements were made with the polychromator described in Chapter 4, of wavelength in two water vapor bands.

To further explore the applicability of optical methods of analysis to high pressure combustion systems the absorbtivities of water vapor were measured at three different wavelengths. The measured absorptivities are then compared to values predicted from the statistical band model developed in section 3-3.

The final experimental effort entailed employment of the line of sight multiple wavelength technique developed in Chapter 3 to determine the temperature gradient along the axis of flame propagation.

The main purpose of the experimental work was to take a closer look at the applicability of optical analysis of high pressure and high temperature system, particularly, with respect to the measurement of temperatures, temperature gradients, and the prediction of optical properties from theoretical considerations. In this context the experiments were performed with the engine variables held at one setting. Pertinent engine data and engine variable settings are given in table 5-1.

5.1 Emission Absorption Temperature Measurements

In order to perform the emission absorption temperature measurements the engine was operated with a dual ignition system with the spark plugs diametrically opposite the optical axis (see Figure 5-1). This was necessary to create a uniform slab of gas across the optical path. Simultaneous emission and absorption measurements were made at 1.8, 2.0, and 2.5 micron. After the integral of the instrument function $G(\lambda)$ is determined at each of the wavelengths of interest equation 3.6-15 may be rearranged to yield an expression for the optically determined temperature in terms of the experimentally measured quantities $V_{om}(\lambda)$, $V_{bm}(\lambda)$, $V_{gm}(\lambda)$, $G(\lambda)$ where

$V_{om}(\lambda)$ = voltage deflection due to the unabsorbed external light source

$V_{gm}(\lambda)$ = voltage deflection due to the emission from the combustion gas

$V_{bm}(\lambda)$ = voltage deflection due to the combustion gas plus the absorbed external source.

$$T = (hc/\lambda k)\left[\ \ln\left\{\frac{2hc^2 G(\lambda)(V_{om}(\lambda) + V_{gm}(\lambda) - V_{bm}(\lambda)}{\lambda^5 V_{gm}(\lambda) V_{om}(\lambda)} + 1\right\}\right]^{-1} \qquad (5.1\text{-}1)$$

Figures (5-3) to (5-6) show results obtained for single expansion strokes. Along with the optically determined temperatures is plotted the bulk temperature. The bulk temperature is a fictitious quantity in that it is a mass average temperature inferred from the instantaneous cylinder pressure, cylinder volume and mass of combustion gas. Since the ideal gas law is applicable to the combustion gases at the temperature and pressures of interest, the bulk temperature is obtained from

$$PV = mRT_b/\overline{MW} \tag{5.1-2}$$

The details of obtaining the mass of charge and molecular weight are given in Appendix I.

The engine cycles which are shown in Figures (5.3) - (5.6) were randomly selected from a series of approximately 100 engine cycles for the same engine conditions. In all cases the scatter observed from cycle to cycle and among the wavelengths is typified in Figures (5.3) - (5.6). Although the scatter in data is significant a couple of observations can be made. Figures (5.3) - (5.6) demonstrate that the spectroscopic temperatures obtained from the infrared radiation of water vapor are within 100°K of the ideal gas temperature.

In terms of the scatter of data between the wavelengths the measurements with the highest level of confidence are those made at 2.5μ and as can be seen exhibit the least scatter. This is due in part to the higher absorbtivity at 2.5μ which means a measurement with a higher degree of confidence. The average standard deviation of the measurements presented were evaluated from[60]

$$\sigma = \frac{\sum_{i=1}^{N} (x_i - \overline{x})^2}{N - 1}$$

and exhibit values of

$$\sigma_{2.5} = 24 \text{ °K}$$

$$\sigma_{2.0} = 75 \text{ °K}$$

$$\sigma_{1.8} = 134 \text{ °K}$$

Looking at the results of the analytical model and the spark plug configuration employed in these measurements one might conclude that the optically determined temperatures should be lower than the ideal gas temperature. This results from the fact that the optical path traverses the coolest section predicted from the non-uniform model. One factor that has not been discussed is the quench layer near the cylinder wall.

Since the ideal gas temperature is a mass average temperature the cool quench layer will tend to weight the experimentally measured value below the mass average value in the bulk gases away from the cylinder wall. An estimate of this can be made in the following manner. Daniel has measured quench zone thicknesses in a propane fueled engine[61] and showed that the correlation proposed by Friedman and Johnston could be used to predict quench zone distances. This correlation takes the form

$$q_D = 0.0035\ (1/P)^{0.91}\ (535/T)^{0.5}$$

for stoichiometric and rich mixtures. In the above expression the terms have the following meaning

q_D = quench zone distance, inch

p = pressure, atm.

T = temperature in the quench zone, °R

If the assumption is made that the quench zone temperature is on the order of the coolant temperature, then for typical conditions in the post flame gas approximately 2% of the mass is contained in the quench layer near the combustion chamber walls and piston surface. This has the effect of lowering the calculated mass average or bulk temperature of the gases not in the quench by approximately 50°K. Thus, the fact that the spectroscopic temperature and the bulk temperature are the same is not inconceivable. Since this quench layer also exists near the optical windows, question arises as to its effect on the spectroscopic measurements. At the wavelengths used, this quench zone is virtually transparent and makes a negligible contribution to the radiation.

5.2 Absorptivities of Water Vapor

Since Newhall used infrared spectroscopy to determine nitric oxide levels in an engine cylinder it has been of interest to check ones ability to predict absorptivities of radiating species. Since the water vapor concentration is not highly dependent on temperature and can, to a high degree of accuracy be predicted from chemical equilibrium considerations, it is of interest to compare the measured absorptivities with those predicted by the statistical band model.

Typical comparisons are shown in Figures (5.7), (5.8), and (5.9) for wavelengths of 1.8, 2.0, and 2.5 microns respectively. Each figure represents comparisons between measured absorptivities and predicted values for a single engine cycle. As can be seen the measured and predicted values are within 10%. Since the band model parameters have an uncertainty at least of the order of 10% the comparison between measured and predicted values are very good.

It is the feeling of the author that these results are extremely important in instilling a deeper confidence in ones ability to measure species concentrations in high pressure combustion systems.

5.3 Absorption Emission Temperatures Along A Non Isothermal Path

Following the experiments with the dual ignition system described in section 5.1 configuration with a single spark plug was employed. In this configuration the spark plug was located just above the front window. As can be seen in Figure (5-2) this resulted in the polychromator "looking" directly along the axis of flame propagation. Thus, according to the non-uniform model the radiation entering the optical system originates from a non-isothermal slab of gas.

As was discussed in section (3.1) the radiation from this non isothermal path at wavelength λ is given by equation (3.1-5) and the temperature distribution can be obtained from the solution of the set of equations (3.1-7). However, some information can be obtained regarding the spatial temperature distribution by simple emission absorption considerations. When the data obtained from the "gradient" configuration (Figure 5-2) is interpreted in terms of the emission absorption technique, equation (5.1-1), the result is an average of the form

$$(1-\bar{\tau}(\lambda,T))I_b(\lambda,\bar{T}) = \int_0^L [1-\tau(\lambda,T)]I_b(\lambda,T)dr \qquad (5.3\text{-}1)$$

where

$T = T(r)$

Thus the average temperature $\overline{T}$ which is measured is a function of the temperature distribution T(r) and the transmittance of the gas. The exponential temperature dependence of Planck's function tends to weight $\overline{T}$ towards the high temperature regions. While the transmittance weights $\overline{T}$ in the following manner: high transmittance weight $\overline{T}$ to regions far from the detector while low transmittances weight $\overline{T}$ towards regions close to the detector. Physically this means that at wavelengths of high transmittance the spectrometer can look deep into the gas layer. While at wavelengths of low transmittance the spectrometer sees the gas near the surface. The measured transmittance at 2.5, 2.0 and 1.8 microns are of the order of 0.3, 0.75, 0.75 respectively. Thus the temperature determined at 2.5 microns should be greater than the temperature determined at 2.0 or 1.8 microns.

Figures (5-10) to (5-13) show typical emissions-absorption temperature histories for engine cycles with the spark plug in the "gradient" configuration. As can be seen the temperature measured at 2.5 microns is not in any statistical sense greater than the temperature determined at 2.0 or 1.8 microns. One of two conclusions can be drawn from these measurements: either 1) a large temperature gradient does not exist or 2) the experimental uncertainty is too large to make the refined measurements. As will be shown the problems can probably be attributed to experimental measurements (see Appendix II).

Another indication of the temperature gradient can be made by looking at the temperatures measured at 2.5 microns. The average transmittance of the combustion gases at this wavelength is on the order of 0.3. Therefore, the emission-absorption technique tends to weight the temperature to that nearest the detector. In this context one would expect the temperatures measured at 2.5 microns to be higher in the "gradient" configuration than the "isothermal" configuration (see figures (5-1) and (5-2)). This is so since the temperature near the detector in the "gradient" configuration is the hottest according to the nonuniform model, where in the "isothermal" configuration the temperature across the optical path should be more or less isothermal and the lowest in the cylinder.

The 2.5 micron temperature histories from 15 "isothermal" engine cycles have been averaged and are plotted in figure 5-14 along with the average bulk temperatures. As was discussed in section 5.1 the average values for the "isothermal" configuration are almost the same as the bulk temperatures for that configuration. However, for the "gradient" configuration the average spectroscopic temperature, determined at 2.5 microns, is on the order of 75°K higher than the bulk temperature. Thus, in light of the discussion in the previous paragraph there is a strong indication that a temperature gradient exists across the combustion chamber. The differences between the bulk temperatures for the two configurations is attributable to the dual and single ignition systems used in the "isothermal" and "gradient" configuration respectively.

5.4 Temperature Gradient Data Reduction:

As was developed in section 3-1 the radiation emerging from a nonisothermal layer of radiating and absorbing gas can be approximated by an incremental equation given by (3.1-7). Again using the consideration of the weighting effect of the instrument function equation (3.1-7) takes on the form

$$I_m(L,\lambda) = I_o(0,\bar{\lambda})\bar{\tau}_m(\lambda) + \sum_{i=1}^{N} I_b(\bar{\lambda},T_i)\{[\tau_m(\lambda)]_{i+1}^{N}-[\tau_m(\lambda)]_{i}^{N}\}$$

$[\tau_m(\lambda)]_{i+1}^{N}$ = measured or calculated transmittance of zones (i+1) to N

$[\tau_m(\lambda)]_{i+1}^{N}$ = measured or calculated transmittance of zones i to N

It is observed that the only unknowns in equation (3.1-7) are the N zonal Planck functions. Hence, if measurements are made at N wavelength one has left to solve a set of N x N non linear algebraic equations in order to determine the N zonal Planck functions. These may then be inverted to determine the N zonal temperatures. The solution to such a set of equations is not a trivial one. Krakow[23] has made measurements of the emergent intensity from three flat flames in series at three different wavelengths. In order to arrive at a solution he approximated the Planck function by a function with a temperature sensitive term and a wavelength sensitive term and used an iterative scheme to find a solution. In this study it was felt that with the availability of the CDC 6400 computer a solution to the set of equations could be obtained without approximating the Planck functions. Thus, a general iterative scheme utilizing Newton's method was employed to solve the set of equations. A general description of Newton's method is given in Appendix IIIand a Fortran listing of the data reduction program is shown in Appendix V.[62]

Data was collected with the engine in the "gradient" configuration at 1.8, 2.0, and 2.5 microns. The optical path could then be broken into either two or three isothermal zones as shown in figure 5-15 which results in the solution of a system of 2x2 or 3x3 equations respectively.

Due to the extensive amount of computer time required the solutions were only carried out for crank shaft angles near the ocurrence of peak cycle pressure. The data at 2.0 and 2.5 microns was used to determine the temperatures in the two zone approximation. In order to instill further confidence in the results, data collected at 2.0 and 2.5 microns with the engine in the "isothermal" spark plug configuration was also input in the data reduction scheme. Since the dual ignition configuration should produce a more isothermal condition along the optical path than the single ignition "gradient" configuration it is of interest to compare the results. Table 5-2 lists some of the results obtained from the two zone data reduction scheme. In table 5-2 the cycles marked "I" are "isothermal" data and the cycles marked "G" are the "gradient" data. Also, zone 1 is the zone furthest from the detector, and the spark plug in the "gradient" configuration and zone 2 is closest to the detector.

As can be seen in table 5-2 the two zone data reduction definitely shows the existence of a temperature gradient. Cycles I-1 to I-3 yield results which are either isothermal to approximately 100°K or yield a temperature distribution with the temperature in the region furthest from the detector which is hotter by approximately 400°K than the region closer to the detector. From the geometry of the dual ignition system it was expected that the temperature distribution should be essentially isothermal, or at least more isothermal than the single spark plug "gradient" configuration. On the other hand, the results for cycles G-2 to G-4 all show temperature distributions with the hotter region being close to the detector. These results have been plotted in figure 5-16 along with the results of the model developed in chapter 2. As is seen in figure 5-16 the model predicts a temperature difference of 600°K at the end of flame travel and the two zone data reduction yields an average difference of 700-800°K. Since the results of the error analysis in Appendix II yield a probable uncertainty on the order of 150°K in the difference between the two zonal temperatures, the comparison between the model and the experiment is fairly good.

The difference between the analytical bulk temperature and the experimental bulk temperature of about 200°K can be attributed to heat transfer during the compression and combustion processes and the fact that combustion is not 100% complete as is assumed in the analytical model. Hence a better comparison is shown in figure 5-17 where the results are replotted with respect to the bulk temperature. As is seen in this figure the comparison is good.

Another factor which needs to be considered is the fact that the analytical model assumes each zone adiabatic. Hence, any heat transfer from the first zone to burn (which is the hottest and has the longest residence time) to the cylinder wall during the combustion process would tend to reduce the temperature difference of 600°K calculated in chapter 2. An estimate of this may be obtained using a heat transfer correlation proposed by Annand(10)

$$Nu = 0.26\ (Re)^{0.75}$$

to calculate the heat transfer from the first zone to the cylinder wall during the time increment for the remainder of flame travel. In the above correlation the Reynold's number is based on the cylinder bore and the mean piston speed. This quantity of heat which is transferred is then equated to an energy loss in the first zone

$$Q = hA(T_{gas} - T_{wall})\Delta t = c_p\ m\ \Delta T$$

where ΔT is the change in temperature of the first zone due to heat transfer to the walls. Performing this calculation for the conditions of the first zone yields a value of 50°K for ΔT. Hence, if heat transfer to the cylinder walls was taken into account in the analytical model the temperature difference across the combustion chamber would only be reduced by approximately 50°K.

Next the data from all three wavelengths was used to formulate a three zone model (figure 5-15). As can be seen in table 5-3 the results of this analysis were similar to the two zone analysis. In table 5-3 zone 1 is the zone further from the spark plug, zone 2 is the center of the chamber and zone 3 is closest to the spark plug. The "isothermal" cycles show essentially an isothermal distribution and the "gradient" cycles yield temperature distributions with the coolest zone being zone 1. In the three zone formulation problems of convergence and uniqueness were encountered which prohibited obtaining more definitive results.

5.5 Discussion of Results and Conclusions

A number of observations can be made from the results of the experimental investigation. It was observed that the utlization of the emission absorption technique could be used to measure the temperature of the combustion gas products in the engine cylinder. In these measurements it was found that the most reliable results were obtained when the transmittance of the gas was of the order of 0.3. However, in all cases it was found that the temperature was of the order of the ideal bulk gas temperature. Thus it appears that the water vapor energy states are in equilibrium. This substantiates the conclusion reached by Smith[9] and more recently the results of Lavoie[65] that the spectroscopic temperatures determined from the radiation of the $A^2\Sigma \rightarrow X^2\pi$ transition of the OH radical yield abnormally high results.

With regards the multiple wavelength temperature gradient measurements the two zone formulation yielded reasonably good results. However, definitive results could not be obtained with the three zone formulation. This was due to problems in obtaining unique solutions and in obtaining convergence.

Two paths are available in pursuing future work. First is to further investigate the multiple wavelength technique with three and more zones. This could involve a study in a constant volume bomb using hydrogen and oxygen whereby the only infrared active product would be water vapor. Since only single firings would be used fouling of the windows would not be a problem. Also, problems of mixture motion due to induction processes along with mixing with the residual gas would be avoided. With careful control over the initial mixture reproducibility could be achieved and windows could be mounted along with optical path to determine the temperature distribution.

The other approach would be to indirectly determine the temperature map by direct sampling for nitric oxide. Since the nitric oxide levels are almost entirely determined by the temperature history sampling an engine running on a premixed propane/air system at various locations around the cylinder should yield an indication of the temperature distribution.

From the work presented the following conclusions may be formulated:

1) The non uniform model of the burned gas region and the kinetic formation of nitric oxide can account for experimental observations of the

formation of nitric oxide in an engine cylinder.

2) The non uniform model predicts a temperature difference of 650°K across the engine cylinder and that this difference has a profound effect on the kinetic formation of NO. In the hot region near the spark plug the model predicts the NO to almost reach its peak equilibrium value and then decomposes to approximately 50°ATC where it freezes. In the colder region far from the point of ignition the NO freezes before it reaches the peak equilibrium value.

3) The emission-absorption technique can be used to determine the temperature of the combustion products. The temperatures which are measured are within 100°K of the bulk gas temperature.

4) The statistical band model predicts the transmittance of the 1.8 and 2.7 micron bands of water vapor in the combustion products to within 10% of the measured values.

5) Comparisons between the emission-absorption temperatures of the "gradient" and "isothermal" engine configurations indicate that a gradient exists along the path of flame travel.

6) The multiple wavelength single line of sight temperature distribution measurements indicate the existence of a temperature gradient along the path of flame travel. The two zone formulation yielded an average temperature difference of about 750°K between the two zones. Considering the experimental uncertainty of about 150°K this is in good agreement with the predictions of the analytical model.

Table 5-1

CFR Engine Parameters

Bore	8.25 cm
Compression Ratio	7:1
Manifold Pressure	14.7psia
Ignition Timing	38°BTDC
Engine Speed	1200rpm
Fuel	Propane
Equivalence Ratio	1.00

TABLE 5-2

Two Zone Data Reduction

Cycle	Crank Shaft Angle (deg atc)	Bulk Temperature (°K)	Zonal Temperatures	
			T_1 (°K)	T_2* (°K)
I-1	4.50	2608	2659	2565
I-1	7.50	2560	2380	2693
I-2	7.50	2477	2796	2382
I-2	10.50	2446	2775	2347
I-4	4.50	2527	2559	2599
I-4	7.50	2494	2538	2592
G-2	16.50	2522	2155	3094
G-2	19.50	2496	2133	3209
G-3	9.00	2577	2380	2907
G-3	15.00	2502	2225	2956
G-3	18.00	2490	2417	2739
G-4	10.50	2566	2235	3004
G-4	13.5	2538	2219	3063
G-4	16.5	2485	2236	2964
G-4	19.5	2457	2353	2770

Zone #1: furthest from detector
Zone #2: center of chamber

* for (G) cycles zone #2 is adjacent to point of ignition

TABLE 5-3

Three Zone Data Reduction

Cycle	Crankshaft Angle (deg atc)	Bulk Temperature (°K)	Zonal Temperatures		
			T_1 (°K)	T_2 (°K)	T_3* (°K)
I-1	4.5	2608	2625	2600	2575
I-1	7.5	2560	2586	2517	2578
I-2	7.5	2477	2958	1660	3125
I-4	4.5	2527	2918	1890	3230
G-2	16.5	2522	2166	2548	3109
G-3	9.0	2577	2360	3277	2755
G-4	13.5	2538	2521	2461	3278

Zone #1: furthest from detector
Zone #2: center of chamber
Zone #3: nearest detector

*for (G) cycles zone #3 is adjacent to point of ignition

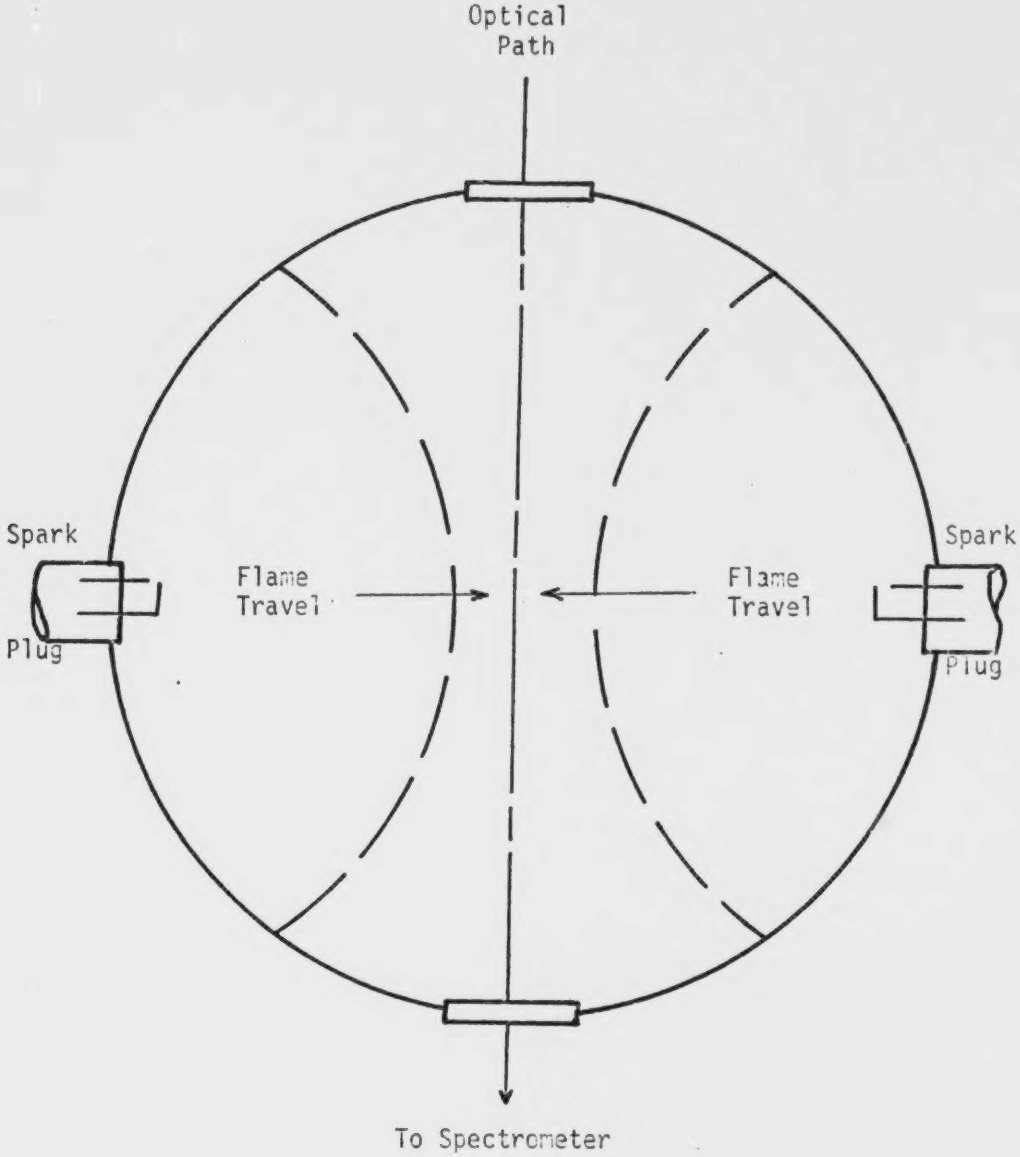
Optical Path
Spark Plug
Flame Travel
Flame Travel
Spark Plug
To Spectrometer

Figure 5-1

ISOTHERMAL CONFIGURATION

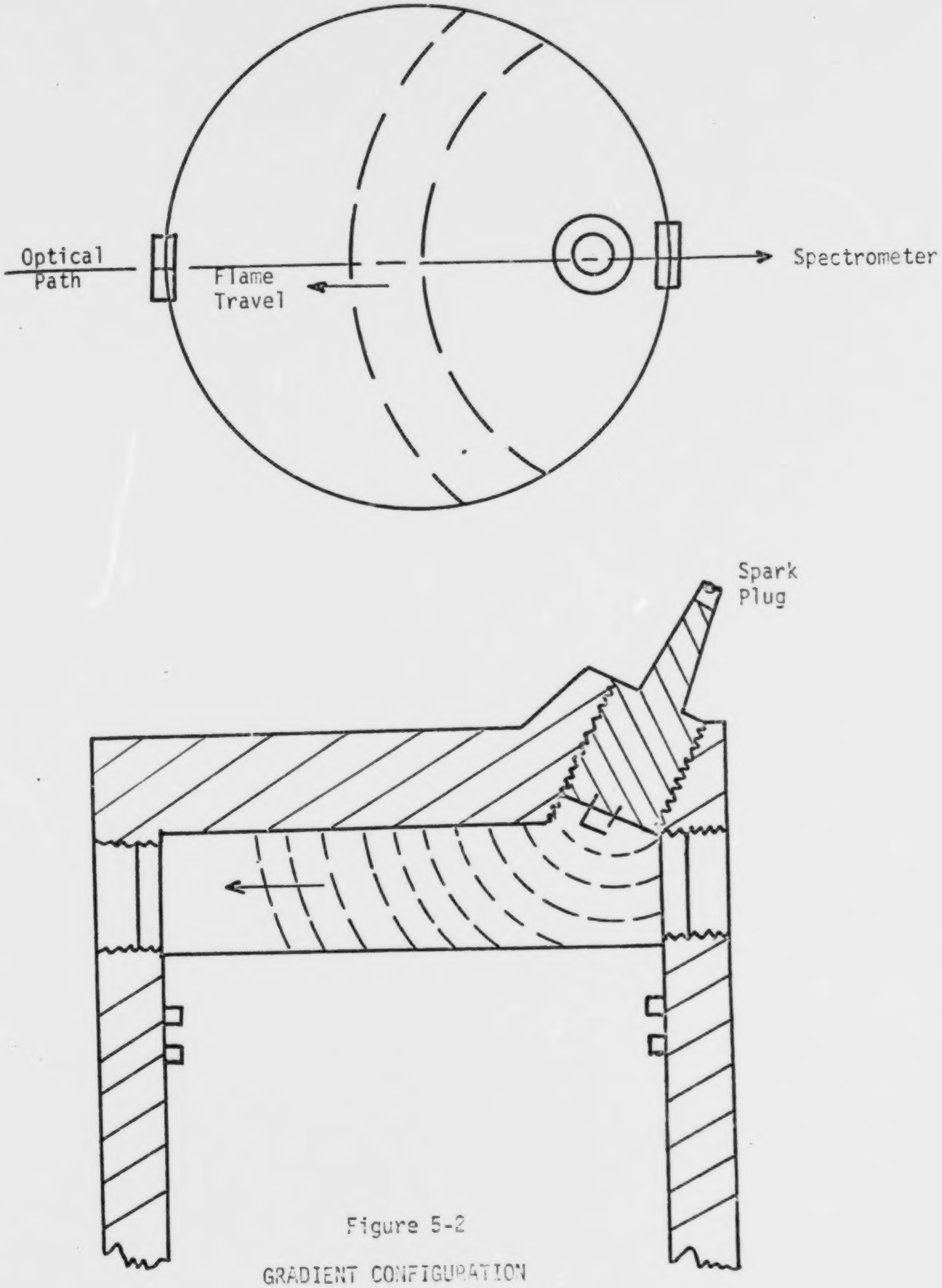
Optical Path
Flame Travel
Spectrometer
Spark Plug

Figure 5-2

GRADIENT CONFIGURATION

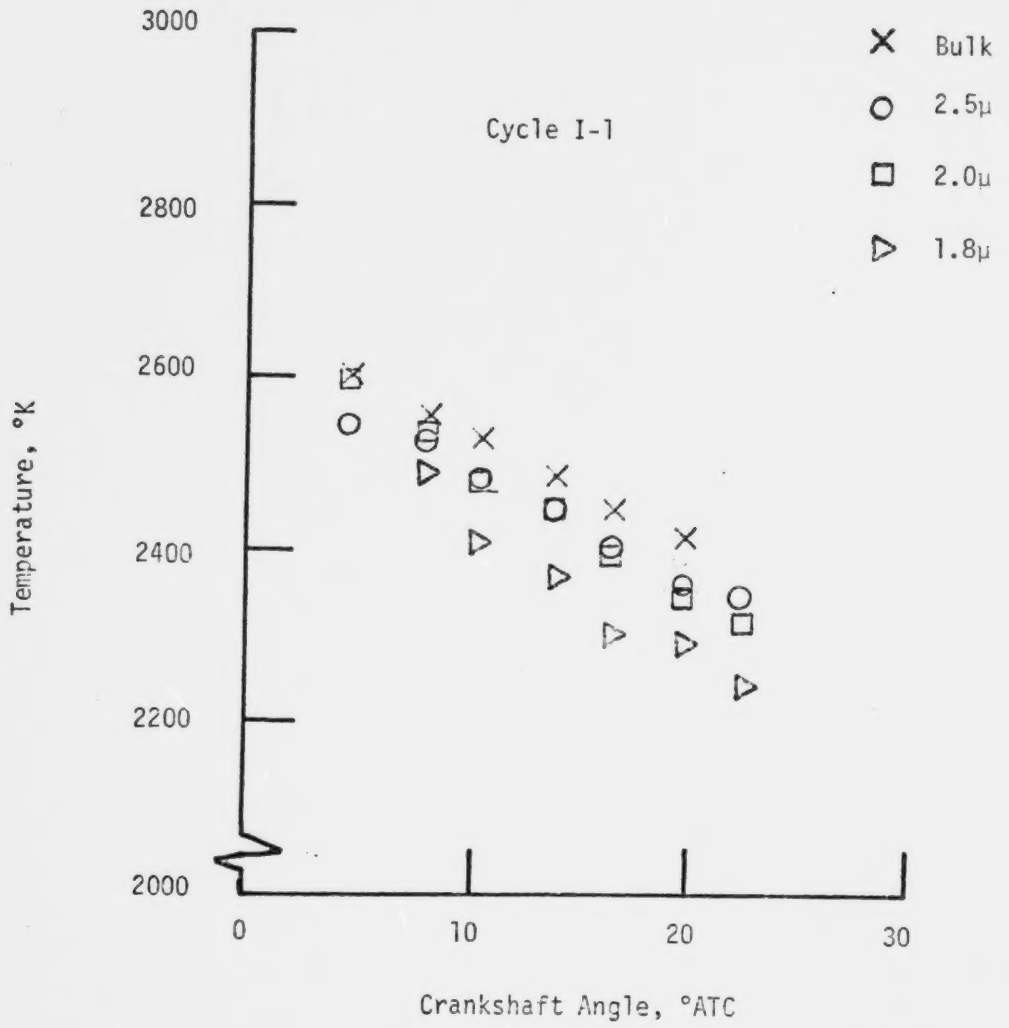

Figure 5-3

CYCLE I-1 EMISSION - ABSORPTION
TEMPERATURE HISTORY

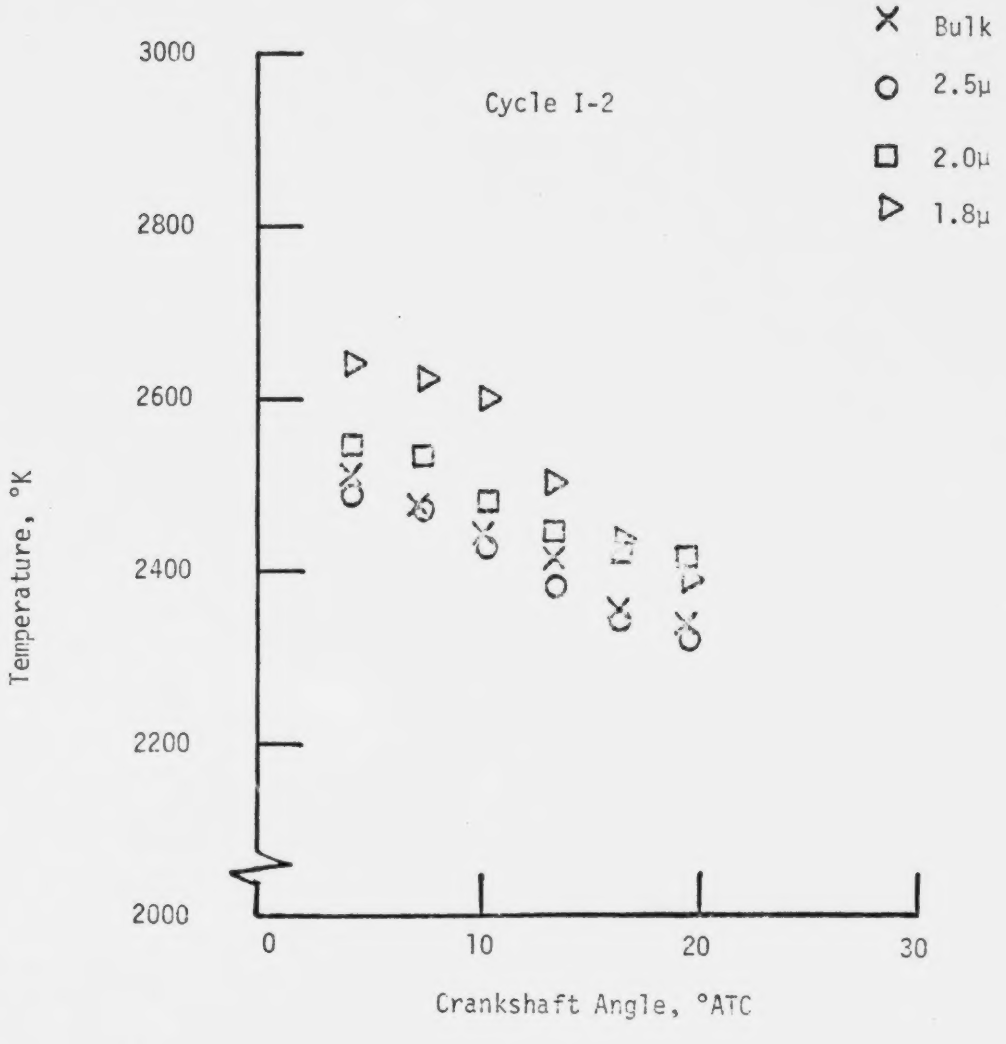

Figure 5-4

CYCLE I-2 EMISSION-ABSORPTION
TEMPERATURE HISTORY

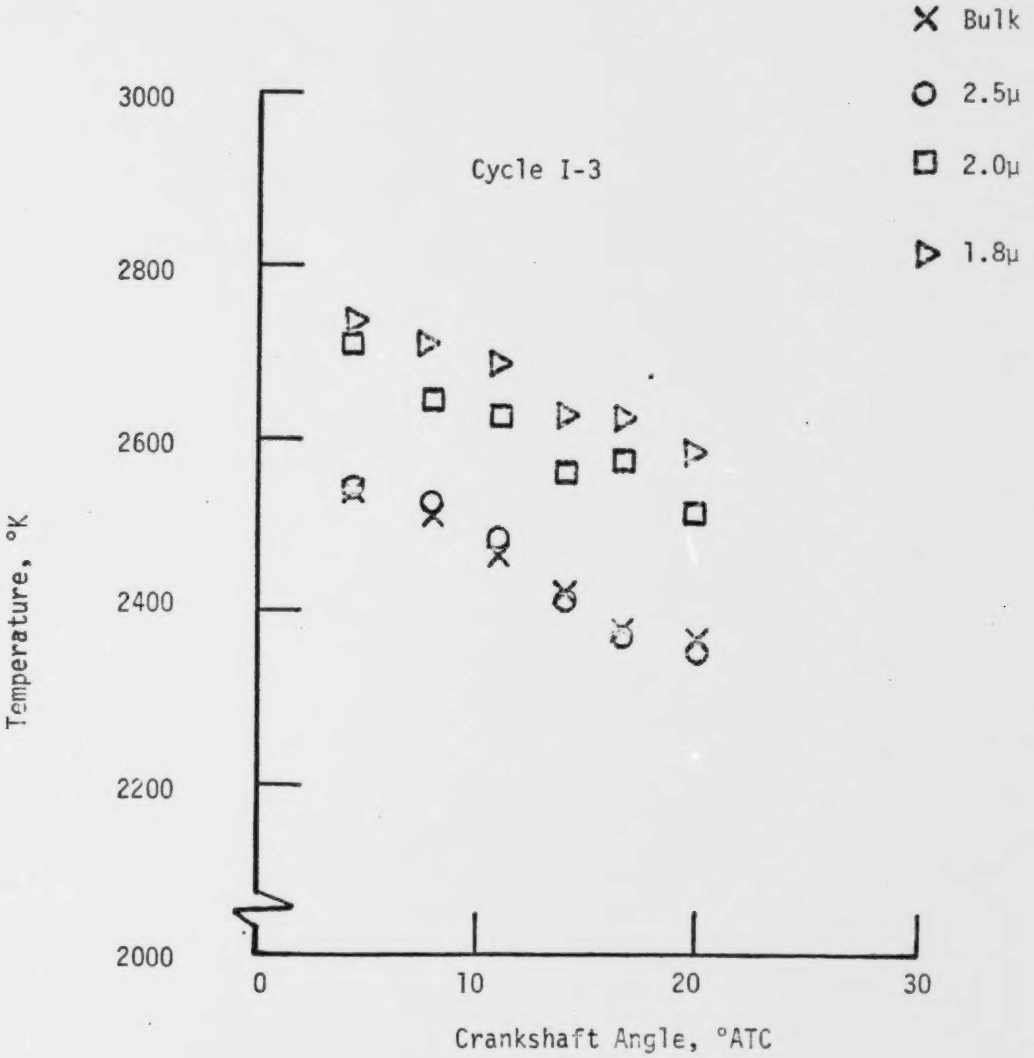

Figure 5-5

CYCLE I-3 EMISSION-ABSORPTION
TEMPERATURE HISTORY

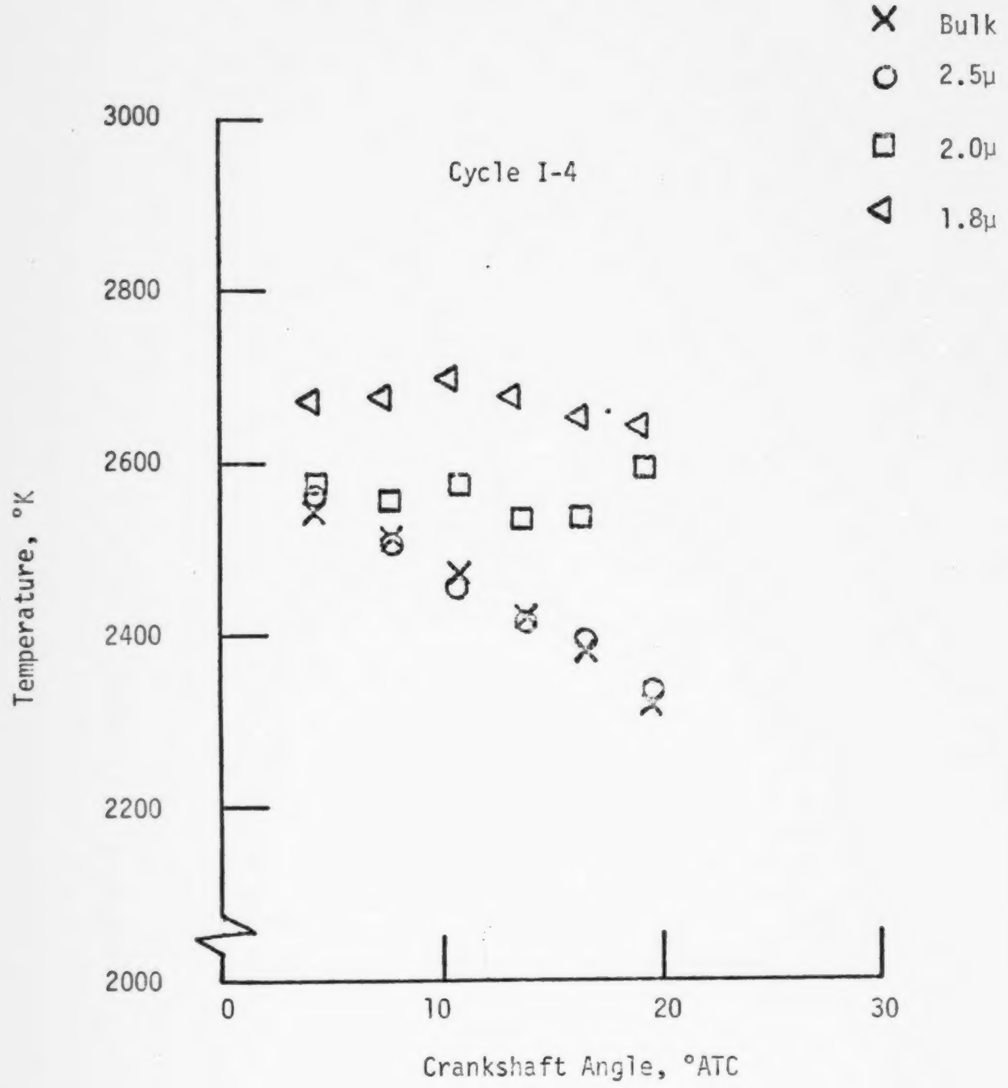

Figure 5-6

CYCLE I-4 EMISSION-ABSORPTION
TEMPERATURE HISTORY

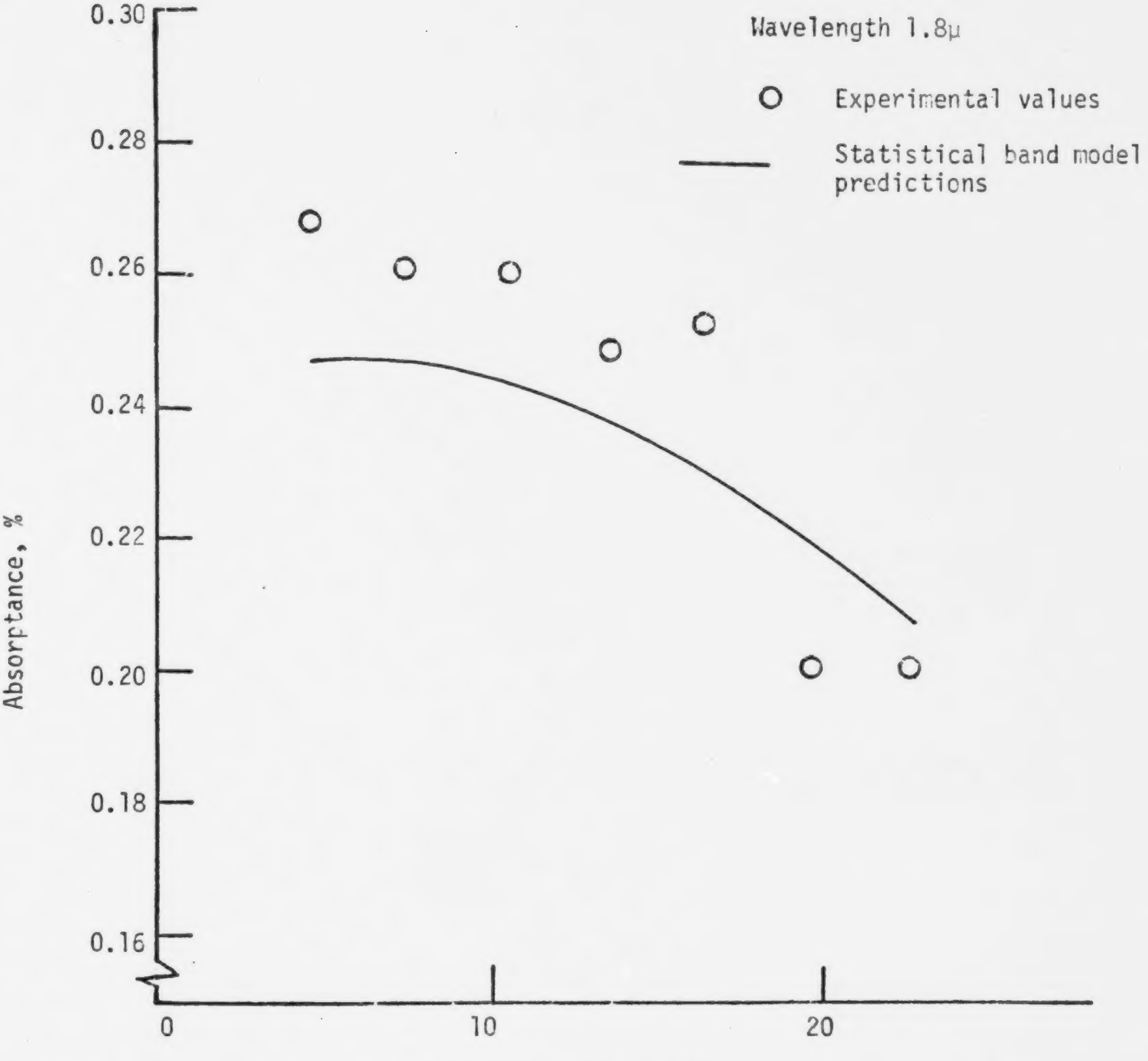

Figure 5-7

EXPERIMENTAL ABSORPTIVITY OF WATER VAPOR AT 1.8 MICRONS

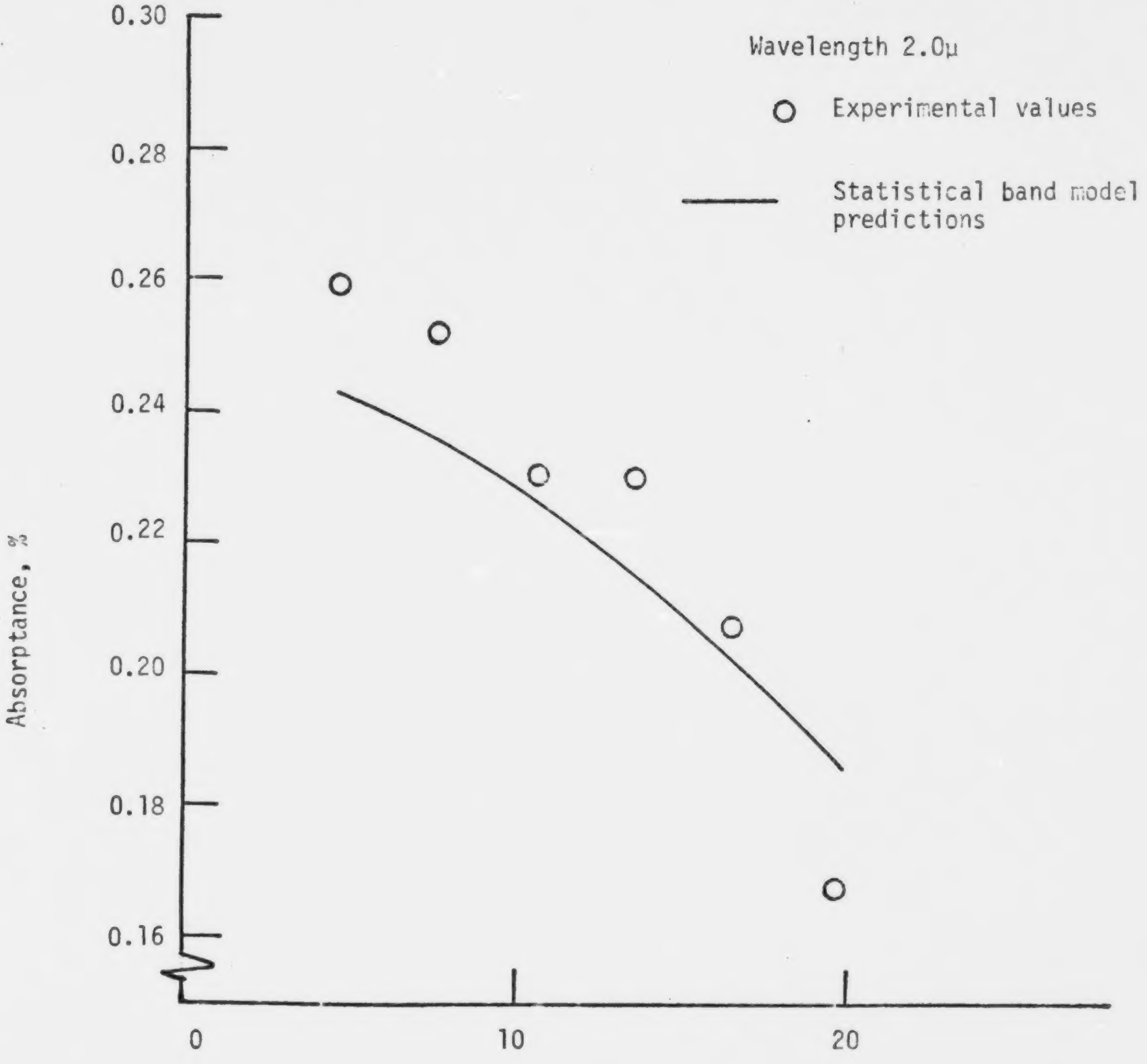

Figure 5-8

EXPERIMENTAL ABSORPTIVITY OF WATER VAPOR
AT 2.0 MICRONS

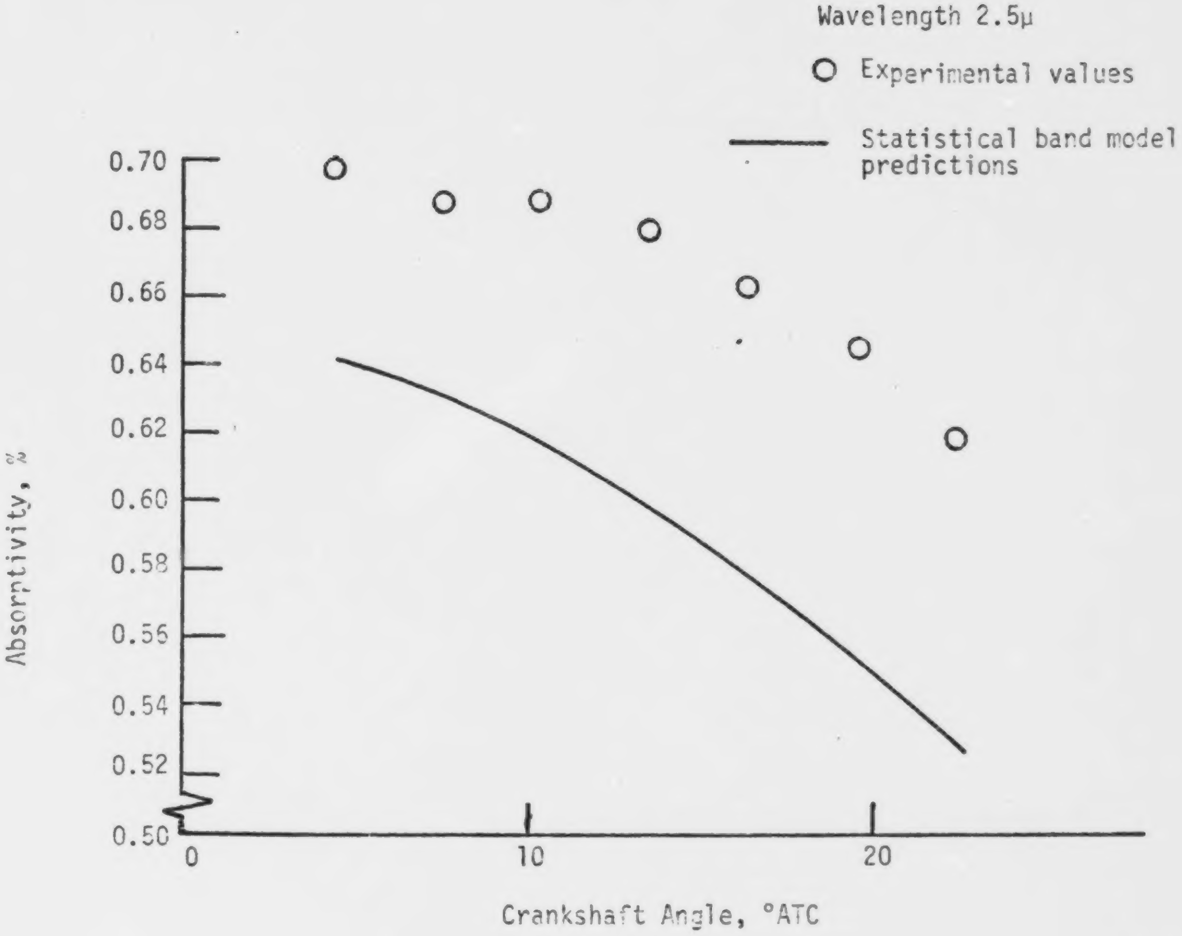

Figure 5-9

EXPERIMENTAL ABSORPTIVITY OF WATER VAPOR
AT 2.5 MICRONS

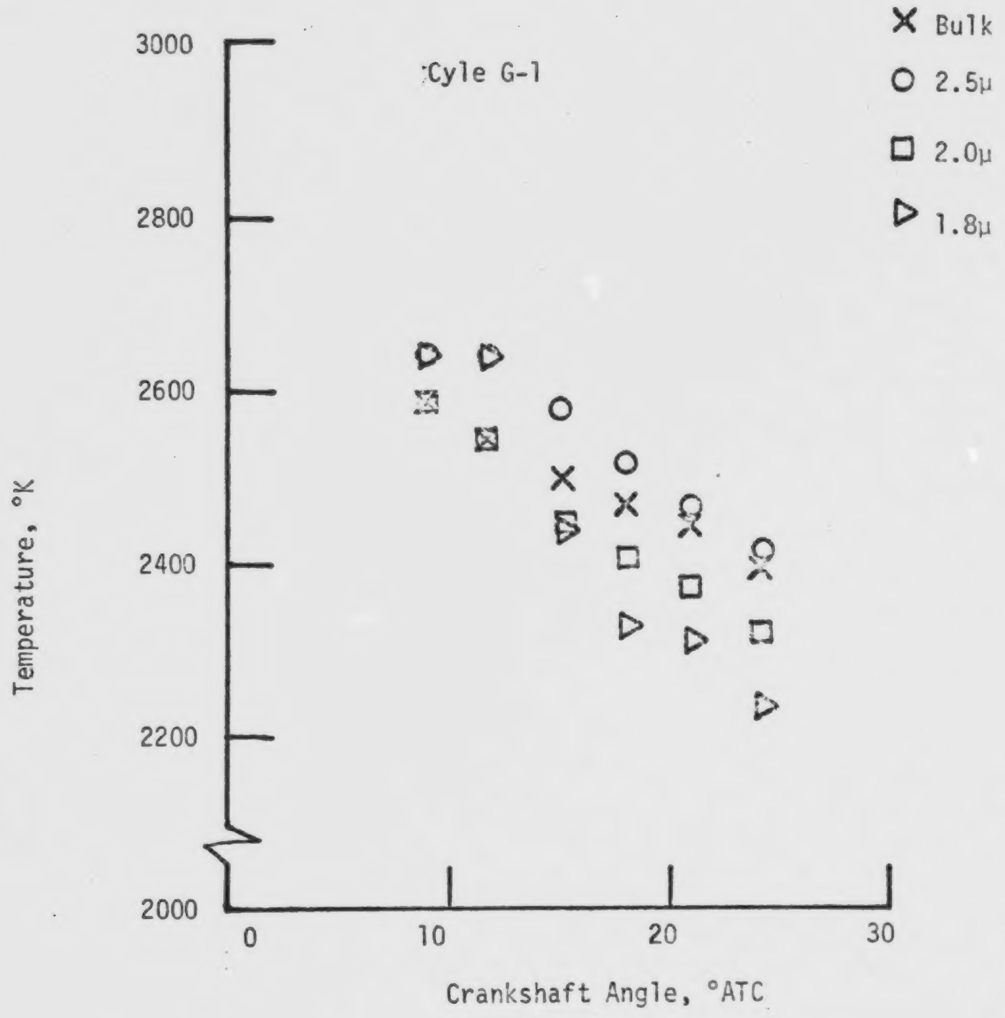

Figure 5-10

CYCLE G-1 AVERAGE EMISSION-ABSORPTION TEMPERATURE HISTORY

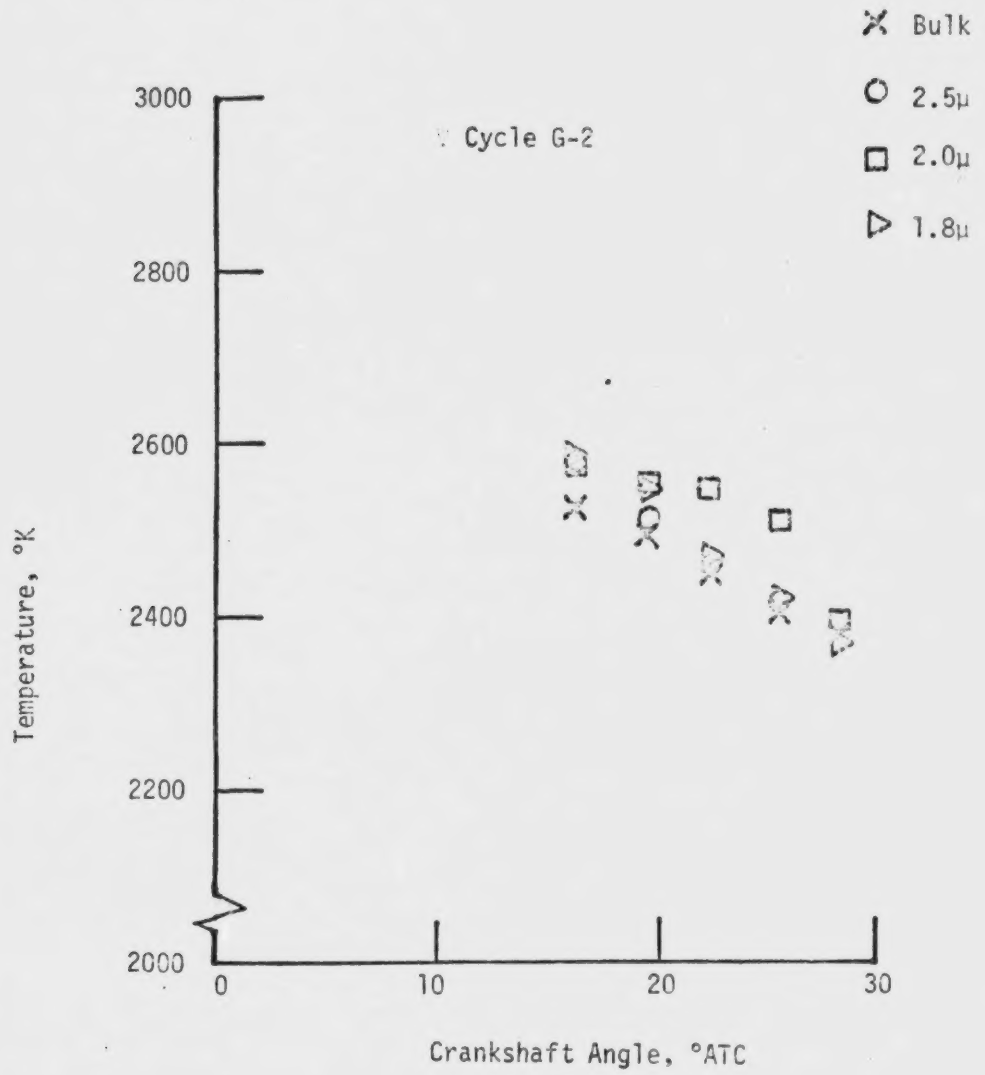

Figure 5-11

CYCLE G-2 AVERAGE EMISSION-ABSORPTION TEMPERATURE HISTORY

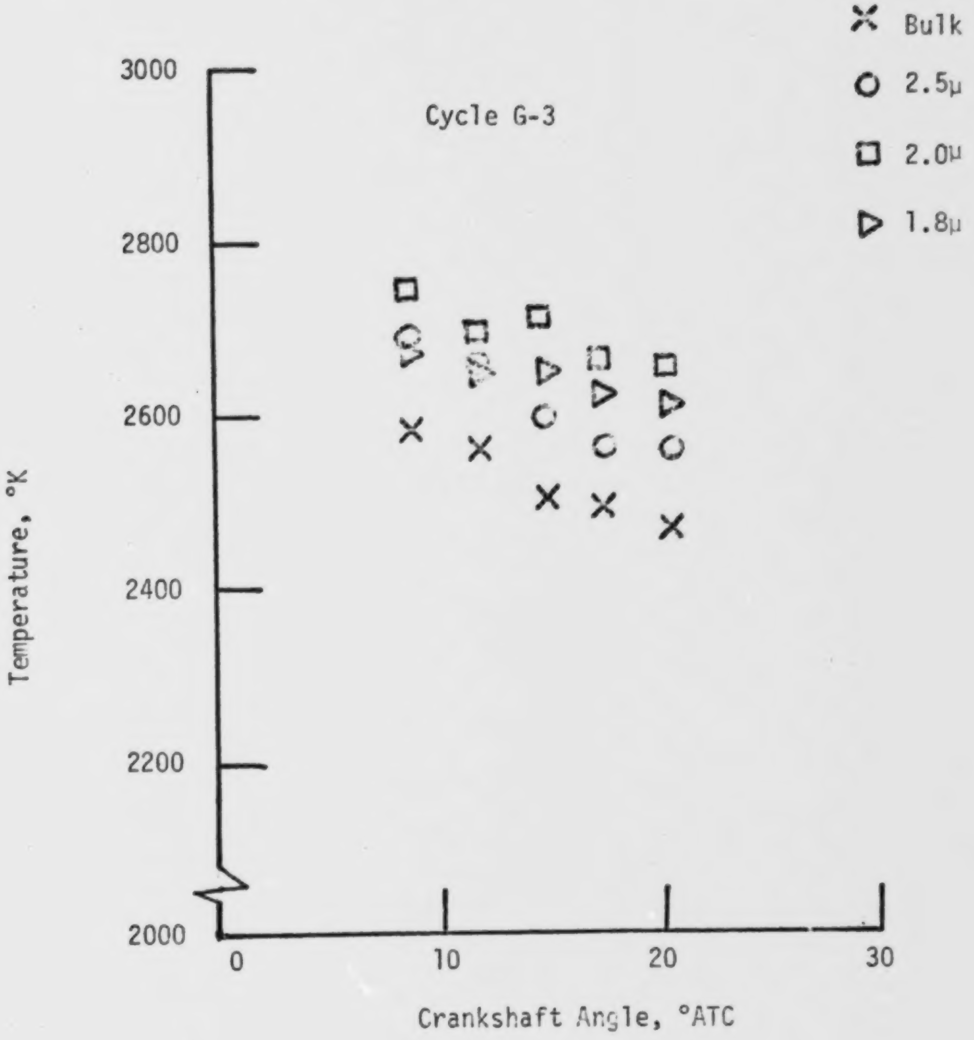

Figure 5-12

CYCLE G-3 AVERAGE EMISSIONS ABSORPTION TEMPERATURE HISTORY

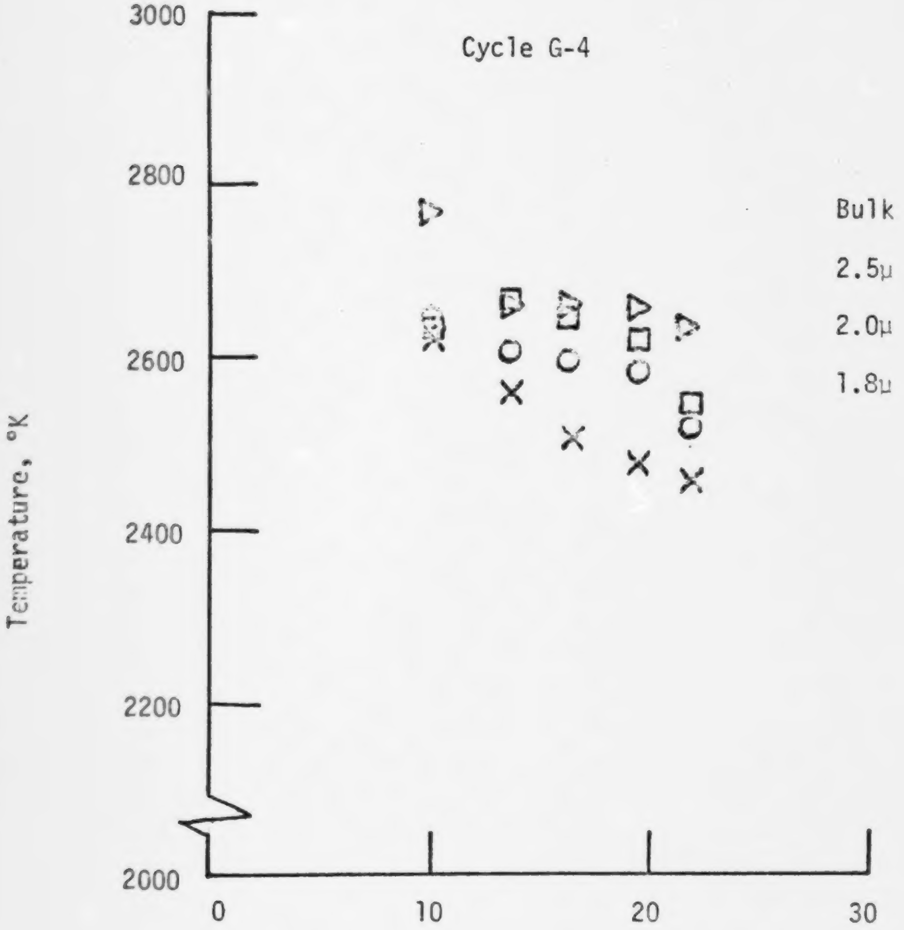

Crankshaft Angle, °ATC

Figure 5-13

CYCLE G-4 AVERAGE EMISSION ABSORPTION TEMPERATURE HISTORY

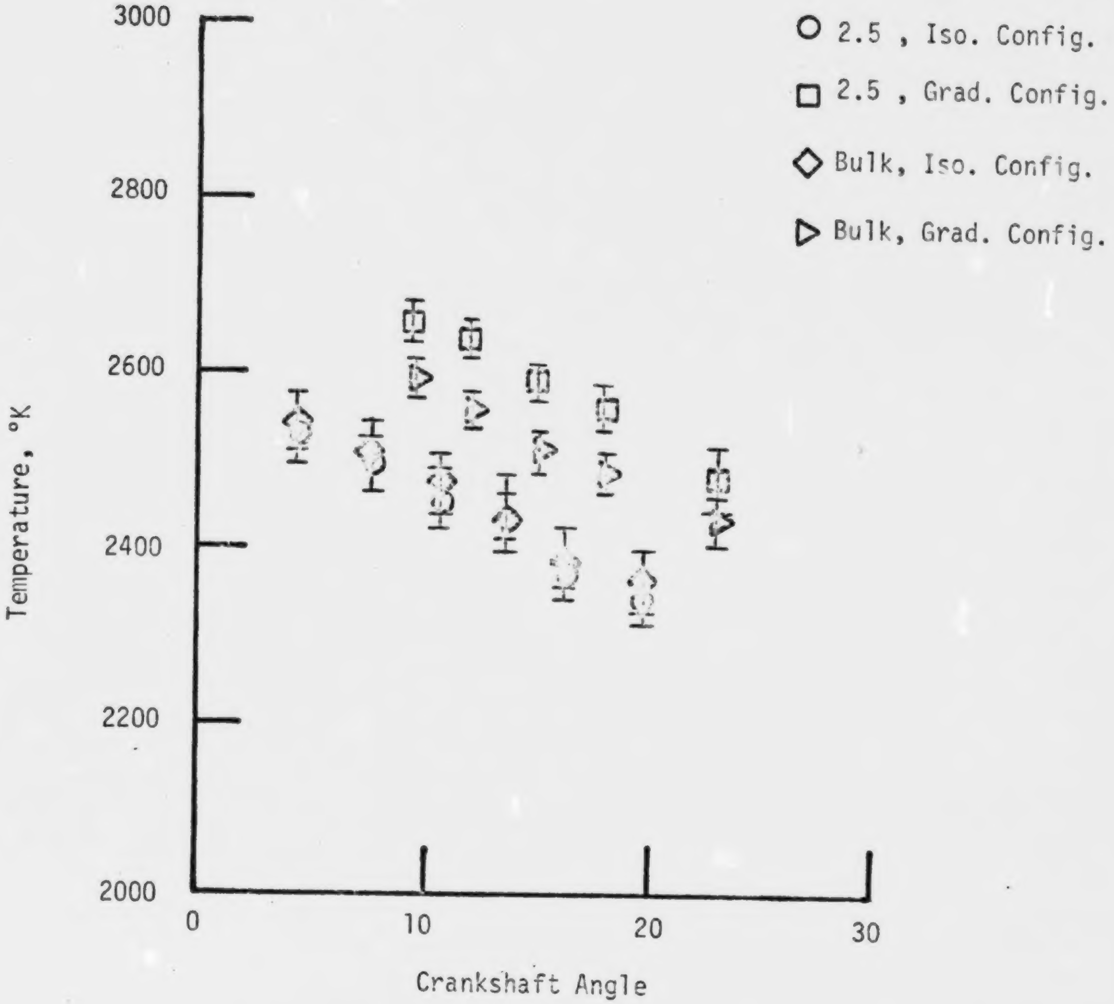

Average Temperature with 2σ Bars

Figure 5-14

AVERAGE 2.5μ TEMPERATURE HISTORIES
FOR THE "ISOTHERMAL" AND "GRADIENT"
CONFIGURATIONS

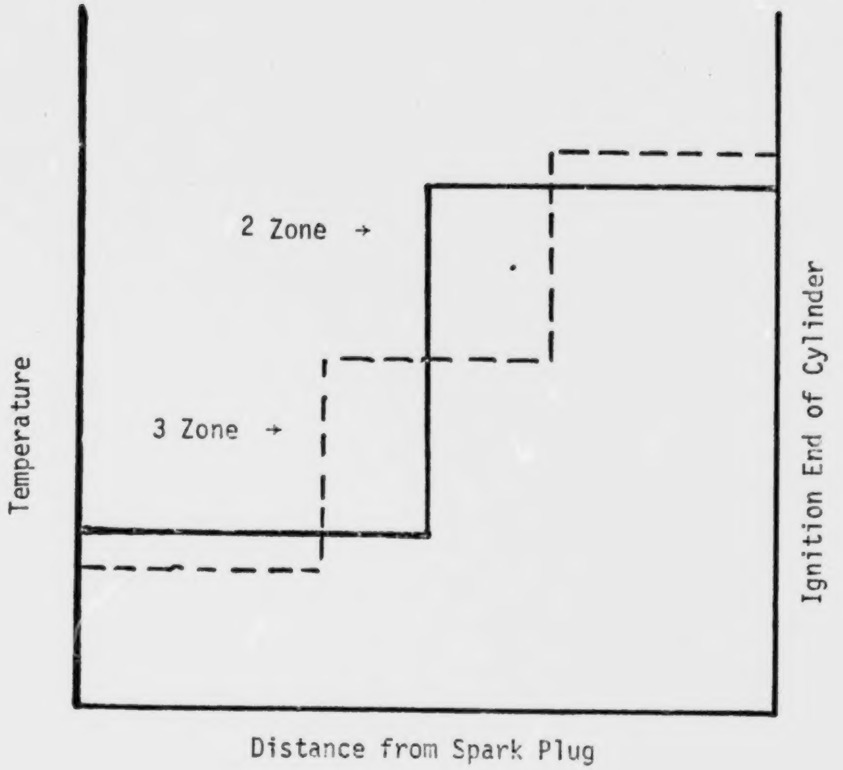
2 Zone →
3 Zone →
Temperature
Ignition End of Cylinder
Distance from Spark Plug

Figure 5-15

SCHEMATIC OF ZONAL TEMPERATURE
DISTRIBUTION DATA REDUCTION

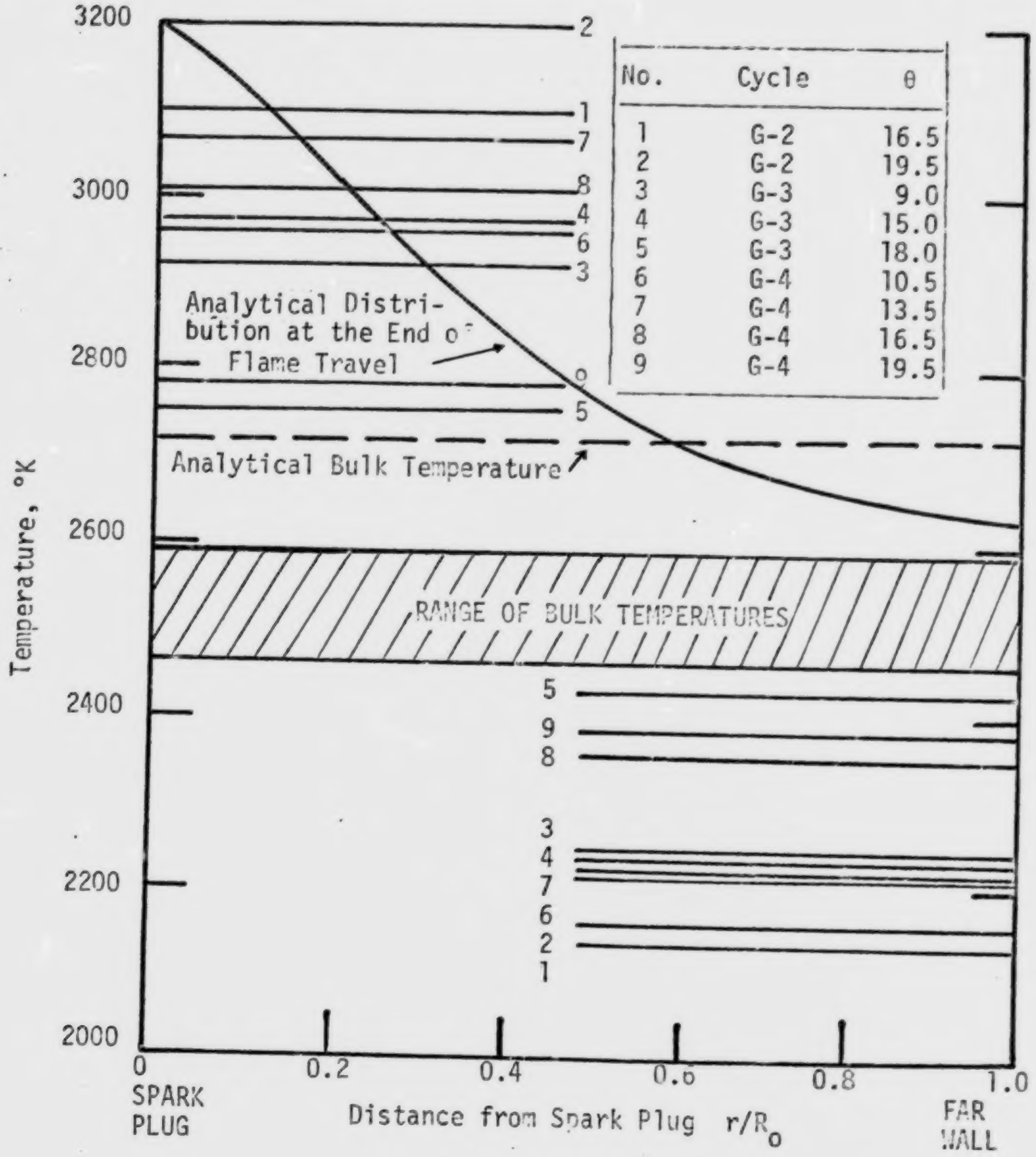

No.	Cycle	θ
1	G-2	16.5
2	G-2	19.5
3	G-3	9.0
4	G-3	15.0
5	G-3	18.0
6	G-4	10.5
7	G-4	13.5
8	G-4	16.5
9	G-4	19.5

Figure 5-16

TWO ZONE TEMPERATURE DISTRIBUTION

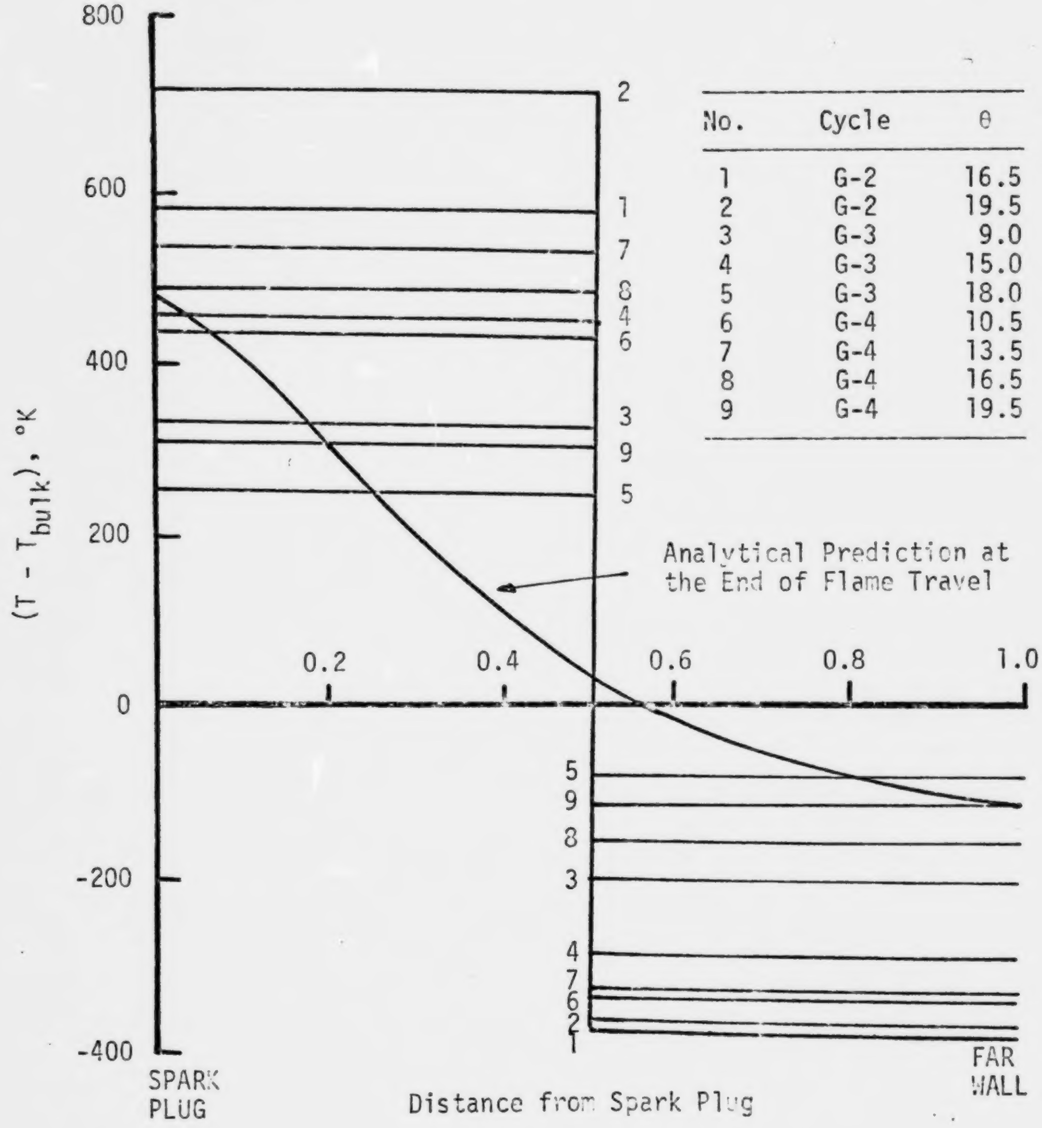

No.	Cycle	θ
1	G-2	16.5
2	G-2	19.5
3	G-3	9.0
4	G-3	15.0
5	G-3	18.0
6	G-4	10.5
7	G-4	13.5
8	G-4	16.5
9	G-4	19.5

Figure 5-17

RELATIVE TWO ZONE TEMPERATURE DISTRIBUTION

REFERENCES

1. Hopkinson, Proceedings of the Royal Society, 77, 327, 1906.

2. Lewis, von Elbe, Combustion, Flames and Explosions of Gases, 2nd Edition, Academic Press, New York, 1961.

3. Strehlow, R., Fundamentals of Combustion, International Textbook Co., Penn., 1968.

4. Rassweiler, G. M., Withrow, L., SAE J., 36, 125, 1935.

5. Starkman, E. S., Stewart, H. E., Zvonow, V. A., Paper 690020, SAE International Automotive Engineering Congress, Detroit, Michigan 1969.

6. Lavoie, G. A., Heywood, J. B., Keck, J. C., Combustion Science and Technology, 1, 313, 1970.

7. Obert, E. F., Internal Combustion Engines, 3rd Edition, International Textbook Co., Penn., 1968.

8. Final Summary Report, CRC Project No. CM-1-58, Coordinating Research Council, New York, New York, 1960.

9. Smith, D. S., Ph.D. Thesis, University of California, Berkeley, Calif., 1969.

10. Taylor, C. F., Taylor, E. S., The Internal Combustion Engine, 2nd Edition, International Textbook Co., Penn., 1961.

11. Eyzat, P., Guibet, J. C., SAE Paper No. 680124, 1968.

12. JANAF Thermochemical Tables, Dow Chemical Company, Midland, Michigan 1965.

13. Alperstein, M., Bradow, R. L., Review of Scientific Instruments, 36, 1029, July 1965.

14. Newhall, H. K., Starkman, E. S., SAE Paper No. 670122, 1967.

15. Newhall, H. K., Shahed, S. M., WSCI Paper No. 70-3, Spring Meeting 1970, Western States Section of the Combustion Institute, Berkeley California, 1970.

16. Bell, A. W., et al., WSCI Paper No. 70-5, Spring Meeting, 1970 Western States Section of the Combustion Institute, Berkeley, Calif. 1970.

17. Starkman, E. S., Sawyer, R. F., Carr, R. C., Johnson, G. L., Muzio, L. J., JAPCA, 20, 2, February, 1970.

18. Wray, K. L., Teare, J. D., J. Chem. Phys., 36, 2582, 1962.

19. Tien, C. L., Pelech, I., J. Quant. Spect. and Rad. Trans., 8, 685, 1968.

20. Young, L. A., AIAA J., 3, 4, 610, 1965.

21. Freeman, M. P., Katz, S., J. Opt. Soc. Am., 50, 8, 826, 1960.

22. Krakow, B., AIAA J., 3, 1359, 1965.

23. Krakow, B., Appl. Opt., 5, 201, 1966.

24. Tourin, R. H., Krakow, B., Appl. Opt., 2, 237, 1965.

25. Conrath, B., NASA TND-2940, 1965.

26. Tourin, R. H., Spectroscopic Gas Temperature Measurement, Elsevier Publishing Company

27. Newhall, H. K., Ph.D. Thesis, University of California, Berkeley, California, 1966.

28. Chandrasekhar, S., Radiative Transfer, Oxford University Press, London, 1950.

29. Kourganoff, V., Basic Methods in Transfer Problems, Oxford University Press, London, 1952.

30. Penner, S. S., Quantitative Molecular Spectroscopy and Gas Emissivities, Addison-Wesley, Reading, Massachusetts, 1959.

31. Rossman, T. G., et al., AD 656-775, DDC, Washington, D. C.

32. Ferriso, C. C., Ludwig, Appl. Opt., 4, 1, 1965.

33. Tien, C. L., "Thermal Radiation Properties of Gases," in Advances in Heat Transfer, Vol. 5, Academic Press, New York, 1968.

34. Malkmus, W., J. Opt. Soc. Am., 53, 8, 951, 1963.

35. Malkmus, W., Thomson, A., J. Quant. Spect. and Rad. Trans., 2, 17, 1962.

36. Oppenheim, U. P., Ben Aryeh, Y., J. Quant. Spect. and Rad. Trans., 4, 559, 1964.

37. Abu-Romia, M. M., Tien, C. L., J. Quant. Spect. and Rad. Trans., 6, 143, 1966.

38. Ferriso, C. C., Ludwig, C. B., Thomson, A. L., J. Quant. Spect. and Rad. Trans., 6, 241, 1966.

39. Penzias, G. J., MacLay, G. J., 10th Symposium (International) on Combustion, 189, 1965.

40. Oppenheim, U. P., Goldman, A., 10th Symposium (International) on Combustion, 185, 1965.

41. MacLay, G. J., Babrov, H. J., AD 446-254, DDC, Washington, D. C. 1964.

42. Goody, R. M., Atmospheric Radiation, Oxford Press, London, 1964.

43. Baer, R. M., "G2 Cal NLIN," Computer Center Library, University of California, Berkeley, California, June 1967.

44. Huffaker, R. M., J. Quant. Spect. Rad. Trans., 8, 87, 1968.

45. Starkman, E. S., Sawyer, R. F., Carr, R. C., "The Influence of Fuel Composition on Emissions of Carbon Monoxide and Oxides of Nitrogen," Paper presented at SAE Midyear Meeting, Detroit, 1970.

46. Smith, D. S., Starkman, E. S., Review of Scientific Instruments, 40, 12, 1541, 1969.

47. Vincenti, W. G., Kruger, C. H., Introduction to Physical Gas Dynamics, John Wiley and Sons, New York, 1965.

48. Millikan and White, J. Chem. Phys., 39, 3209, 1963.

49. Callear, A. B., Applied Optics, Supplement 2, 145, 1965.

50. Herzfeld, K. F., Litovitz, T. A., Absorption and Dispersion of Ultrasonic Waves, Academic Press, New York, 1959.

51. Ferriso, C. C., Breeze, J. C., Ludwig, C. B., Malkmus, W., J. Chem. Phys., 42, 402, 1965.

52. Ferriso, C. C., Ludwig, C. B., J. Chem. Phys., 41, 1668, 1964.

53. Patch, R. W., J. Quant. Spec. Rad. Trans., 5, 137, 1965.

54. Tsurch, D. E., Williams, D., Appl. Opt., 1, 587, 1962.

55. Breeze, J. C., Ferriso, C. C., J. Chem. Phys., 43, 3253, 1965.

56. Horning, Trans., SAE, 26, 1931.

57. Sawyer, R. A., Experimental Spectroscopy, Dover, New York, 1963.

58. Harrison, G. R., Lord, R. C., Loofbourow, J. R., Practical Spectroscopy, Prentice Hall, New York, 1948.

59. Stair, R., Johnston, R., Halbach, J. of Research of the NBS-A, Physics and Chemistry, 64A, 4, 1960.

60. Bevington, P. R., Data Reduction and Error Analysis for the Physical Sciences, McGraw-Hill, New York, 1969.

61. Daniel, W. A., 6th Symposium (International) on Combustion, 1956.

62. Baer, R. M., "C4 Cal Simex," Computer Center Library, University of California, Berkeley, California, June 1969.

63. Holman, J. P., Experimental Methods for Engineers, McGraw-Hill, New York, 1966.

64. Henrici, P., Elements of Numerical Analysis, John-Wiley and Sons, New York, 1964.

65. Lavoie, G. A., "Spectroscopic Measurements of Nitric Oxide in Spark Ignition Engines", Fluid Mechanics Laboratory Publication No. 70-4, M.I.T., 1970.

APPENDIX I

Sample Calculations and Data

A1.1 Sample Calculations

All data reduction was performed on a CDC 6400 digital computer at the University of California Computer Center, Berkeley Campus.

A sample calculation of the ideal gas temperature, transmittance, and emission-absorption temperature is presented for illustrative purposes.

A point in cycle I-1 has been used for these calculations. The operating conditions are shown in the tables below

Engine Conditions	
Fuel	propane
Compression ratio	7:1
Engine speed	1200 rpm
Ignition	38° btc
$\dot{M}_f$	0.059 lbm/min
$\dot{M}_a$	0.850 lb/min

Test Point Data	
Crank angle (θ)	4.5° atc
Pressure (P)	785 psia
Volume (V)	0.00368
$\overline{MW}$	27.3 lbm/lb mole
Wavelength (λ)	2.5 microns
V_{om}	0.280 volts
V_{gm}	0.355 volts
V_{bm}	0.440 volts

Ideal Gas Temperature

$$T = \frac{PV}{m\,\frac{R}{MW}}$$

$$m = m_{residual} + m_{propane} + m_{air}$$

$$= m_{residual} + (\dot{m}_f + \dot{m}_a)(2/rpm)$$

An average value of 3% may be taken for the value of the residual

$$m = 1.03\ (\dot{m}_f + \dot{m}_a)(2/rpm)$$

$$R = \frac{PV\ \overline{MW}}{1.03\ (\dot{m}_f + \dot{m}_a)(2/rpm)\ R}$$

$$T = \frac{PV\ \overline{MW}}{1.03\ (\dot{m}_f + \dot{m}_a)(2/rpm)\ R}$$

$$= \frac{(785)(144)(0.00368)(27.3)}{1.03(0.059+0.850)(2/1200)(1545)}$$

T = 4710°R or 2610°K

Transmittance

$$\tau_m = \frac{V_{bm} - V_{gm}}{V_{om}}$$

$$\tau_m = (0.440-0.355)/0.280$$

$$\tau_m = 0.304$$

Instrument Function

$$G' = \int_{\Delta\lambda} g(\lambda,\Delta\lambda)d\lambda = \frac{V_{std.}}{I_{std.}}$$

at 2.5 microns

$$I_{std.} = 16.70 \times 10^{10} \quad \left(\frac{erg}{cm^3\text{-sec-ster}}\right)$$

and the voltage deflection was measured to be

$V_{std.} = 0.0600$ volts

hence

$G' = 3.48 \times 10^{-13}$

Emission Absorption Temperature

$$T = \frac{hc}{\lambda k} \{\ln[\frac{2hc^2}{\lambda^5} \frac{(1-\tau_m(\lambda))}{V_{gm}} G'(\lambda) + 1]\}^{-1}$$

$$T = [\frac{(6.63\text{x}10^{-27})(3\text{x}10^{10})}{(2.5\text{x}10^{-4})(1.38\text{x}10^{-16})}] [\ln\{\frac{2(6.63\text{x}10^{-27})(3\text{x}10^{10})^2}{(2.5\text{x}10^{-4})^5}$$

$$\frac{(1-0.304)}{(0.355)} (3.48\text{x}10^{-13})+1\}]^{-1}$$

T = 2525°K

A1.2 Data

The data used in calculating the results for cycle I-1 to I-4 and G-1 to G-4 are given in tabulated form on the following pages.

CYCLE I-1

ENGINE SPEED	1200 rpm
IGNITION	38 deg btc (single)
COMPRESSION RATIO	7:1
$\dot{m}_f$	0.059 lb/min
$\dot{m}_a$	0.850 lb/min
$V_{om}(2.5)$	0.280 volts
$V_{om}(2.0)$	0.054 volts
$V_{om}(1.8)$	0.050 volts

ϕ (deg atc)	P (atm)	2.5μ V_{gm} (volts)	2.5μ V_{bm} (volts)	2.0μ V_{gm} (volts)	2.0μ V_{bm} (volts)	1.8μ V_{gm} (volts)	1.8μ V_{bm} (volts)
4.5	53.5	0.355	0.440	0.0244	0.0640	0.0214	0.0580
7.5	51.5	0.342	0.430	0.0220	0.0620	0.0190	0.0560
10.50	49.5	0.327	0.415	0.0190	0.0600	0.0170	0.0540
13.50	46.8	0.310	0.400	0.0174	0.0590	0.0154	0.0530
16.50	44.2	0.290	0.385	0.0160	0.0580	0.0140	0.0514
19.50	41.5	0.270	0.370	0.0140	0.0566	0.0110	0.0510
22.50	38.1	0.250	0.360	0.0130	0.0560	0.0100	0.0500

CYCLE I-2

ENGINE SPEED	1200 rpm
IGNITION	38 deg btc (single)
COMPRESSION RATIO	7:1
$\dot{m}_f$	0.059 lb/min
$\dot{m}_a$	0.850 lb/min
$V_{om}(2.5)$	0.280 volts
$V_{om}(2.8)$	0.054 volts
$V_{om}(1.8)$	0.050 volts

ϕ	P	2.5μ		2.0μ		1.8μ	
(deg atc)	(atm)	V_{gm} (volts)	V_{bm}	V_{gm} (volts)	V_{bm}	V_{gm} (volts)	V_{bm}
4.5	51.5	0.335	0.420	0.0240	0.0630	0.0226	0.0600
7.5	49.9	0.320	0.410	0.0220	0.0620	0.0210	0.0590
10.5	47.9	0.305	0.395	0.0206	0.0606	0.0194	0.0580
13.5	45.5	0.290	0.380	0.0190	0.0596	0.0180	0.0560
16.5	42.5	0.272	0.365	0.0170	0.0586	0.0164	0.0544
19.5	40.2	0.250	0.355	0.0150	0.0580	0.0140	0.0530

CYCLE I-3

ENGINE SPEED	1200 rpm
IGNITION	38 deg btc (single)
COMPRESSION RATIO	7:1
$\dot{m}_f$	0.059 lb/min
$\dot{m}_a$	0.850 lb/min
$V_{om}(2.5)$	0.280 volts
$V_{om}(2.8)$	0.054 volts
$V_{om}(1.8)$	0.050 volts

ϕ (deg atc)	P (atm)	2.5μ V_{gm} (volts)	2.5μ V_{bm} (volts)	2.0μ V_{gm} (volts)	2.0μ V_{bm} (volts)	1.8μ V_{gm} (volts)	1.8μ V_{bm} (volts)
4.5	52.2	0.345	0.435	0.0260	0.0664	0.0280	0.0640
7.5	50.5	0.330	0.425	0.0250	0.0650	0.0260	0.0626
10.5	48.2	0.315	0.410	0.0234	0.0640	0.0244	0.0614
13.5	45.5	0.300	0.390	0.0220	0.0624	0.0224	0.0596
16.5	42.8	0.282	0.375	0.0204	0.0620	0.0210	0.0590
19.5	40.5	0.260	0.365	0.0190	0.0606	0.0184	0.0574

CYCLE I-4

ENGINE SPEED	1200 rpm
IGNITION	38 deg btc (single)
COMRPESSION RATIO	7:1
$\dot{m}_f$	0.059 lb/min
$\dot{m}_a$	0.850 lb/min
$V_{om}(2.5)$	0.280 volts
$V_{om}(2.8)$	0.054 volts
$V_{om}(1.8)$	0.050 volts

ϕ (deg atc)	P (atm)	2.5μ (volts)		2.0μ (volts)		1.8μ (volts)	
		V_{gm}	V_{bm}	V_{gm}	V_{bm}	V_{gm}	V_{bm}
4.5	51.9	0.345	0.435	0.0230	0.0630	0.0240	0.0610
7.5	50.2	0.335	0.420	0.0220	0.0624	0.0230	0.0606
10.5	48.2	0.325	0.405	0.0204	0.0620	0.0210	0.0600
13.5	45.5	0.310	0.392	0.0194	0.0610	0.0196	0.0590
16.5	42.8	0.285	0.376	0.0176	0.0604	0.0180	0.0580
19.5	39.8	0.265	0.362	0.0150	0.0600	0.0170	0.0574

CYCLE G-1

ENGINE SPEED	1200 rpm
IGNITION	38 deg btc (dual)
COMPRESSION RATIO	7:1
$\dot{m}_f$	0.059 lb/min
$\dot{m}_a$	0.850 lb/min
$V_{om}(2.5)$	0.280 volts
$V_{om}(2.8)$	0.054 volts
$V_{om}(1.8)$	0.050 volts

ϕ (deg atc)	P (atm)	2.5μ V_{gm} (volts)	2.5μ V_{bm} (volts)	2.0μ V_{gm} (volts)	2.0μ V_{bm} (volts)	1.8μ V_{gm} (volts)	1.8μ V_{bm} (volts)
9.0	51.5	0.375	0.467	0.0200	0.0620	0.0180	0.0580
12.0	48.9	0.360	0.460	0.0190	0.0610	0.0164	0.0550
15.0	46.2	0.342	0.440	0.0170	0.0590	0.0150	0.0540
18.0	43.50	0.320	0.420	0.0156	0.0580	0.0140	0.0520
21.0	40.82	0.295	0.400	0.0136	0.0570	0.0120	0.0514
24.0	37.8	0.270	0.380	0.0120	0.0560	0.0106	0.0500

CYCLE G-2

ENGINE SPEED	1200 rpm
IGNITION	38 deg btc (dual)
COMPRESSION RATIO	7:1
$\dot{m}_f$	0.059 lb/min
$\dot{m}_a$	0.850 lb/min
$V_{om}(2.5)$	0.280 volts
$V_{om}(2.8)$	0.054 volts
$V_{om}(1.8)$	0.050 volts

ϕ	P	2.5μ		2.0μ		1.8μ	
(deg atc)	(atm)	V_{gm} (volts)	V_{bm}	V_{gm} (volts)	V_{bm}	V_{gm} (volts)	V_{bm}
16.5	45.5	0.337	0.437	0.0204	0.0620	0.0200	0.0580
19.5	42.8	0.315	0.415	0.0184	0.0610	0.0170	0.0564
22.5	39.8	0.290	0.395	0.0160	0.0600	0.0150	0.0544
25.5	36.8	0.270	0.380	0.0144	0.0590	0.0124	0.0530
28.5	34.5	0.245	0.365	0.0122	0.0570	0.0104	0.0520

CYCLE G-3

ENGINE SPEED	1200 rpm
IGNITION	38 deg btc (dual)
COMPRESSION RATIO	7:1
$\dot{m}_f$	0.059 lb/min
$\dot{m}_a$	0.850 lb/min
$V_{om}(2.5)$	0.280 volts
$V_{om}(2.8)$	0.054 volts
$V_{om}(1.8)$	0.050 volts

ϕ	P	2.5μ		2.0μ		1.8μ	
(deg atc)	(atm)	V_{gm} (volts)	V_{bm}	V_{gm} (volts)	V_{bm}	V_{gm} (volts	V_{bm}
9.0	51.2	0.375	0.475	0.0244	0.0660	0.0260	0.0620
12.0	49.2	0.355	0.460	0.0236	0.0650	0.0250	0.0610
15.0	46.2	0.340	0.442	0.0210	0.0640	0.0226	0.0600
18.0	43.8	0.320	0.427	0.0200	0.0630	0.0210	0.0590
21.0	41.2	0.295	0.415	0.0180	0.0620	0.0190	0.0580

CYCLE G-4

ENGINE SPEED	1200 rpm
IGNITION	38 deg btc
COMPRESSION RATIO	7:1
$\dot{m}_f$	0.059 lb/min
$\dot{m}_a$	0.850 lb/min
$V_{om}(2.5)$	0.280 volts
$V_{om}(2.8)$	0.054 volts
$V_{om}(1.8)$	0.050 volts

ϕ (deg atc)	P (atm)	2.5μ		2.0μ		1.8μ	
		V_{gm} (volts)	V_{bm}	V_{gm} (volts	V_{bm}	V_{gm} (volts)	V_{bm}
10.5	50.2	0.365	0.462	0.0230	0.0640	0.0250	0.0630
13.5	47.85	0.355	0.450	0.0220	0.0640	0.0240	0.0600
16.5	44.8	0.335	0.440	0.0206	0.0630	0.0220	0.0600
19.5	42.2	0.310	0.425	0.0190	0.0620	0.0200	0.0590
22.5	39.8	0.288	0.405	0.0170	0.0604	0.0184	0.0580

CALIBRATION DATA		
Wavelength (microns)	$I_{std.}$ (erg/sec-cm -ster)	$V_{std.}$ (volts)
2.5	16.70 x 10	0.0600
2.0	28.50 x 10	0.0110
1.8	39.50 x 10	0.0100

APPENDIX II

Error Analysis

A2.0 Root Mean Square Error

In this section propagation of experimental errors and their effects on the absolute values of the experimentally measured temperatures will be evaluated. These uncertainties are calculated from the root mean square error (r.m.s.) (see references (60) (63) for a detailed discussion).

The r.m.s. error is defined in the following manner. If a quantity Y is determined by the measurement of independent variables $x_1, x_2, \ldots x_n$ and the functional relationship $Y = f(x_1, x_2, x_3, \ldots x_n)$ then the uncertainty in the value of Y, U_Y due to uncertainties in the independent variables is given by

$$U_Y = \frac{dY}{Y} = \left[\sum_{i=1}^{N} \left(\frac{\partial \ln Y}{\partial \ln x_i} \quad \frac{dx_i}{x_i}\right)^2\right]^{1/2} \qquad \text{A3-1}$$

or

$$dY = \left[\sum_{i=1}^{N} \left(\frac{\partial Y}{\partial x_i} \; dx_i\right)^2\right]^{1/2} \qquad \text{A3-2}$$

A2.1 Bulk Temperature

$$T = \left[\frac{PV\,\overline{MW}}{R}\right] \left[\frac{RPM}{2.06\,(\dot{m}_f + \dot{m}_a)}\right]$$

Performing the differention equation A3-1 becomes

$$U_T = \left(\frac{dP}{P}\right)^2 + \left(\frac{dV}{V}\right)^2 + \left(\frac{d\,\overline{MW}}{\overline{MW}}\right)^2 + \left(\frac{d(RPM)}{RPM}\right)^2 + \left(-\,\frac{d(\dot{m}_f + \dot{m}_a)}{\dot{m}_f + \dot{m}_a}\right)^2 \qquad \text{A3-3}$$

Below are estimated uncertainties in the measured independent variables.

$$\frac{dP}{P} = 0.02$$

$$\frac{dv}{v} = 0.01$$

$$\frac{d\,\overline{MW}}{\overline{MW}} = 0.004$$

$$\frac{d(RPM)}{RPM} = 0.003$$

$$\frac{d(\dot{m}_f + \dot{m}_a)}{(\dot{m}_f + \dot{m}_a)} = 0.01$$

Substituting the above uncertainties along with typical experimental values of the independent variables the uncertainty in the calculated bulk temperature is

$$\frac{dT}{T} = 0.025$$

which for typical experimental values is approximately 60°K.

A2.2 Emission-Absorption Temperature

$$T_{E-A} = \frac{hc}{\lambda k} \{\ln[\frac{2hc^2}{x^5} \frac{(1 - \tau_m(\lambda))}{V_{gm}} G'(\lambda) + 1]\}^{-1}$$

Applying equation A3.2 to the equation above

$$dT_{E-A} = [(\frac{\partial T_{E-A}}{\partial \lambda})^2 d\lambda^2 + (\frac{\partial T_{E-A}}{\partial V_{gm}})^2 dV_{gm}{}^2 + (\frac{\partial T_{E-A}}{\partial G'})^2 dG'^2$$

$$(\frac{\partial T_{E-A}}{\partial \tau_m})^2 d\tau_m{}^2]^{1/2}$$

Performing the differentiation and defining

$$f = \frac{2hc^2}{\lambda^5} \frac{(1 - \tau_m(\lambda))}{V_{gm}} G'(\lambda)$$

$$dT_{E-A} = \frac{(hc/\lambda k)}{[\ln(f+1)]^2} \left(\frac{f}{f+1}\right) \{[\frac{5f-(1+f)\ln(f+1)}{f}]^2 \left(\frac{d\lambda}{\lambda}\right)^2 + \left(\frac{dV_{gm}}{V_{gm}}\right)^2$$

$$+ \left(\frac{dG'(\lambda)}{G'(\lambda)}\right)^2 + \left(\frac{\tau_m(\lambda)}{1-\tau_m(\lambda)}\right)^2 \left(\frac{d\tau_m(\lambda)}{\tau_m(\lambda)}\right)^2\}^{1/2} \qquad \text{A3.4}$$

the transmittance $\tau_m(\lambda)$ is given in terms of the experimentally measured quantities

$$\tau_m(\lambda) = \frac{V_{bm}(\lambda) - V_g(\lambda)}{V_{om}(\lambda)}$$

and its uncertainty is dependent on the uncertainties of $V_{bm}(\lambda)$, $V_g(\lambda)$, $V_{om}(\lambda)$. Applying equation A3-1 to the above equation for the transmittance

$$\frac{d\,\tau_m(\lambda)}{\tau_m(\lambda)} = [\left(\frac{dV_{bm}(\lambda)}{V_{bm}(\lambda) - V_{gm}(\lambda)}\right)^2 + \left(\frac{dV_{gm}(\lambda)}{V_{bm}(\lambda) - V_{gm}(\lambda)}\right)^2 +$$

$$\left(\frac{dV_{om}(\lambda)}{V_{om}(\lambda)}\right)^2]^{1/2}$$

Typical values of $V_{bm}(\lambda)$, $V_{gm}(\lambda)$ and $V_{om}(\lambda)$ along with estimates of the uncertainties are shown below for typical conditions near the peak pressure portion of the cycle.

Wavelength →	2.4μ	2.0μ	1.8μ
V_{om}, volts	0.275	0.056	0.053
V_{gm}, volts	0.355	0.0244	0.0214
V_{bm}, volts	0.440	0.064	0.058
dV_{om}, dV_{gm}, dV_{bm}	0.005	0.001	0.001

Substituting these values into the above expression the uncertainties in the measured transmittances is

$$\left(\frac{d\tau_m(2.5)}{\tau_m(2.5)}\right)_{2.5\mu} = 8.5\%, \qquad \tau_m(2.5) = 0.309$$

$$\left(\frac{d\tau_m(2.0)}{\tau_m(2.0)}\right)_{2.0\mu} = 4.0\%, \qquad \tau_m(2.0) = 0.695$$

$$\left(\frac{d\tau_m(1.8)}{\tau_m(1.8)}\right)_{1.8\mu} = 4.3\%, \qquad \tau_m(1.8) = 0.692$$

Typical values of experimental data are shown in the table below, for the three wavelengths, along with estimates of these uncertainties,

Value ↓	Wavelength →	2.5	2.0	1.8
$\tau_m(\lambda)$		0.309	0.695	0.692
$V_{gm}(\lambda)$		0.355	0.0244	0.0214
$G'(\lambda)$		3.84×10^{-13}	3.86×10^{-14}	2.78×10^{-14}
$d\lambda/\lambda$		.001	.001	.001
$d\tau_m/\tau_m$		0.085	0.040	0.043
dV_{gm}/V_{gm}		0.014	0.04	0.046
dG'/G'		.01	.01	.01

Substituting these values into equation A3.4 the uncertainties of the temperature determined from the emission absorption technique are

$$\Delta T_{E-A}\ (2.5\mu) = 40°K \quad \text{or } 1.6\%$$

$$\Delta T_{E-A}\ (2.0\mu) = 84°K \quad \text{or } 3.4\%$$

$$\Delta T_{E-A}\ (1.8\mu) = 81°K \quad \text{or } 3.2\%$$

A2.3 Calculated Transmittance

An estimate of the uncertainty in the calculated value of the transmittance can be obtained from a simplified Beer's law expression

$$\tau = e^{-(s/d)_{stp}(T_o/T)\, P_T\, x_{H_2O}\, l}$$

According to equation A3-4

$$U_\tau = \varepsilon \left[\left(\frac{d\ s/d}{s/d}\right)^2 + \left(\frac{dT}{T}\right)^2 + \left(\frac{dP_T}{P_T}\right)^2 + \left(\frac{d\ x_{H_2O}}{x_{H_2O}}\right)^2\right]^{1/2}$$

where

$$\varepsilon = \left(\frac{s}{d}\right)_{stp} \left(\frac{T_o}{T}\right) P_T\, x_{H_2O}\, l$$

Substituting the following estimated values of the uncertainties

$\frac{d(s/d)}{s/d} = 0.1$, $s/d = 0.2$

$\frac{dT}{T} = 0.02$, $T = 2500°k$

$\frac{dP_T}{P_T} = 0.02$, $P = 50$ atm

$\frac{dx_{H_2O}}{x_{H_2O}} = 0.02$, $x_{H_2O} = 0.15$

$l = 8.25$ cm

The uncertainty in the calculated values of the transmittances is

$$U_\tau = 5\%$$

A2.4 Temperature Distribution

An estimate of the probable uncertainty in the determination of a temperature distribution can be obtained by simplifying equation (3.1-7) to two zones. To this approximation the emergent intensity at wavelength λ is given by

$$I(L,\lambda) = I_b(\lambda,T_1)(1-\tau_1)(\tau_2) + I_b(\lambda,T_2)(1-\tau_2)$$

rearranging this equation the temperature in zones #1 is given by

$$T_1 = \frac{hc}{\lambda k}\left[\ln\left\{\frac{2hc^2}{\lambda^5}\left(\frac{(1-\tau_1)\,\tau_2}{\frac{V_{gm}}{G'} - \frac{2hc^2}{\lambda^5}\left(e^{hc/\lambda T_2}-1\right)(1-\tau_2)}\right)+1\right\}\right]^{-1}$$

The uncertainty in the zonal temperature T_1 is obtained from equation A3.2

$$dT_1 = \left\{\left(\frac{\partial T_1}{\partial V_{gm}}\right)^2 dV_{gm}^{\,2} + \left(\frac{\partial T_1}{\partial G'}\right)^2 dG'^2 + \left(\frac{\partial T_1}{\partial \tau_1}\right)^2 d\tau_1^{\,2} + \left(\frac{\partial T_1}{\partial \tau_2}\right)^2 d\tau_2 + \left(\frac{\partial T_1}{\partial T_2}\right)^2 dT_2^{\,2}\right\}^{1/2}$$

The uncertainty in T_1 due to an uncertainty in the wavelength λ has been neglected since it is negligible compared to the other terms.

Performing the differentiation the uncertainty is given by

$$dT_1 = \frac{T_1^{\,2}}{A(H+1)}\left\{\left(\frac{H}{BG'}\right)^2\left[dV_{gm}^{\,2} + \left(\frac{V_{gm}}{BG'}\right)^2 dG'^2\right] + H^2\left[\left(\frac{d\tau_1}{1-\tau_1}\right)^2 + \left(\frac{d\tau_2}{\tau_2}\right)^2\right] + \left(\frac{HDA}{BT_2^{\,2}}\right) e^{A/T_2}\, dT_2^{\,2}\right\}^{1/2}$$

where

$$A = \frac{hc}{\lambda k} \quad , \qquad D = \frac{2hc^2}{\lambda^5}$$

$$B = \frac{V_{gm}}{G'} - D(e^{A/T_2} - 1)(1-\tau_2)$$

$$H = \frac{D}{B}\ (1-\tau_1)\tau_2$$

Substituting the values in the previous table for 2.5 microns along with the following estimated values

$\tau_1 = \tau_2 = 0.55$

$d\tau_1 = d\tau_2 = 0.05$

$T_1 = 2300°K$

$T_2 = 2700°K$

$dT_2 = 100°K$

into the above equation yields an uncertainty of

$$\frac{dT_1}{T_1} = 1\% \text{ or } 25°K$$

in the calculated value of T_1. Since the actual determination of T_1 entails the solution of a set of either two or three equations it is anticipated that the actual uncertainty is probably double or triple (50°K, 75°K) than the value of 25°K calculated above.

APPENDIX III

Solution of Non Linear Algebraic Equations

Newton's method was used to solve the system of nonlinear equations for the zonal temperatures in section 5-4. Newtons method for the solution of a system of three equations and three unknowns will be developed in this section since this was the order of the system employed in section 5-4.

The problem at hand is finding the solution to the following sytem of equations.

$$Z_1(x_1,X_2,X_3) = 0$$

$$Z_2(x_1,x_2,x_3) = 0$$

$$Z_3(x_1,x_2,x_3) = 0$$

where Z_1, Z_2, and Z_3 are defined and differentiable in a volume V in (X_1,X_2,X_3) space around the desired solution $x_1=x_{1s},x_2=x_{2s},x_3=x_{3s}$.

Newtons method proceeds as follow: If (x_1,x_2,x_3) is a point in the vicinity of the correct solution and $x_1+\delta,x_2+\varepsilon,x_3+\xi$ is a better approximation to the solution we may find δ,ε and ξ by expanding z_1, z_2, z_3 in a Taylor series.[64]

$$\left[Z_i(x_1+\delta,x_2+\varepsilon,x_3+\xi) = Z_i(x_1,x_2,x_3)+(\partial Z_i/\partial x_1)\delta+(\partial Z_i/\partial x_2)\varepsilon + (\partial Z_i/\partial x_3)\xi\right]_{i=1,2,3}$$

where the Taylor series has been truncated after the first term.

Setting the above equations equal to zero one is left with a linear system of equations in terms of the corrections δ,ε,ξ.

$$\left[(\partial Z_i/\partial x_1)\delta + (\partial Z_i/\partial x_2)\varepsilon + (\partial Z_i/\partial x_3)\xi = -Z_i(x_1,x_2,x_3) \right]_{i=1,2,3}$$

The linear system above may easily be solved for δ, ε, ξ with Gaussian elimination. The functions are then expanded around the new point $(x_1+\delta, x_2+\varepsilon, x_3+\xi)$ and new correction terms are found $\delta',\varepsilon',\xi'$. The process is repeated until the correction terms are negligible.

Question now arises as to the uniqueness of the solution found from the method described above. It can be shown that if the Jacobian determinant is non zero at the solution (x_1^0,x_2^0,x_3^0) of Z_1,Z_2,Z_3 then there is no other solution to the system of equations other than (x_1^0,x_2^0,x_3^0) in a certain vicinity of (x_1^0,x_2^0,x_3^0). [64]

APPENDIX IV

Fortran Listing - Analyticl Combustion Model

```
C      MAIN PROGRAM
       REAL NORA,NORB
       REAL T[illegible]),MO(20,40),MWT(40),MNO(20,40),MT(40),[illegible]
       DIMENSION XY(11,30,40),T(30,40),P(40),V(30),[illegible](30,40),
      1AMO(30),[illegible](30),VO(30),CO(30),GAM(30,40),CP(30,40),[illegible],[illegible](30),
      2VZ(30),[illegible](30,40),R(30,40),MU(30),X1(11),X2(11),[illegible](40),[illegible](40)
      3VCO(30),ZZ(40),TIME(40)
       REAL [illegible],NORN,MW(30,40)
       REAL DEN(30,40)
       COMMON/[illegible]/A(11)
       COMMON/[illegible]/ALF,UFF,HFF
       COMMON/[illegible]/AN(11)
       COMMON/[illegible]/W,X,YFL,ZFL,YSTOA,ZSTOA,PHE
       COMMON/[illegible]A/AM,BM,CM,DM,RHO,AMWO
       COMMON/[illegible]/BORE
       COMMON/AS[illegible]/KLM
       COMMON/TRIG/ML
       COMMON/ROCK/LJK
       INTEGER W
       REAL MCON
       REAL MCOPC
       DATA(AM(LL),LL=1,11)/0.5,0.,0.,-0.5,0.5,0.,0.,0.5,0.,0.5,0./
       DATA(A(I),I=1,11)/1,2,3,4,6,7,9,12,13,14,15/
25     READ 100,PHE
100    FORMAT(F5.3)
       IF(PHE.EQ.0.)GO TO 26
       PRINT 105,PHE
105    FORMAT(1H1,50X,*PHE=*,F5.3)
C      PROPANE
       IYP=0
       IZP=0
       JAMM=0
       AMWF=44.
       W=3.
       X=8.
       YFL=0.
       ZFL=0.
       YSTOA=10.
       ZSTOA=37.7
       UFF=-22874.
       HFF=-24750.
       AF=-0.966
       BF=0.07279
       CF=-0.00003755
       DF=7.58E-09

       AMWO2=32.
       AMWN2=28.
       AO2=6.085
       BO2=0.00363
       CO2=-1.709E-06
       DO2=3.133E-10
       AN2=6.903
      BN2=-0.0003753
      CN2=1.95E-06
      DN2=-5.851E-10
      UFO2=0.
      UFN2=0.
C     EVALUATE XI AND YI FOR THE UNBURNED MIXTURE
      AA=1.0+((YSTOA+ZSTOA)/(2.*PHE))
      XUF=1./AA
      XUO2=(YSTOA/(2.*PHE))/AA
      XUN2=(ZSTOA/(2.*PHE))/AA
C     MEAN CP COEFF.
      AM=XUF*AF+XUO2*AO2+XUN2*AN2
      BM=XUF*BF+XUO2*BO2+XUN2*BN2
      CM=XUF*CF+XUO2*CO2+XUN2*CN2
      DM=XUF*DF+XUO2*DO2+XUN2*DN2
C     BVEL IS THE RATE OF PROPAGATION OF THE FLAME INTO THE UNBURNED G
      AMWU=XUF*AMWF+XUO2*AMWO2+XUN2*AMWN2
      RMU=82.054/AMWU
C     THE INDUCTION CONDITIONS ARE
      TIN=298.
      PIN=1.0
C     THE VOLUME AT BDC IS
      CALL VOLUME(180.,VBDC,EZBC)
C     THE VOLUME AT THE POINT OF IGNITION IS
      CALL VOLUME(-40.,VSPK,EZO)
C     THE THERMODYNAMIC STATE AT THE IGNITION POINT IS
      CALL ISENV(TIN,PIN,VBDC,TI,PI,VSPK)
      TMASS=PIN*VBDC*AMWU/(82.05**TIN)
      VI=VSPK/TMASS
C     NOW THE FIRST INCREMENT OF MASS WILL BURN
      DELANG=5.
      BVEL=500.
      NJK=0
      THET=-40.
      TIM=0.
      THET=THET+DELANG
      RPM=1200.
      DELTIM=DELANG/(6.*RPM)
      TIM=TIM+DELTIM
      CALL VOLUME(THET,VOL,EZ(1))
      DRAD=BVEL*DELTIM
C     THE INITIAL PROPAGATION IS
      RU=DRAD
C     THE VOLUME OF THE UNBURNED MASS CONSUMED IS
      CALL VH(0.,RU,VCON,EZO)
      MCON=VCON/VI
C     THE PER CENT OF THE MASS CONSUMED IS
      MCOPC=(MCON/TMASS)*100.
C     NOW WE ARE SET FOR THE FIRST ITERATION
C     ASSUME A FINAL PRESSURE PF
      PRINT342,PI,TI
342   FORMAT(5X,*PI=*,F10.5,*TI=*,F7.2)
      CALL ISENV(TI,PI,VSPK,TFT,PF,VOL)
      PF=PF+5.
```

```
3       CALL ISENUN(TI,PI,VI,TUF,PF,VUF)
        CALL UNENG(TI,UI,HI)
        CALL UNENG(TUF,UF,HF)
        AMS(1)=MCON
C       THE WORK DONE ON THE UNBURNED GAS IS
        WKU=(TMASS-MCON)*(UF-UI)
C       USING THE TRAPEZOIDAL RULE TO FIND THE WORK ON THE PISTON
        WKT=0.01255*(PF+PI)*(VOL-VSPK)
C       THE WORK DONE BY THE BURNING ZONE
        WKS=(WKT+WKU)/AMS(1)
        LUK=4
        CALL BURN(TI,PI,VI,UI,TFB,PF,VFB,UFB,WKS,XB,SB,GAB,CVAB,CPAB,MW(1
       11))
        LUK=0
C       NOW CHECK THE VOLUME
        AVOL=VFB*MCON+VUF*(TMASS-MCON)
        DVOL=VOL-AVOL
        IF(ABS(DVOL/VOL).LT.0.001)GO TO 4
        PNEW=PF*((AVOL/VOL)**1.4)
        PF=PF+(0.55*(PNEW-PF))
        GO TO 3
4       CONTINUE
C       THE FIRST ZONE HAS BURNED ( THE FIAL STATE POINTS ARE
        P(1)=PF
        TU(1)=TUF
        AMU(1)=TMASS-AMS(1)
        VU(1)=VUF
        T(1,1)=TFB
        V(1,1)=VFB
        VOLE(1)=VOL
        THETA(1)=THET
        VCU(1)=VCON
        TIME(1)=TIM
C       K REPRESENTS THE CONDITIONS AFTER THE K-TH INCREMENT OF MASS HAS
C       BURNED
        K=0
5       K=K+1
        NXYP=1
        BVEL=500.+(40.+THETA(K))+0.36*((40.+THETA(K) )**2)
C       ZONE LOCATION ROUTINE
34      CONTINUE
        IF(IYP.EQ.1)K=K+1
        IF(IYP.EQ.1)JNZ=K
        IF(IYP.EQ.1)NJK=1
        IF(IYP.EQ.1)IZP=1
        IYP=0
        IF(ITP.EQ.1)IYP=0
        KZONE=K
        IF(IZONE.EQ.1)KZONE=JNZ
        EZ=ZZ(K)
        AL=BORE/2.
        R(1,K)=JRAD
        XB1=R(1,K)/(2*AL)
800     XOLD=XB1
```

```
      XR2=XR1**2
      CD=(2*XR2-1.)*ACOS(XR1)-XR1*SQRT(1.-XR2)
      CE=-ACOS(0.)
      GG=2*(AL**2)*EZ*(CD-CE)-V(1,K)*AMS(1)
      GP=8*(AL**2)*EZ*XR1*ACOS(XR1)
      XR1=XR1-(GG/GP)
      IF(ABS(XR1-XOLD).GT.0.01)GO TO 800
      R(1,K)=XR1*2*AL
      NZ=K+1
      IF(K.LT.2)GO TO 803
      DO 802 I=2,NZONE
      R(I,K)=R(I-1,K)+1.
      XRI=R(I,K)/(2.*AL)
      IF(XRI.GT.1.0)GO TO 861
  862 CONTINUE
  801 XOLDD=XRI
      XRI2=XRI**2.
      XRII=R(I-1,K)/(2.*AL)
      IF((XRII-1.))866,861,861
  866 CONTINUE
      IF((XRI-1.))865,861,861
  865 CONTINUE
      XRII2=XRII**2
      FI=(2*XRI2-1.)*ACOS(XRI)-XRI*SQRT(1.-XRI2)
      FI2=(2*XRII2-1.)*ACOS(XRII)-XRII*SQRT(1.-XRII2)
      GGG=2*(AL**2)*EZ*(FI-FI2)-V(I,K)*AMS(I)
      GGP=8*(AL**2)*EZ*XRI*ACOS(XRI)
      XRI=XRI-(GGG/GGP)
      IF(ABS(XRI-XOLDD).GT.0.01)GO TO 801
      R(I,K)=XRI*2*AL
      GO TO 802
  861 R(I,K)=10.
  802 CONTINUE
      IF(IZONE.EQ.1)GO TO 660
      IF(NJK.EQ.1)GO TO 600
      IF(IZP.EQ.1)GO TO 600
  803 CONTINUE
C     INCREMENT THE CRANKANGLE, TIME, ETC.
      TIME(K+1)=TIME(K)+DELTIM
      THETA(K+1)=THETA(K)+DELANG
      CALL VOLUME(THETA(K+1),VOLE(K+1),ZZ(K+1))
      DRAD=BVEL*DELTIM
      P(K+1)=2.*P(K)
      RP=R(K,K)+DRAD
      IF(RP.GT.3.99)GO TO 701
C     THE VOLUME CONSUMED
      CALL VB(R(K,K),RP,VCU(K+1),ZZ(K+1))
C     THE MASS CONSUMED
      AMS(K+1)=VCU(K+1)/VU(K)
      AMB=0.
      DO 870 I=1,NZ
  870 AMB=AMB+AMS(I)
      AMU(K)=TMASS-AMB
      PRINT300,K,TMASS,AMU(K),AMS(K),AMB
```

```
 350    FORMAT(1H1,*K=*,I2,/,4(5X,E10.4,/))
        PMB=(AMB-AMS(K+1))*100./TMASS
        IF(PMB.GE.100.)GO TO 650
        IF(PMB.EQ.100.)GO TO 704
 642    CONTINUE
 6      CALL ISENUN(TU(K),P(K),VU(K),TU(K+1),P(K+1),VU(K+1))
        JK=JK+1
        IF(JK.EQ.50)GO TO 25
        CALL UNENG(TU(K),UU(K),HU(K))
        CALL UNENG(TU(K+1),UU(K+1),HU(K+1))
 C      ISENTROPIC COMPRESSION OF THE UNBURNED GAS
        JK=0
        GO TO 205
 204    WKU=0.
        VOLU=0.
        VU(N)=0.
        TU(N)=0.
 205    CONTINUE
        GO TO 702
 701    CONTINUE
        AMS(K+1)=AMU(K-1)
 704    CONTINUE
        CALL UNENG(TU(K),UU(K),HU(K))
        UU(K+1)=0.
        NXP=1
        WKU=0.
        AMU(K)=0.
        PMB=100.
        PMB=(AMB-AMS(K+1))/TMASS
        IYP=1
        AMB=TMASS
 702    CONTINUE
 C      ISENTROPIC COMPRESSION OF THE BURNED GAS ZONES
        DO 8 L=1,K
        CALL ISENNG(T(L,K),P(K),V(L,K),S(L,K),U(L,K),T(L,K+1),P(K+1),
       1V(L,K+1),S(L,K+1),U(L,K+1),X1,X2,GAM(L,K),GAM(L,K+1),MW(L,K+1))
        DO 7 I=1,11
        XY(I,L,K)=X1(I)
 7      XY(I,L,K+1)=X2(I)
 8      CONTINUE
 C EVALUATION OF THE WOK DONE BY THE BURNING ZONE
        IF(NXP.EQ.1)GO TO 703
        WKU=AMU(K)*(UU(K+1)-UU(K))
 703    CONTINUE
 206    CONTINUE
        WKB=0.
 C      THE WORK BY THE BURNED GAS
        DO 9 I=1,K
        WKB=WKB+AMS(I)*(U(I,K+1)-U(I,K))
 9      CONTINUE
 C      THE WORK ON THE PISTON DURING THE INREMENT
        IF(K.EQ.1)GO TO 351
        A1=(P(K+1)-P(K))/(VOLE(K+1)-VOLE(K))
        A2=(P(K-1)-P(K))/(VOLE(K-1)-VOLE(K))
```

```
      A3=VOLE(K+1)-VOLE(K-1)
      IF(A3.EQ.0.0)GO TO 351
      CW=(A1-A2)/A3
      BW=((P(K-1)-P(K))/(VOLE(K-1)-VOLE(K)))-CW*(VOLE(K-1)+VOLE(K))
      AW=P(K)-BW*VOLE(K)-CW*VOLE(K)**2
      A4=AW*(VOLE(K+1)-VOLE(K))
      A5=0.5*BW*(VOLE(K+1)**2-VOLE(K)**2)
      A6=0.333*CW*(VOLE(K+1)**3-VOLE(K)**3)
      WKS=A4+A5+A6
      WKS=WKS*0.0241
      GO TO 352
351   CONTINUE
      WKS=0.5*(P(K+1)+P(K))*(VOLE(K+1)-VOLE(K))*0.0241
352   CONTINUE
      WKT=WKU+WKB+WKS
      WKT=WKT/AMS(K+1)
C     EVALUATE PROPERTIES OF THE BURNING ZONE
      CALL BURN(TU(K),P(K),VU(K),UU(K),T(K+1,K+1),P(K+1),V(K+1,K+1),
     1U(K+1,K+1),WKT,XB,S(K+1,K+1),GAM(K+1,K+1),CV(K+1,K+1),CP(K+1,K+1)
     1MW(K+1,K+1))
      IF(NLM.EQ.3)GO TO 640
      IF(ML.EQ.1)GO TO 643
      GO TO 641
643   P(K+1)=P(K+1)/1.1
      GO TO 642
640   P(K+1)=P(K+1)*1.2
      GO TO 642
641   CONTINUE
      DO 10 I=1,11
10    AY(I,K+1,K+1)=XB(I)
C     VOLUME CHECK
      VOLU=AMU(K)*VU(K+1)
      VOLB=0.
      NZ=K+1
      DO 363 I=1,NZ
363   VOLB=VOLB+AMS(I)*V(I,K+1)
      VOLT=VOLU+VOLB
      DVOL=VOLE(K+1)-VOLT
      IF(ABS(DVOL/VOL).LT.0.001)GO TO 22
      IF(ABS(DVOL).LT.1.0)GO TO 22
      PNEW=P(K+1)*((VOLT/VOLE(K+1))**1.4)
      P(K+1)=P(K+1)+(0.2*(PNEW-P(K+1)))
      IZONE=0
      GO TO 5
22    CONTINUE
C      ALL THE PRINT STATEMENTS GO HERE
      LM=0
660   CONTINUE
      KZONE=K
      IF(IZONE.EQ.1)KZONE=JNZ
      TB(K)=P(K)*VOLE(K)*27.5/TMASS*(1/82.054)
      CALL EQUILIB(TB(K),P(K),AJZ,XZ)
      ANOB=XZ(6)
      JAMM=JAMM+1
      PRINT 101,K
101   FORMAT(1H1,////,50X,*K=*,I3)
      PRINT 371,THETA(K)
371   FORMAT(//,30X,*CRANK SHAFT ANGLE=*,F8.2)
      PRINT 863,PMB
863   FORMAT(20X,F6.2,1X,*PER CENT OF THE MASS HAS BEEN BURNED*)
      PRINT 372,VOLE(K)
372   FORMAT(20X,*THE COMBUSTION CHAMBER VOLUME (CC.) = *,F7.3)
      PRINT106,AMS(K)
106   FORMAT(20X,*THE MASS CONSUMED DURING THIS INCREMENT IS  *,E10.4)
      PRINT 31,K,TB(K),ANOB
31    FORMAT(50X,*TB(*,I2,*)= *,F7.2,2X,*NO(BULK)= *,E10.4)
      PRINT 104,K,P(K),K,TU(K),K,VU(K)
104   FORMAT(///,1X,*P(*,I2,*)= *,F7.3,10X,*TU(*,I2,*)= *,F7.2,10X,
     1*VU(*,I2,*)= *,E16.8)
      DO 400 I=1,KZONE
      PRINT 401,I,K,T(I,K),I,K,MW(I,K),I,K,R(I,K)
401   FORMAT(10X,*T(*,I2,*,*,I2,*) =*,F7.2,15X,*MW(*,I2,*,*,I2,*) = *,
     1E16.8,15X,*R(*,I2,*,*,I2,*)= *,F7.4)
400   CONTINUE
      PRINT 450
450   FORMAT(///,3X,*ZONE*,9X,*XH*,8X,*XOH*,7X,*XH2*,6X,*XH2O*,
     17X,*XN*,8X,*XNO*,7X,*XN2*,7X,*XO*,8X,*XO2*,7X,*XCO*,6X,*XCO2*)
      DO 452 J=1,KZONE
      PRINT 451,J,K,(XY(I,J,K),I=1,11)
451   FORMAT(//,1X,*(*,I2,*,*,I2,*)*,5X,11(F8.5,2X))
      IF(PRE.EQ.1.0)GO TO 25
452   CONTINUE
      IF(IYP.EQ.1)GO TO 340
      GO TO 600
679   K=K+1
      IYP=0
      JNZ=K
      GO TO 660
681   CONTINUE
      IF(NXYP.EQ.3)GO TO 656
      IF(PMB.EQ.100.)GO TO 656
      IF(NJK.EQ.1)GO TO 636
      GO TO 5
656   CONTINUE
C  ISENTROPIC EXPANSION OF THE BURNED GAS
657   CONTINUE
      IF(THETA(K).GT.90.)GO TO 601
      P(K+1)=P(K)*0.9
      NXYP=3
      LM=1
      VOLB=0.
      DO 659 L=1,JNZ
      CALL ISENBG(T(L,K),P(K),V(L,K),S(L,K),U(L,K),T(L,K+1),P(K+1),
     1V(L,K+1),S(L,K+1),U(L,K+1),X1,X2,GAM(L,K),GAM(L,K+1),MW(L,K+1))
      VOLB=VOLB+AMS(L)*V(L,K+1)
      DO 658 I=1,11
      XY(I,L,K)=X1(I)
658   XY(I,L,K+1)=X2(I)
```

```
659   CONTINUE
      CALL TEFIN(VOLB,THETA(K),THETA(K+1))
      K=K+1
      TU(K)=0.
      VU(K)=0.
      CALL VOLUME(THETA(K),VOLE(K),ZZ(K))
      KMAX=K
      IZONE=1
      GO TO 340
661   CONTINUE
      DO 979 I=1,KMAX
      K=1
      PRINT 973
973   FORMAT(1H1,3X,*ZONE*,2X,*TIME STEP  NO KINETIC  NO EQUILIB*,
     1*RATIO KIN/EQ*)
       NOMA=0.
      NOKO=0
978   K=K+1
      IF(K.EQ.KMAX)GO TO 979
      DEN(I,K)=P(K)*MW(I,K)/(82.054*T(I,K))
      CALL NOKIN(T(I,K),DEN(I,K),XY(9,I,K),XY(7,I,K),XY(8,I,K),
     1XY(5,I,K),NOKO,NOKN,DELTIM,MW(I,K))
      RAT=NOKN/XY(5,I,K)
      PRINT974,I,K,NOKN,XY(5,I,K),RAT
974   FORMAT(3X,I2,3X,I2,3X,F10.9,2X,F10.9,3X,E10.4)
      NOKO=NOKN
      IF(K.EQ.(KMAX-1))NOMA=NOKN*AMS(I)/MW(I,K)
      IF(I.EQ.KMAX.AND.K.EQ.(KMAX-1))NOKB=NOMA*TPASS/28
      GO TO 978
979   PRINT 987,NOKB
987   FORMAT(10X,*KINETIC NO MOLE FRACTION AT FROZEN POINT  *,E10.4)
20    STOP
      END
      SUBROUTINE EQUILIB(T,P,AMMC,XC)
      COMMON/EQ/TEQ,PEQ,K,XH2,XH2O,XCO,XCO2,XN2,XNO,XOH,XH,XO,XN,XO2
      COMMON/JANE/W,X,YFL,ZFL,YSTOA,ZSTCA,PHE
      COMMON/SOME/SMH,SMOH,SMH2,SMH2O,SMN,SMNO,SMN2,SMO,SMO2,SMCO,SMCO
      COMMON/ASFG/LM
      DIMENSION XC(11)
      TEQ=1.8*T
      PEQ=14.7*P
      K=1
      IF(PHE-1.)4,4,5
 4    CALL SPECY1
      GO TO 6
 5    CALL SPECY2
      IF(LM.EQ.7)GO TO 9
 6    K=K
      XC(1)=XH
      XC(2)=XOH
      XC(3)=XH2
      XC(4)=XH2O
      XC(5)=XN
      XC(6)=XNO
      XC(7)=XN2
      XC(8)=XO
      XC(9)=XO2
      XC(10)=XCO
      XC(11)=XCO2
      IF(K-2)200,8,8
 8    XO2=0.
      XN2=0.
      XH2O=0.
      XCO2=0.
      XCO=0.
      XOH=0.
      XN=0.
      XO=0.
      XNO=0.
      XH2=0.
      XH=0.
      MM=1
      IF(MM.EQ.1)GO TO 980
 987  PRINT 981
 981  FORMAT(*SPECIES NEGATIVE*)
 980  CONTINUE
      AMMC=2.*XH2+28.*XN2+18.*XH2O+17.*XOH+1.*XH+30.*XNO+14.*XN+32.*XO
     1+16.*XO+44.*XCO2+28.*XCO
 9    RETURN
      END
      SUBROUTINE SPECY1
      COMMON/JANE/W,X,YFL,ZFL,YSTOA,ZSTOA,PHE
      COMMON/EQ/TEQ,PEQ,K,XH2,XH2O,XCO,XCO2,XN2,XNO,XOH,XH,XO,XN,XO2
      COMMON/SOME/SMH,SMOH,SMH2,SMH2O,SMN,SMNO,SMN2,SMO,SMO2,SMCO,SMCO,
      T=TEQ
      YS=(YFL+YSTOA/PHE)
      ZS=(ZFL+ZSTOA/PHE)
      A=1./(W+(X+ZS)/2.)
      B=30000.0/EXP(T/620.)
      G=0.0
      G35=0.0
      G36=0.0
      G37=0.0
      G38=0.0
      P=PEQ/14.7
      G1=SQRT(P)
C     EQUILIBRIUM CONSTANT EVALUATION FOLLOWS
      XK1=10.**(1.11059-205.213*(100./T)+0.21953*ALOG(T))
      XK2=10.0**(2.38548-235.575*(100./T)+0.11952*ALOG(T))
      XK3=10.0**(3.46218-449.882*(100./T))
      XK4=10.0**(3.0455-400.976*(100./T)+0.32653*ALOG(T))
      XK5=10.0**(2.98031-267.867*(100./T)+0.08329*ALOG(T))
      XK6=10.0**(5.69695-42.5732*(100./T)-0.60653*ALOG(T)+(2.9687E-03)
     1T/100.))
      XK7=10.0**(2.24799-315.992*(100./T)+0.1563 *ALOG(T))
C     THE TRIAL VALUES FOR A AND B ARE NOW USED TO COMPUTE DISTRIBUTUI
    1 ALFA=(XK5*B+XK1)/(G1*(B+1.))
      BETA=(XK7*B+XK3)/G1
      XH2=0.0625*(SQRT(ALFA*ALFA+8.*A*X/(B+1.))-ALFA)**2
      XN2=0.0625*(SQRT(BETA*BETA+8.*A*ZS)-BETA)**2
      XH2O=B*XH2
      XOH=XK5*B*SQRT(XH2)/G1
      XH=XK1*SQRT(XH2)/G1
      XNO=XK7*B*SQRT(XN2)/G1
      XN=XK3*SQRT(XN2)/G1
      XO2=XK4*B*B/P
      XO=XK2*SQRT(XO2)/G1
      XCO2=A*W*B/(B+XK6)
      XCO=XK6*XCO2/B
      G4=(XH2O+XOH+XNO+XCO+XO+2.*(XO2+XCO2))/YS
      SUMM=XH2+XH2O+XCO2+XCO+XN2+XO2+XOH+XNO+XN+XH+XO
C     THE VALUE OF B IS NOW TESTED AND ADJUSTED
      G=G+1.
      G5=G4/A
      IF(G5-1.0015)2,2,3
    2 IF(G5-0.9985)5,5,15
    3 C=G5
      D=B
      IF(G35-1.)4,10,10
    4 B=B/1.01
      G36=2.
      IF(G-1000.)1,1,100
    5 E8=G5
```

```
      XOH=(XK5*XH2O)/(SQRT(XH2)*G1)
      XO2=(XK4*XH2O**2)/(XH2**2*P)
      XO=(XK2*SQRT(XO2))/G1
      XNO=(XK7*XH2O*SQRT(XN2))/(XH2*G1)
      XN=(XK3*SQRT(XN2))/G1
      IF(N-10)3,3,4
    3 E=SUM*XH
      F=SUM*XOH
      G=SUM*XO2
      H=SUM*XO
      XJ=SUM*XNO
      ZK=SUM*XN
      GO TO 2
    4 SUMX=XH+XH2+XOH+XH2O+XCO+XCO2+XN2+XN+XNO+XO2+XO
      IF(XH2O)100,200,200
  200 XMOLE=(6.65/453.)*(YSTOA+YFL*PHE)/(YSTOA*(XH2O+XOH+XNO+2.*XCO2+
     1XCO+2.*XO2+XO))
      SMH=XH*SUM
      SMH2=XH2*SUM
      SMOH=XOH*SUM
      SMH2O=XH2O*SUM
      SMN=XN*SUM
      SMNO=XNO*SUM
      SMN2=XN2*SUM
      SMO=XO*SUM
      SMO2=XO2*SUM
      SMCO=XCO*SUM
      SMCO2=XCO2*SUM
      RETURN
 100  K=3
      RETURN
 20   LM=7
      PRINT 800
 800  FORMAT(7X,*I AM RETURNING WITH LM=7, TOO BAD*)
      RETURN
      END
      SUBROUTINE SPECY2
      COMMON/NANE/W,X,YFL,ZFL,YSTOA,ZSTOA,PHE
      COMMON/EQ/TEQ,PEQ,R,XH2,XH2O,XCO,XCO2,XN2,XNO,XOH,XH,XO,XN,XO2
      COMMON/SUME/SMH,SMOH,SMH2,SMH2O,SMN,SMNO,SMN2,SMO,SMO2,SMCO,SMCO2
      COMMON/MSFG/LM
      LM=0
      YS=(YFL+YSTOA/PHE)
      ZS=(ZFL+ZSTOA/PHE)
      R=1.987
      P=PEQ/14.7
      T=TEQ
C     EQUILIBRIUM CONSTANT EVALUATION FOLLOWA
      XK1=10.0**(1.11059-205.213*(100./T)+0.21953*ALOG(T))
      XK2=10.0**(2.38546-235.575*(100./T)+0.11962*ALOG(T))
      XK3=10.0**(3.46216-449.882*(100./T))
      XK4=10.0**(3.0455-460.976*(100./T)+0.32653*ALOG(T))
      XK5=10.0**(2.98031-267.867*(100./T)+0.08529*ALOG(T))
      XK6=10.0**(6.69695-42.5732*(100./T)-0.60635*ALOG(T)+(2.9687E-03)*
     1T/100.))
      XK7=10.0**(2.24799-415.992*(100./T)+0.15632*ALOG(T))
    1 G1=SQRT(P)
    5 N=0
      A=0.0
      B=0.0
      C=0.0
      D=0.0
      E=0.0
      F=0.0
      G=0.0
      H=0.0
      ZJ=0.0
      ZK=0.0
    2 ALFA=(YS-F-2.0*G-H-ZJ-W)
      BETA=((X-E-F)/2.0)
      THETA=BETA-ALFA
      N=N+1
      GAMA=((XK6*THETA)+ALFA+W)
      A=((SQRT(GAMA**2+4.0*(XK6-1.0)*ALFA*W))-GAMA)/(2.0*(XK6-1.0))
      B=W-A
      C=ALFA-A
      D=THETA+A
      ZI=(ZS/2.0-ZJ-ZK)
      SUM=A+B+C+D+E+F+G+H+ZI+ZK+ZJ
      XN2=ZI/SUM
      XCO2=A/SUM
      XCO=B/SUM
      XH2O=C/SUM
      XH2=D/SUM
      IF(XN2.LT.0.)GO TO 20
      IF(XCO2.LT.0.)GO TO 20
      IF(XH2O.LT.0.)GO TO 20
      IF(XH2.LT.0.)GO TO 20
      XH=XK1*SQRT(XH2)/G1
      HB=B
      IF(G36-1.0)6,10,10
    6 B=B*1.01
      G35=2.0
      IF(B-1000.0)1,1,100
   10 B=B+((D-HB)/(C-EB))*(1.0-G5)
   15 G35=0.0
      G36=0.0
C     THE VALUE OF A IS NOW TESTED AND ADJUSTED
      IF(SUMM-1.0015)22,22,23
   22 IF(SUMM-0.9985)25,25,35
   23 CA=SUMM
      DA=A
      G37=2.0
      IF(G38-1.0)24,30,30
   24 A=A*0.9990
      GO TO 1
   25 EA=SUMM
      HA=A
      G38=2.0
      IF(G37-1.0)26,30,30
   26 A=A*1.001
      GO TO 1
   30 A=A+(1.0-SUMM)*((DA-HA)/(CA-EA))
      G37 = 0.0
      G38=0.0
      GO TO 1
   35 XMOLB=(6.65/453.)*(YSTOA+YFL*PHE)/(YSTOA*(XH2O+XOH+XNO+XCO+
     12.0*XCO2+2.0*XO2+XO))
      SMH2=XH2  /A
      SMH2O=XH2O/A
      SMN2=XN2/A
      SMOH=XOH/A
      SMH=XH/A
      SMNO=XNO/A
      SMN=XN/A
      SMO2=XO2/A
      SMO=XO/A
      SMCO2=XCO2/A
      SMCO=XCO/A
      RETURN
  100 K=3
      RETURN
      END
      SUBROUTINE THERMO(TI,I,DUM,ACP,ACV,AH,AU,AS)
      COMMON /COEF/Z(14, 100)
      IF (I .EQ. 0) GO TO 15
      IF (TI .LT. 298.0) GO TO 14
      IF (TI .LE. 6000.0) GO TO 10
   14 PRINT 20, TI
   20 FORMAT (57H1* * * ERROR * * * PROPERTIES SUBROUTINE ENTERED WITH
     * =      F12.4/65H THIS SUBROUTINE IS VALID ONLY FOR 298 LE T LE 6
     *000 (DEG. KELVIN).     /28H ALL PROPERTIES SET TO ZERO.        )
 15   ACP=0.0
      ACV=0.0
      AH=0.0
      AU=0.0
      AS=0.0
      RETURN
   10 T = TI * 0.001
      TLOG = ALOG(T)
      IF (TI .LT. 1200.0) GO TO 32
      ACP= (((Z(5,I)/T + Z(4,I))/T + Z(3,I))/T + Z(2,I))/T + Z(1,I)
      AH= (-((Z(5,I)/(3.0 * T) + Z(4,I) * 0.5)/T + Z(3,I))/T + Z(1,I) *
     1    T + Z(2,I) * TLOG) * 1000.0 + Z(11,I)
      AS= -(((Z(5,I)/(4.0 * T) + Z(4,I)/3.0)/T + Z(3,I) * 0.5)/T
     1    + Z(2,I))/T + Z(1,I) * TLOG + Z(12,I)
      AU = AH-(1.986*TI)+(591.8*(1.-DUM))
      ACV = ACP-1.986
      RETURN
 32   ACP= (((Z(10,I) * T + Z(9,I)) * T + Z(8,I)) * T + Z(7,I)) * T
     1    + Z(6,I)
      AH= ((((Z(10,I) * 0.2 * T + Z(9,I) * 0.25) * T + Z(8,I)/3.0)
     1    * T + Z(7,I) * 0.5) * T + Z(6,I)) * T) * 1000.0 + Z(13,I)
      AS= (((Z(10,I) * 0.25 * T + Z(9,I)/3.0) * T + Z(8,I) * 0.5) * T
     1    + Z(7,I)) * T + Z(6,I) * TLOG + Z(14,I)
      AU = AH-(1.986*TI)+(591.8*(1.-DUM))
      ACV = ACP-1.986
      RETURN
      END
      BLOCK DATA
      COMMON /NAMES/X(100) /COEF/A(14,100)
      DATA X(1), (A(I),   I = 1, 14)/1HH, 4.9680, 4*0.0, 4.9680, 4*0.0,
     1     5.0019350E 04, 3.3406185E 01, 5.0619450E 04, 3.3406266E 01/
      DATA X(2), (A(I), I = 15, 28 )/2HOH, 10.1977, -6.1819, 8.6045,
     1    -10.3492, 5.2727, 7.4904, -1.5811, 1.1168, 0.8126, -0.5117,
     1     9.2883748E 03, 4.8436598E 01, 7.1568579E 03, 5.3401276E 01/
      DATA X(3), (A(I), I = 29, 42 )/2HH2, 12.0548, -23.8674, 52.9484,
     1    -61.0090, 27.9132, 6.1563, 4.6572, -9.6723, 8.7834, -2.7044,
     1     2.3450323E 04, 2.8057320E 01,-1.9718572E 03, 3.7630774E 01/
      DATA X(4), (A(I), I = 43, 56 )/3HH2O, 15.5208, -6.7693, 0.7168,
     1    -2.1223, 2.0974, 8.0455, -1.6538, 7.2725, -4.7628, 1.1469,
     1    -6.6547119E 04, 4.9139755E 01,-6.0169430E 04, 5.5115362E 01/
      DATA X(5), (A(I), I = 57, 70 )/3HNH3, 20.6650, -57.9455, 128.120
     1    -147.7532, 62.9049, 6.9777, 2.2529, 13.0714, -12.648, 3.8128
     1     4.3631974E 04, 3.1600208E 01,-1.3241079E 04, 5.3332740E 01/
      DATA X(6), (A(I), I = 71, 84 )/1HN, 10.62, -47.1592, 137.1048,
     1    -170.5377, 76.3122, 4.9680, 4*0.0,
     1     1.8292449E 05, 2.6229125E 01, 1.1148445E 05, 4.2628206E 01/
      DATA X(7). (A(I), I = 85, 98 )/2HNO, 9.0120, -3.4797, 7.1128,
     1    -9.1937, 4.1679, 8.1959, -7.8995, 18.6601, -14.9907, 4.2114,
     1     2.1178274E 04, 5.7426483E 01, 1.9351847E 04, 6.1921241E 01/
      DATA X(8), (A(I), I = 99, 112)/3HNO2, 13.9764, 0.0495, -1.9601,
     1    0.3637, 0.1327, 6.4906, 6.9902, 5.665, -10.6396, 3.9047,
     1    -1.9033203E 01, 6.9435328E 01, 5.6522440E 03, 6.2970502E 01/
      DATA X(9), (A(I), I = 113,126)/2HN2, 9.7348, -4.9604, 11.2348,
     1    -15.2917, 7.2883, 7.5309, -4.0628, 8.9494, -5.9095, 1.3277,
     1     1.4029634E 03, 5.1879732E 01,-2.1305015E 03, 5.5756405E 01/
      DATA X(10), (A(I), I = 127, 140)/4HN2O4, 31.7937, 0.0390, -4.253
     1    0.5238, 0.3965, 6.0206, 55.9402, -55.3576, 27.3413, -5.4586,
     1    -1.6038732E 04, 9.9773053E 01,-1.6727734E 03, 6.5577847E 01/
      DATA X(11), (A(I), I = 141, 154)/5HARGON, 4.968, 4*0.0, 4.968,
     1    4*0.0. 572.54, 8.589, 572.34, 8.589/
      DATA X(12), (A(I), I = 155, 168)/1HO, 6.5043, -11.2237, 30.2196,
     1    -35.2570, 15.0609, 5.9210, -3.7076, 5.5073, -4.2596, 1.1778,
     1     7.4108364E 04, 4.0509590E 01, 5.7915481E 04, 4.6514378E 01/
      DATA X(13), (A(I), I = 169, 182)/2HO2, 10 789, -0.9278, -17.2354
     1    32.8711, -17.7558, 7.1663, -3.3697, 12.9769, -12.15422, 3.73
     1    -12037.1, 55.2074, -2077.11, 52.2139/
      DATA X(14), (A(I), I = 183, 196)/2HCO, 9.6744, -4.2373, 9.0746,
     1    -12.0826, 5.6379, 7.5994, -4.8861, 11.5395, -8.508, 2.1666,
     1    -2.6044471E 04, 5.3704839E 01,-2.5920508E 04, 5.7422856E 01/
      DATA X(15), (A(I), I = 197, 210)/3HCO2, 16 9476,-12.9426, 31.593
     1    -40.905, 18.7665, 4.4269, 19.8606, -19.3181, 10.484, -2.4332
     1    -85655.4, 58.2216, -96102.7, 51.9249/
      DATA X(16), (A(I), I = 211, 224)/2HNH, 10.6258, -8.6165, 16.155,
     1    -19.58, 9.1421, 7.0276, -0.1593, -0.7821, 2.4793, -1.0542,
     1     8.4771347E 04, 4.7069777E 01, 7.8915417E 04, 5.1855210E 01/
      DATA X(17), (A(I), I = 225, 238)/3HNH2, 13.8594, 0.7371, -11.701
     1    9.5884, -2.2753, 8.1132, -2.6151, 9.4520, -6.1015, 1.3205 ,
     1     2.4866788E 04, 5.4643742E 01, 3.7696005E 04, 5.6721053E 01/
      DATA X(18), (A(I), I = 239, 252)/2HO3, 15.6988, -9.3506, 21.8249
     1    -25.7779, 11.0363, 4.1187, -23.986, -24.6949, 11.6854, -2.146
```

```
1      3.9322316E 04, 6.6648750E 01, 3.2002931E 04, 5.5914119E 01/
 DATA X(19), (A(I), I = 253, 266)/3HHO2, 13.8775, 0.479, -7.0429,
1     6.3668, -1.7049, 6.5932, 5.1772, 4.0242, -7.0123, 5.5811,
1     -6.8387161E 03, 6.4548731E 01, 1.2894812E 03, 5.9144846E 01/
 DATA X(20), (A(I), I = 267, 280)/3HNO3, 19.874, -0.0133, -1.7247,
1     -0.0324, 0.1778, 0.0418, 52.9640, -61.5724, 34.3239, -7.4811,
1      6.6432361E 03, 7.7971633E 01, 1.5115214E 04, 4.7065499E 01/
 DATA X(21), (A(I), I = 281, 294)/3HN2O, 17.8993, 0.0745, -2.8842,
1     0.9113, 0.1206, 4.8717, 19.5613, -19.5098, 10.6848, -2.4944,
1      1.0475310E 04, 6.5102379E 01, 1.7441977E 04, 5.3392043E 01/
 DATA X(22), (A(I), I = 295, 308)/4HN2O5, 35.7626, 0.2224, -3.0719
1     2.1412, -1.3445, 4.278, 90.8232, -112.16, 66.0569, -15.1753,
1     -1.4170811E 04, 1.1737206E 02,-1.7409778E 03, 6.5343178E 01/
 DATA X(23), (A(I), I = 309, 322)/4HN2O3, 24.8388, 0.0327, -3.2819
1     0.4805, 0.3115, 8.2741, 32.2296, -26.1611, 12.1205, -2.0867,
1      5.9662612E 03, 9.5772105E 01, 1.6129000E 04, 7.5475454E 01/
 DATA X(24), (A(I), I = 323, 336)/4HN2H4, 11.0813, 1.6517,-20.5423
1     21.9078, -5.2600, -0.0994, 55.6829, -58.5689, 33.9183,-7.9077
1     -1.3160316E 04, 7.2677629E 01, 2.0800695E 04, 4.2632857E 01/
 DATA X(25), (A(I), I = 337, 350)/4HH2O2,19.0425,-12.0586,41.3547,
1     -72.5995, 40.0792, 3.9051, 30.5698, -3 .1344, 20.2595,-4.4805
1     -2.4525195E 04, 6.5531603E 01,-3.4749546E 04, 5.2547609E 01/
 DATA  X(26),(A(I),  I=351,  364)/2HCL,4.96 1,-.0156,.7991,-.529,
1     .0914, 3.9351, 7.2600, -12.2765, 8.6247, -2.2303,
1      2.8297739E+04, 4.6197422E+01, 2.7518460E+04, 4.2527310E+01/
 DATA  X(27),(A(I),  I=365,  378) /3HCLF,10.4417,-7.8862,19.0001.
1   -21.7856,9.2864,3.3624,11.6299,-15.9252,10.4094,-2.6256,
1     -5.4419748E+03, 5.8846732E+01,-1.4134970E+04, 5.5705954E+01/
 DATA  X(28),(A(I),  I=379,  392) /4HCLF3,19.8739,-0.0167,-.5364,
1     -.1627,.0631,4.8639,55.206,-84.7306,60.0684,-16.1547,
1     -4.5541890E+04, 6.8535088E+01,-4.1141194E+04, 6.0002236E+01/
 DATA  X(29),(A(I),  I=393,  406)/3HHCL, 10.1739, -6.3120, 11.5705
1   -14.6795, 6.9881, 7.1633, -1.1303, 1.4015, 0.7740, -0.0486,
1     -2.0058697E+04, 4.9565303E+01,-2.4161787E+04, 5.3583731E+01/
 DATA  X(30),(A(I),  I=407,  420)/3HCL2, 9.8970, 2.4226, -22.9320,
1   41.2439, -22.5592, 6.0344, 11.0491, -19.9797, 12.1298, -3.2770
1     -1.3547081E+04, 6.2863010E+01,-2.1614711E+03, 5.7953370E+01/
 DATA  X(31),(A(I),  I=421,  434)/1HF, 4.9681, -0.0017, 0.1544,
1   -0.0596, 0.0122, 5.6727, -0.6264, -0.9443, 1.5790, -0.5974,
1      1.7643235E+04, 4.4340640E+01, 1.7202486E+04, 4.4998551E+01/
 DATA  X(32),(A(I),  I=435,  448)/2HHF, 10.1111, -5.7291, 5.6438,
1     -6.2623, 3.3915, 6.2433, 0.9808, -2.8117, 3.2628, -1.0048,
1     -6.6144277E+04, 4.5936160E+01,-6.6865046E+04, 4.9596484E+01/
 DATA  X(33),(A(I),  I=449,  462)/2HNF, 10.4354, -7.8564, 19.7037,
1   -21.6615, 9.2537, 5.8068, 5.7654, -3.0293, -0.4875, 0.6175,
1      6.2727936E+04, 5.7688795E+01, 5.7539129E+04, 5.5871673E+01/
 DATA  X(34),(A(I),  I=463,  476)/2HF2, 11.8913, -15.4898, 37.3794
1     -42.6463, 18.1507, 5.3631, 10.0646, -11.7606, 6.6993, -1.4824,
1      1.2086829E+04, 5.1948074E+01,-1.9560384E+03, 5.2396458E+01/
 DATA  X(35),(A(I),  I=477,  490)/3HNF3, 19.8725, -0.0004, -1.2319
1      0.0009, 0.0889, 1.1423, 58.2015, -70.4100, 50.3135, -14.5192,
1     -3.9621240E+04, 8.1441471E+01,-3.2720053E+04, 4.9396670E+01/
 DATA  X(36),(A(I),  I=491,  504)/3HNF2, 13.9123, -0.0149, -0.7579
1     -0.0544, 0.0930, 4.2384, 26.6572, -31.7839, 18.4058, -4.1419,
1      3.9112903E+03, 7.3538518E+01, 7.8993041E+03, 5.8162548E+01/
 DATA  X(37),(A(I),  I=505,  518)/4HN2F4, 31.7967,-.0057, -2.2279,
1  -.0121, .1705, -2.001, 104.7948, -140.9845, 90.3883, -22.4798,
1    -1.7447159E+04, 1.0154142E+02,-4.9775844E+03, 4.3809028E+01/
 DATA  X(38),(A(I),  I=519,  532)/4HN2F2, 19.8705, 0.0290, -1.9187
1  0.2525, 0.0783, 1.6130, 49.7348, -80.6048, 36.0154, -8.4463,
1      6.1337863E+03, 8.0085122E+01, 1.4170932E+04, 5.1585459E+01/
 DATA  X(39),(A(I),  I=533,  546)/4HN2H2, 13.8229, 0.7082, -12.929
1, 9.1422, -1.8806, 6.1334, 5.4530, 15.8998, -18.8135, 6.1547,
1      3.0596606E+04, 6.2950445E+01, 4.8721519E+04, 5.7462409E+01/
 DATA  X(40),(A(I), I = 547, 560)/4HN2H3, 31.6813, 1.6517,-20.5423
1    21.9078, -5.2600, -0.0994, 55.6829, -57.5689, 33.9183,-7.9077
1      5.7116830E+03, 7.2665829E+01, 3.9672655E+04, 4.2620867E+01/
 DATA  X(41),(A(I), I=561, 574)/4HCLF5, 31.7991, -0.0315, -0.8141,
1  -0.1623, 0.1109, 6.083, 97.6125, -152.1507, 110.0591, -29.904,
1    -7.2213936E+04, 1.1138118E+02,-6.5000179E+04, 6.1494895E+01/
 END
```

```
      SUBROUTINE  ISENBG(T1,P1,V1,S1,U1,T2,P2,V2,S2,U2,X1,X2,GAM1,GAM2,
     1AW*2)
      DIMENSION X1(11),X2(11)
      CALL TPROP(T1,P1,V1,CV1,CP1,U1,H1,S1,AM*1,GAM1,X1)
      ABC=(1.-GAM1)/GAM1
      T2=T1*((P1/P2)**ABC)
      JK=0
 1    CALL TPROP(T2,P2,V2,CV2,CP2,U2,H2,S2,AM*2,GAM2,X2)
      JK=JK+1
      IF(JK.EQ.50)GO TO 25
      DELS=S1-S2
      TNEW=T2*EXP(DELS/CP2)
      IF(ABS(DELS/S1).LT.0.001)GO TO 2
      IF(ABS(TNEW-T2).LT.1.0)GO TO 2
      T2=T2+0.5*(TNEW-T2)
      GO TO 1
 2    RETURN
 25   RETURN
      END
      SUBROUTINE BURN(T1,P1,V1,U1,T2,P2,V2,U2,WKD,X2,S2,GAM2,CV2,CP2,
     1AMW2)
      DIMENSION X2(11)
      COMMON/ASFG/LM
      COMMON/ASD/KLM
      COMMON/THIG/ML
      COMMON/ROCK/LJK
      ML=0
      KLM=0
      DELT=0.
      JK=0
      T2=2300.
      B=U1-WKD
    1 DELT=0.5*DELT
      JK=JK+1
      IF(JK.EQ.50)GO TO 25
      T2=T2+DELT
      IF(LJK.EQ.5)GO TO 9
      IF(T2.LT.1500.)GO TO 7
      IF(T2.GE.3200.)GO TO 5
    9 CONTINUE
      CALL THROP(T2,P2,V2,CV2,CP2,U2,H2,S2,AMW2,GAM2,X2)
      IF(LM.EQ.1)GO TO 5
      DELU=B-U2
      DELT=DELU/CV2
      IF(DELT.GT.100.)GO TO 2
      IF(DELT.LT.-100.)GO TO 3
      IF(ABS(DELT).LT.1.0)GO TO 4
      IF(ABS(DELU/B).LT.0.001)GO TO 4
      GO TO 1
    2 DELT=100.
      GO TO 1
    3 DELT=-100.
      GO TO 1
    7 ML=1
    4 RETURN
    5 KLM=3
   25 RETURN
      END
      SUBROUTINE ISENUN(T1,P1,V1,T2,P2,V2)
      COMMON/GINA/AM,BM,CM,DM,RMU,AMWU
      X1=1.986*ALOG(P2/P1)
      X2=AM*ALOG(T1)+BM*T1+(CM/2.)*(T1**2.)+(DM/3.)*(T1**3.)
      T2=T1+100.
      NN=0
1     TOLD=T2
      NN=NN+1
      IF(NN.EQ.100)GO TO 3
      X3=AM*ALOG(T2)+BM*T2+(CM/2.)*(T2**2.)+(DM/3.)*(T2**3.)
      FT2=X3-X2-X1
      DX3=AM/T2+BM+CM*T2+DM*(T2**2.)
      T2=T2-FT2/DX3
      IF(ABS(T2-TOLD).GT.1.0)GO TO 1
      V1=RMU*T1/P1
      V2=RMU*T2/P2
3     RETURN
      END


      SUBROUTINE VB(R1,R2,V,Z)
      COMMON/ENG/BORE
      BL=BORE/2.
      X1=R1/BORE
      X2=R2/BORE
      F1=(2.*(X1**2.)-1.)*ACOS(X1)-X1*SQRT(1.-(X1**2))
      F2=(2.*(X2**2)-1.)*ACOS(X2)-X2*SQRT(1.-(X2**2))
      F3=2.*Z*(BL**2)
      V=F3*(F2-F1)
      RETURN
      END


      SUBROUTINE NOKIN(T,RHO,XO2,XN2,XO,XN,KNOO,KNON,DT,W)
      REAL KNOO,KNON
      F1=(7.E13)*EXP(-75000./(1.986*T))
      F2=(13.3E09)*T*EXP(-7080./(1.986*T))
      B1=1.55E13
      B2=3.2E09*T*EXP(-39100/(1.986*T))
      C=RHO/W
      A=F1*XN2*XO+F2*XO2*XN-B1*XN*KNOO-B2*XO*KNOO
      B=F1*XO/2.+F2*XN/2+B1*XN+B2*XO
      Y=A/B*(1.-EXP(-B*C*DT))
      KNON=KNOO+Y
      RETURN
      END
      SUBROUTINE TPROP(T,P,V,CV,CP,U,H,S,AMW,GAM,X)
      DIMENSION X(11)
      DIMENSION XCV(11),XCP(11),XU(11),XH(11),XS(11)
      COMMON/LARRY/A(11)
      COMMON/DIVA/AN(11)
      COMMON/ASFG/LM
      CALL EQUILIB(T,P,AMW,X)
      IF(LM.EQ.7)GO TO 2
      CV=0.
      CP=0.
      S=0.
      U=0.
      H=0.
      DO 1 I = 1,11
      CALL THERMO(T,A(I),AN(I),XCP(I),XCV(I),XH(I),XU(I),XS(I))
      CV=CV+X(I)*XCV(I)
      CP=CP+X(I)*XCP(I)
      U=U+X(I)*XU(I)
      H=H+X(I)*XH(I)
1     S=S+X(I)*(XS(I)-1.986*ALOG(X(I)*P))
      GAM=CP/CV
      CV=CV/AMW
      CP=CP/AMW
      U=U/AMW
      H=H/AMW
      S=S/AMW
      V=82.054*T/(P*AMW)
2     RETURN
      END

      SUBROUTINE THETIN(VT,AG,AQW)
      K=0
      AGW=AQ+5.
1     CALL VOLUME(AGW,VTN,ZG)
      KZZ=0
      K=K+1
      A=(VT-VTN)/VT
      IF(K.EQ.100)STOP
      IF(ABS(A).LT.0.02)GO TO 4
      IF(A.GT.0.02)GO TO 3
      AGW=AGW-1.
      KZZ=1
      IF(KZZ.EQ.2)GO TO 4
      GO TO 1
3     AGW=AGW+1.
      KZZ=2
      IF(KZZ.EQ.1)GO TO 4
      GO TO 1
4     CONTINUE
      RETURN
      END
      SUBROUTINE ISENV(T1,P1,V1,T2,P2,V2)
      COMMON/GINA/AM,BM,CM,DM,RMU,AMWU
      AM=AM-1.986
      X1=-1.986*ALOG(V2/V1)
      X2=AM*ALOG(T1)+BM*T1+(CM/2.)*(T1**2.)+(DM/3.)*(T1**3.)
      T2=T1+100.
      NN=0
 1    TOLD=T2
      NN=NN+1
      IF(NN.EQ.100)GO TO 3
      X3=AM*ALOG(T2)+BM*T2+(CM/2.)*(T2**2.)+(DM/3.)*(T2**3.)
      FT2=X3-X2-X1
      DX3=AM/T2+BM+CM*T2+DM*(T2**2.)
      T2=T2-FT2/DX3
      IF(ABS(T2-TOLD).GT.1.0)GO TO 1
      P2=P1*(V1/V2)*(T2/T1)
 3    RETURN
      END


      SUBROUTINE VOLUME(THANG,VCC,ZG)
C     THIS ROUTINE CALCULATES THE COMBUSTION CHAMBER VOLUME
      COMMON/ENG/BORE
      CR=7.
      EL1=25.4
      EL2=5.72
      BORE=10.
      ARC=ABS(THANG)*0.01745
      AP=(3.14/4)*(BORE**2)
      A=(2/(CR-1.))+(1.-COS(ARC))
      B=1.-SQRT(1.-(((EL2/EL1)*SIN(ARC))**2.))
      VCC=AP*((EL2*A)+(EL1*B))
      ZG=VCC/AP
      RETURN
      END


      SUBROUTINE UNENG(T,U,H)
      COMMON/GINA/AM,BM,CM,DM,RMU,AMWU
      COMMON/DIANA/XUF,UFF,HFF
      UFM=XUF*UFF
      US=(AM-1.986)*(T-298.)+(BM/2.)*((T**2.)-8.88E04)+(CM/3.)*
     1((T**3.)-2.644E07)+(DM/4.)*((T**4.)-7.88E09)
      U=(UFM+US)/AMWU
      HFM=XUF*HFF
      HS=US+1.986*(T-298.)
      H=(HFM+HS)/AMWU
      RETURN
      END
```

APPENDIX V

Fortran Listing - Data Reduction

```
      PROGRAM DADRED(INPUT,OUTPUT)
      REAL SC(3)
      DIMENSION TRBER(3)
      DIMENSION TRCGS(3)
      DIMENSION TOC(4)
      DIMENSION TRCG(3),TE(3),EMI(3)
      DIMENSION VO(4),VB(4),TT(4),EM(4),TO(4)
      INTEGER CNTROL(6)
      DIMENSION T(4)
      REAL A(20,20),D(20,3)
      INTEGER PIC
      COMMON/LEN/ZP
      COMMON/A/PRESS
      COMMON/SPEC/WL(4),CI(4),VG(4)
      COMMON/ENG/AL(4)
      COMMON/BEER/NQ
      COMMON/ALFA/PHI
C   READ EXPERIMENTAL DATA
1     READ100,PIC,RPM,AIR,FUEL,TA,DIVT
100   FORMAT(I5,F5.0,F5.2,F5.1,F5.2,F6.4)
      IF(PIC.EQ.0)STOP
      READ101,(SC(I),I=1,3)
101   FORMAT(3F4.2)
      READ101,(VO(I),I=1,3)
      VO(1)=2.8
      VO(2)=2.7
      VO(3)=2.5
2     READ102,THETA,PRESS,(VG(I),VB(I),I=1,3)
102   FORMAT(8F4.2)
      IF(PRESS.EQ.0.)GO TO 1
      PRESS=PRESS+0.5
      THETA=90.*THETA/DIVT
      NN=3
      AL(1)=AL(2)=AL(3)=2.75
      CI(1)=2.79E12
      CI(2)=25.9E12
      CI(3)=35.9E12
      WL(1)=2.5
      WL(2)=2.0
      WL(3)=1.8
C    DETERMINE THE EQUIVALENCE RATIO
      PHI=FUEL*TA/(15.9*AIR)
      PRINT800,PHI
800   FORMAT(10X,*PHI=*,F5.3)
      IF(PHI.LE.1.05.AND.PHI.GE.1.0)PHI=1.0
      IF(PHI.LE.1.1.AND.PHI.GT.1.05)PHI=1.1
C    DETERMINE THE IDEAL BULK GAS TEMPERATURE
      AIRM=226.5*AIR/TA
      TMAS=1.03*(AIRM+FUEL)
      AMW=27.5
      PRESS=314.7+98.4*(PRESS-2.4)
      PRESS=PRESS*144.
      TB=(PRESS*VOL(THETA)*AMW/1545)/(2*TMAS/RPM)
      PRESS=PRESS/144.
      TB=TB/1.8
      V=VOL(THETA)
      PRINT295,PRESS,V,TB,TMAS,RPM
  295 FORMAT(2X,5(E10.4,5X))
C     DETERMINE THE AVERAGE EMISSION ABSOPTION TEMPERATURE
      NQ=0
      DO 9 I=1,NN
      VO(I)=VO(I)*SC(I)
      VG(I)=VG(I)*SC(I)
    9 VB(I)=VB(I)*SC(I)
      C=3.0E10
      BK=1.38E-16
      H=6.625E-27
      ZP=8.25
      DO 3 I=1,NN
      TO(I)=(VB(I)-VG(I))/VO(I)
      EM(I)=1.-TO(I)
      VO(I)=VO(I)/SC(I)
      P=CI(I)*VG(I)/EM(I)
      WL(I)=WL(I)*0.0001
      C1=2.*H*C**2
      C2=1.4388
      A=(WL(I)/C2)*ALOG((C1/(P*WL(I)**5))+1.)
      TT(I)=1./A
    3  TOC(I)=TR(WL(I),TT(I))
      DO208I=1,3
      NQ=1
  208 TRBER(I)=TR(WL(I),TT(I))
      NQ=0
      DO 11 I=1,3
      TE(I)=TB
   29 TOLD=TE(I)
      EMI(I)=1.-TR(WL(I),TE(I))
      AAA=CI(I)*VG(I)
      F=(AAA/EMI(I))-PL(WL(I),TE(I))
      FNN=(AAA/(1.-TR(WL(I),TE(I)+5.)))-PL(WL(I),TE(I)+5.)
       FN=(AAA/(1.-TR(WL(I),TE(I)-5.)))-PL(WL(I),TE(I)-5.)
      FP=(FNN-FN)/10
      TE(I)=TOLD-F/FP
      COM=TE(I)-TOLD
      IF(COM.LE.25.)GO TO 11
      GO TO 29
   11 PRINT15,I,WL(I),EMI(I),TE(I)
   15 FORMAT(2X,*I= *,I1,*   WAVE LENGTH= *,F4.2,*EMISS THEO*,F8.6
     1,*T(THEO) =*,F7.2)
       ZP=2.75
C     SET UP INITIAL VALUES FOR SOLUTION OF THE SET OF NON LINEAR EQS
       T(1)=T(2)=T(3)=TB
       T(1)=TB-200
       T(2)=TB
       T(3)=TB+200
       NN=3
C     CALL SIMEX TO SOLVE THE EQS
```

```
      CNTROL(1)=NN
      CNTROL(2)=200
      CNTROL(3)=NN
      CNTROL(4)=-1
      CNTROL(5)=4
      CNTROL(6)=4
      T(4)=100.
      DIM=NN
      CALL SIMEX(T,A,D,DIM,CONVRG,CNTROL)
C     PRINT ALL OF THE RESULTS HERE
      DO10 I=1,NN
      E1=ALOG(TR(WL(I),T(1)))**2
      E2=ALOG(TR(WL(I),T(2)))**2
      E3=ALOG(TR(WL(I),T(3)))**2
      E4=SQRT(E1+E2+E3)
      TRCGS(I)=EXP(E4)
      TRCGS(I)=1./TRCGS(I)
      TRCG(I)=TR(WL(I),T(1))*TR(WL(I),T(2))*TR(WL(I),T(3))
10    WL(I)=WL(I)*10000.
      PRESS=PRESS/14.7
      PRINT200,PIC,RPM,PHI
200   FORMAT(1H1,10X,*RUN= *,I6,3X,*ENGINE SPEED= *,F6.1,*(RPM)*,3X,
     1*EQUIVALENCE RATIO= *,F4.2,/)
      PRINT 201,THETA,PRESS
      PRINT206,TB
201   FORMAT(27X,*THETA= *,F4.1,*(ATC)*,10X,*PRESSURE= *,F5.2,*(ATM)*,
     1/,22X,*TRANSMITTANCES*,/)
206   FORMAT(22X,*T(IDEAL GAS)= *,F6.1,* (K)*,/)
202   FORMAT(1X,3(22X,*T(*,F4.2,*)=*,F6.1,5X,*TTHEO(*,F4.2,*)=*,F6.1/))
      PRINT203,(WL(I),TO(I),WL(I),TOC(I),I=1,3)
      PRINT 202,(WL(I),TT(I),WL(I),TE(I),I=1,3)
203   FORMAT(22X,  *TRM(*,F4.2,*)=*,F5.3,5X,*TRCALC(*,F4.2,*)=*,F5.3,/)
      PRINT 20,(TRCG(I),I=1,3)
20    FORMAT(20X,*TRCG(I)=*,3(F8.6,3X))
      PRINT21,(TRCGS(I),I=1,3)
21    FORMAT(20X,*TRCGS(I)=*,3(F8.6,3X))
      PRINT209,(TRBER(I),I=1,3)
209   FORMAT(20X,*TRBER(I)=*,3(F8.6,3X))
      PRINT204,(I,T(I),I=1,NN)
204   FORMAT(22X,*TEMPERATURE PROFILE*,/,3(22X,*T(*,I1,*)=*,F6.1,*(K)*,
     1/))
      PRINT205,(I,AL(I),I=1,NN)
205   FORMAT(22X,*WHERE THE ZONES ARE OF THE FOLLOWING LENGTHS*,/,22X,
     13(*L(*,I1,*)=*,F4.2,*(CM)*))
      GO TO 2
      GO TO 1

      END
      FUNCTION TR(AW,TZ)
      COMMON/LEN/ZP
      COMMON/A/PRESS
      COMMON/ENG/AL(4)
      COMMON/EQ/TEQ,PJK,K,XH2,XH2O,XCO,XCO2,XN2,XNO,XOH,XH,XO,XN,XO2
      COMMON/BEER/NQ
      I=1
      AL(I)=ZP
      XH2O=0.146
      IF(AW.LT.2.0E-04)GO TO 1
      IF(AW.GT.1.9E-04.AND.AW.LT.2.2E-04)GO TO 2
      IF(AW.GT.2.2E-04)GO TO 3
1     CONTINUE
      A=0.3E-02
      B=0.46617E-04
      C=-0.775E-08
      D=-0.52667E-11
      E=0.14E-14
      GO TO 4
2     CONTINUE
C  WAVELENGTH 2.00 OR 2.0  FIT PARAMETERS GO HERE
      A=-0.2197
      B=0.4801E-03
      C=-0.36045E-06
      D=0.1217E-09
      E=-0.15E-13
      GO TO 4
3     CONTINUE
      A=0.085
      B=0.51583E-03
      C=-0.6035E-06
      D=0.24867E-09
      E=-0.34E-13
      GO TO 4
4     AK=A+B*TZ+C*TZ**2+D*TZ**3+E*TZ**4
      P=PRESS/14.7
      OPD=AK*(273./TZ)*P*XH2O*AL(I)
      IF(NQ.EQ.1)TR=EXP(-OPD)
      IF(NQ.EQ.1)RETURN
      X=SQRT(273./TZ)
      GAM=0.524*P*X*(XH2O*(X+0.1)+(1.-XH2O)*0.18)
      SP=EXP(-0.00106*TZ+1.21)
      AA=GAM/SP
      TR=EXP(-OPD/(1.+(OPD/(3.14*AA))))
      RETURN
      END
```

```
       SUBROUTINE SIM EQS (Z,A,D,DIM,CONVRG,CNTROL)
       LOGICAL   CONVRG, PRINTX, START
      INTEGER DIM, CNTROL(6)
      REAL Z(20),   A(DIM,DIM), D(DIM,3)

C      SIMEX
CHANGE TOLERANCE ON CORRECTIONS FOR DIFFERENT CRITERION FOR
CONVERGENCE.  EPS IS THE RELATIVE CHANGE IN CORRECTIONS............
       EPS = 1.0E-7
      EPS=1.0E-15

       JJ = CNTROL(1)
       CONVRG = .FALSE.
       ITERS = CNTROL(2)
       NPROB = CNTROL(3)
       IF (ITERS .EQ. 0)   ITERS = 20
       CNTROL(2) = 0
CORRECTIONS MAY BE SCALED TO SIZE OF Z(NZ), WHERE  NZ  IS THE VALUE OF
CNTROL(5)....(SEE WRITE-UP).......     .
       NZ = CNTROL(5)
COUNT ITERATIONS IN CNTROL(2)....................
       PRINTX = .FALSE.
       IF (CNTROL(4) .GT. 0)   PRINTX = .TRUE.
       NOTE = CNTROL(6)
       MARK = 0
       MARK X = 0
       NOTE = CNTROL(6)
       G NORM = 0.0
       DO 2  J=1,JJ
       D(J,2) = Z(J)
       D(J,1) = - GRAD(Z,J,0,NPROB)
    2  IF (ABS(D(J,1)) .GT. GNORM)   GNORM = ABS(D(J,1))
       GMIN = GNORM
       IF (CNTROL(4) .NE. 0)   CALL PRINTR (Z,CNTROL,D,DIM)
       START = .FALSE.

COMPUTE MATRICES FOR NEXT ITERATION
CHECK FIRST TO SEE IF ITERATION LIMIT HAS BEEN EXCEEDED.
   15  IF (IABS(CNTROL(2)) .GT. ITERS)  GO TO 200

   20  DO 25  I=1,JJ
       D(I,1) = - GRAD(Z,I,0,NPROB)
       DO 25 J = 1,JJ
   25  A(I,J) = GRAD(Z,I,J,NPROB)
       IF (MARK .GT. 0)  GO TO 140

   40  DTRMNT = 1.0
       MWAY = 0
COMPUTE SOLUTION OF THE LINEARIZED EQUATIONS.........
       M = LINEQF(DIM,JJ,A,D(1,1),DTRMNT,D(1,3))
CAN USE ERASE SPACE IN SIMEQF FOR SAVING CORRECTION VECTOR..........
       DO 44  J=1,JJ
       DEL = ABS(D(J,1))
    44  D(J,3) = D(J,1)

CHECK WHETHER M = 1 CORRESPONDING TO PROPER SOLUTION OF LINEAR EQUATIONS
    50  IF (M .EQ. 1)  GO TO 60

CONTINUE HERE IF SYSTEM OF LINEARIZED EQUATIONS IS SINGULAR.....
CURRENT STRATEGY IS TO SCALE THE EQUATIONS AND TRY ONE MORE TIME......
        MARK = MARK + 1
        IF (MARK .GE. 2)   GO TO 200
        GO TO 20

CONSTRUCT NEXT APPROXIMATION TO SOLUTION.
    60  DO 65  J=1,JJ
        DEL = D(J,3)
        IF (NOTE .EQ. 0)   GO TO 65
        IF (NOTE .NE. 0)   DEL = SIGN(AMIN1(ABS(DEL),Z(NZ)),DEL)
    65  Z(J) = D(J,2) + DEL
        CNTROL(2) = CNTROL(2) + ISIGN(1,CNTROL(2))
        G NORM = 0.
        DO 74 J = 1, JJ
        D(J,1) = - GRAD(Z,J,0,NPROB)
        TEST = ABS(D(J,1))
    74  IF (TEST .GT. GNORM)   GNORM = TEST

        IF (PRINTX)  CALL PRINTR (Z,CNTROL,D,DIM)

    79  TEST = G NORM - G MIN
        IF (TEST .GT. 0)   GO TO 85
        IF (TEST .EQ. 0)   GO TO 200

        G MIN = G NORM
        MARK X = 0
        CNTROL(2) = IABS(CNTROL(2))
        DO 82 J = 1, JJ
    82  D(J,2) = Z(J)
        GO TO 90

CHOP CORRECTION VECTOR SINCE FUNCTION NORM HAS NOT DECREASED.....
    85  DO 86 J = 1, JJ
    86  D(J,3) = 0.2 * D(J,3)
CHANGE CNTROL(2) TO NEGATIVE TO INDICATE SCALING OF CORRECTION....
        CNTROL(2) = -IABS(CNTROL(2))
        MARK X = MARK X + 1
        IF (MARKX .GT. 10)  GO TO 15

CONVERGENCE TEST ON VECTOR INCREMENT
    90  DO 98 J = 1, JJ
        TEST = ABS(D(J,2))
        IF (TEST .GT. 1.0E-7)   TEST = ABS(D(J,3)/TEST)
        IF (TEST .GT. EPS)   GO TO 100
    98  CONTINUE

        CONVRG = .TRUE.
        GO TO 200
```

```
  100  IF (MARK X .EQ. 0)   GO TO 15

       GO TO 60

CONVERT ORIGINAL MATRICES TO SCALED EQUIVALENTS SINCE INVERSION FAILED.
  140  PRINT 141, CNTROL(2)
  141  FORMAT (13H0AT ITERATION   I2, 52H, IN THE EQUATION AX=C THE MATR
      XICES C AND A ARE                     //)
       DO 145 J = 1, JJ
  145  PRINT 146, J, D(J,1), (A(J,K), K =1,JJ)
  146  FORMAT (I4, E15.7, E20.7, 4E15.7/(E39.7, 4E15.7))
       IF (MWAY .GT. 0)  GO TO 40
       MWAY = 1

       DO 170 J = 1,JJ
       ROWMAX = 0.
       DO 155 K = 1, JJ
       AJK = ABS(A(J,K))
       IF (AJK .GT. ROWMAX)  ROWMAX = AJK
  155  CONTINUE
       IF (ROWMAX .LT. 1.E-10)  ROWMAX = 1.
       D(J,1) = D(J,1) / ROWMAX
       DO 160 K = 1, JJ
  160  A(J,K) = A(J,K) / ROWMAX
  170  CONTINUE

CYCLE BACK FOR ATTEMPT TO INVERT SCALED VERSION OF MATRICES.
       GO TO 140

CHANGE THE Z ARRAY TO THE OPTIMAL VALUES FOUND DURING ITERATIONS....
  200  DO 201  J=1,JJ
  201  Z(J) = D(J,2)
       IF (CNTROL(4) .LT. 0)   CALL PRINTR (Z,CNTROL,D,DIM)

       RETURN
       END
      FUNCTION LINEQF(M,N,A,B,DTRMNT,Z)
      REAL    A(M,M), B(M), Z(M)
C.. SOLVES SIMULTANEOUS LINEAR EQUATIONS BY GAUSSIAN REDUCTION.
C.. FORTRAN IV EQUIVALENT OF LNEQS.
       EPS = 1.0E-30
      MDSW=0
      NM1=N-1
      DO 40 J=1,NM1
      J1=J+1
      LMAX=J
      RMAX=ABS(A(J,J))
      DO 8 K=J1,N
      RNEXT=ABS(A(K,J))
      IF (RMAX .GE. RNEXT) GO TO 8
      RMAX=RNEXT
      LMAX=K
    8 CONTINUE
      IF (LMAX .NE. J) GO TO 10
       IF (ABS(A(J,J)) .LT. EPS)   GO TO 94
       GO TO 20
   10 DO 12 L=J,N
      W=A(J,L)
      A(J,L)=A(LMAX,L)
      A(LMAX,L)=W
   12  CONTINUE
       W = B(J)
       B(J) = B(LMAX)
   14  B(LMAX) = W
       DTRMNT = -DTRMNT
   20 Z(J)=1./A(J,J)
      DO 30 K=J1,N
      IF (A(K,J)) 22,30,22
   22 W=-Z(J)*A(K,J)
      DO 24 L=J1,N
      A(K,L)=W*A(J,L)+A(K,L)
       NOTH = 1
   24  CONTINUE
   26  B(K) = W * B(J) + B(K)
   30 CONTINUE
   40 CONTINUE

       IF (ABS(A(N,N)) .LT. 1.0E-30)   GO TO 94

   42 Z(N)=1./A(N,N)
       B(N) = Z(N) * B(N)
      DO 60 K=1,NM1
      J=N-K
      J1=J+1
      W=0.
      DO 56 I=J1,N
       W = A(J,I) * B(I) + W
   56  CONTINUE
   58  B(J) = (B(J) - W) * Z(J)
   60 CONTINUE

      MDSW=1
       IF (DTRMNT .EQ. 0.0)   GO TO 74
   70 DO 72  J=1,N
   72 DTRMNT=DTRMNT*A(J,J)
   74  LINEOF = 1
   80  CONTINUE
      RETURN
CONTINUE HERE FOR SINGULAR OR NEAR-SINGULAR CASE...................
   94  LINEOF = 2
      DTRMNT=0.
      GO TO 80
      END
      SUBROUTINE SIMEX(Z,A,D,DIM,CONVRG,CNTROL)
       LOGICAL   CONVRG, PRINTX
       INTEGER   DIM, CNTROL(6)
CHANGE THESE CARDS IN ORDER TO ALTER.DIMENSIONS..........
       REAL        Z(20), A(20,20), D(20,3)
      DIM=3


CARD 1 CONTAINS SIX CONTROL PARAMETERS.....
CNTROL(1) = NUMBER OF EQUATIONS IN THE CURRENT SYSTEM,
CNTROL(2) = BOUND ON THE NUMBER OF ITERATIONS,
CNTROL(3) = IDENTIFICATION NUMBER OF THE PROBLEM,
CNTROL(4) = NONZERO INTEGER IFF ALL ITERATIONS ARE TO BE PRINTED,
CNTROL(5) = NUMBER OF VARIABLES TO BE READ-IN.
CNTROL(6) = NONZERO CAUSES CORRECTIONS OF AT MOST Z(K), K = CNTROL(5).

 1    CONTINUE
       IF (CNTROL(1) .EQ. 0)   STOP
       LIMIT = CNTROL(2)
       NZ = CNTROL(5)
     3 FORMAT (*1 STARTING VALUES FOR C4 CAL SIMEX *,6I4 /
      X    (5E15.5))
       IF (NZ .EQ. 0)   NZ = CNTROL(1)
       PRINT 3, (CNTROL(J), J=1,6), (Z(K), K=1,NZ)
     5 FORMAT (8F10.3)

       CALL       SIM EQS (Z,A,D,DIM,CONVRG,CNTROL)

       IF (CNTROL(2) .LT. LIMIT)   GO TO 9
       PRINT 8
     8 FORMAT (*0 NUMBER OF ITERATIONS HAS REACHED THE ASSIGNED LIMIT.*)
       RETURN
     9 IF (CONVRG)   PRINT 10
    10 FORMAT (*0 ITERATIONS HAVE CONVERGED.*)
       RETURN

       END
      FUNCTION GRAD (Z,NFN,KDERIV,NPROB)
     REAL Z(20)
      IF (KDERIV .NE. 0)   GO TO 2
      GRAD = YCOMP  (Z,NFN,NPROB)
      RETURN
    2 Y1 = YCOMP (Z,NFN,NPROB)
      REMARK = Z(KDERIV)
      H = 0.0001 * ABS(REMARK)
      IF (H .LE. 0.0001)  H = .0001
      Z(KDERIV) = REMARK + H
      Y2 = YCOMP (Z,NFN,NPROB)
      GRAD = (Y2 - Y1) / H
      Z(KDERIV) = REMARK
      RETURN
      END
      SUBROUTINE PRINTR (Z,CNTROL,D,DIM)
     INTEGER DIM, CNTROL(6)
     REAL Z(20), D(DIM,3)
      JJ = CNTROL(1)
      NN = CNTROL(2)
      PRINT  1, NN, (Z(J), J=1,JJ)
    1 FORMAT (15H0 AT ITERATION  I4 /
     X     12H  VARIABLES    5E15.7/(E27.7,4E15.7))
      PRINT  2, (D(J,1), J = 1, JJ)
    2 FORMAT (12H  FUNCTIONS           5E15.7/(12X,5E15.7))
      RETURN
      END
      FUNCTION YCOMP(Z,NFN,NPROB)
      COMMON/SPEC/WL(4),CI(4),VG(4)
      REAL Z(4)
      GO TO(400,200,300),NPROB
200   YCOMP=PL(WL(NFN),Z(1))*(1.-TR(WL(NFN),Z(1)))*TR(WL(NFN),Z(2))
     1+PL(WL(NFN),Z(2))*(1.-TR(WL(NFN),Z(2)))
      YCOMP=YCOMP-CI(NFN)*VG(NFN)
      RETURN
300   YCOMP=PL(WL(NFN),Z(1))*(1.-TR(WL(NFN),Z(1)))*TR(WL(NFN),Z(2))*
     1TR(WL(NFN),Z(3))+PL(WL(NFN),Z(2))*(1.-TR(WL(NFN),Z(2)))*TR(WL(NF
     2,Z(3))+PL(WL(NFN),Z(3))*(1.-TR(WL(NFN),Z(3)))
      YCOMP=YCOMP-CI(NFN)*VG(NFN)
      RETURN
400   RETURN
      END

      FUNCTION PL(W,AT)
      PL=1.1925E-05/((W**5)*(EXP(1.4388/(W*AT))-1.))
      RETURN
      END
      SUBROUTINE EQUILIB(TTT,PEQ)
      COMMON/EQ/TEQ,PJK,K,XH2,XH2O,XCO,XCO2,XN2,XNO,XOH,XH,XO,XN,XO2
      COMMON/JANE/W,X,YFL,ZFL,YSTOA,ZSTOA,PHE
      COMMON/SOME/SMH,SMOH,SMH2,SMH2O,SMN,SMNO,SMN2,SMO,SMO2,SMCO,SMCO2
      COMMON/ALFA/PHI
      DIMENSION XC(11)
      PHE=PHI
      TEQ=1.8*TTT
      W=3.
      X=8.
      YFL=0.0
      ZFL=0.0
      YSTOA=10.
      ZSTOA=37.7
      K=1
      IF(PHE-1.)4,4,5
4     CALL SPECY1(PEQ)
      GO TO 6
5     CALL SPECY2(PEQ)
6     K=K
      XC(1)=XH
      XC(2)=XOH
      XC(3)=XH2
      XC(4)=XH2O
      XC(5)=XN
      XC(6)=XNO
      XC(7)=XN2
      XC(8)=XO
      XC(9)=XO2
      XC(10)=XCO
      XC(11)=XCO2
      IF(K-2)900,8,8
8     XO2=0.
      XN2=0.
      XH2O=0.
      XCO2=0.
      XCO=0.
      XOH=0.
      XN=0.
      XO=0.
      XNO=0.
      XH2=0.
      XH=0.
      MM=1
      IF(MM.EQ.1)GO TO 980
980   PRINT 981
981   FORMAT(*SPECIES NEGATIVE*)
900   CONTINUE
      AMMC=2.*XH2+28.*XN2+18.*XH2O+17.*XOH+1.*XH+30.*XNO+14.*XN+32.*XO2
     1+16.*XO+44.*XCO2+28.*XCO
       RETURN
       END
      SUBROUTINE SPECY1(PEQ)
      COMMON/ALFA/PHI
      COMMON/EQ/TEQ,PJK,K,XH2,XH2O,XCO,XCO2,XN2,XNO,XOH,XH,XO,XN,XO2
      COMMON/JANE/W,X,YFL,ZFL,YSTOA,ZSTOA,PHE
      COMMON/SOME/SMH,SMOH,SMH2,SMH2O,SMN,SMNO,SMN2,SMO,SMO2,SMCO,SMCO2
      PHE=PHI
      IF(TEQ.LE.2800.)TEQ=2800.
      IF(TEQ.GE.5700.)TEQ=5600.
      T=TEQ
      YS=(YFL+YSTOA/PHE)
      ZS=(ZFL+ZSTOA/PHE)
      A=1./(W+(X+ZS)/2.)
      B=80000.0/EXP(T/620.)
      Q=0.0
      G35=0.0
      G36=0.0
      G37=0.0
      G38=0.0
      P=PEQ/14.7
      G1=SQRT(P)
C     EQUILIBRIUM CONSTANT EVALUATION FOLLOWS
      XK1=10.**(1.11059-205.213*(100./T)+0.21953*ALOG(T))
      XK2=10.0**(2.38548-235.575*(100./T)+0.11962*ALOG(T))
      XK3=10.0**(3.46218-449.882*(100./T))
      XK4=10.0**(3.0455-460.976*(100./T)+0.32653*ALOG(T))
      XK5=10.0**(2.98031-267.867*(100./T)+0.08329*ALOG(T))
      XK6=10.0**(6.69595-42.5732*(100./T)-0.60636*ALOG(T)+(2.9687E-03)*(
     1T/100.))
      XK7=10.0**(2.24799-315.992*(100./T)+0.1563 *ALOG(T))
C     THE TRIAL VALUES FOR A AND B ARE NOW USED TO COMPUTE DISTRIBUTUIOM
    1 ALFA=(XK5*B+XK1)/(G1*(B+1.))
      BETA=(XK7*B+XK3)/G1
      XH2=0.0625*(SQRT(ALFA*ALFA+8.*A*X/(B+1.))-ALFA)**2
      XN2=0.0625*(SQRT(BETA*BETA+8.*A*ZS)-BETA)**2
      XH2O=B*XH2
      XOH=XK5*B*SQRT(XH2)/G1
      XH=XK1*SQRT(XH2)/G1
      XNO=XK7*B*SQRT(XN2)/G1
      XN=XK3*SQRT(XN2)/G1
      XO2=XK4*B*B/P
      XO=XK2*SQRT(XO2)/G1
      XCO2=A*W*B/(B+XK6)
      XCO=XK6*XCO2/B
      G4=(XH2O+XOH+XNO+XCO+XO+2.*(XO2+XCO2))/YS
      SUMM=XH2+XH2O+XCO2+XCO+XN2+XO2+XOH+XNO+XN+XH+XO
C     THE VALUE OF B IS NOW TESTED AND ADJUSTED
      Q=Q+1.
       G5=G4/A
      IF(G5-1.0015)2,2,3
    2 IF(G5-0.9985)5,5,15
    3 C=G5
      D=B
      IF(G35-1.)4,10,10
    4 B=B/1.01
      G36=2.
      IF(Q-1000.)1,1,100
    5 EB=G5
      HB=B
      IF(G36-1.0)6,10,10
    6 B=B*1.01
      G35=2.0
      IF(Q-1000.0)1,1,100
   10 B=B+((D-HB)/(C-EB))*(1.0-G5)
   15 G35=0.0
      G36=0.0
C     THE VALUE OF A IS NOW TESTED AND ADJUSTED
      IF(SUMM-1.0015)22,22,23
   22 IF(SUMM-0.9985)25,25,35
   23 CA=SUMM
      DA=A
      G37=2.0
      IF(G38-1.0)24,30,30
   24 A=A*0.9990
      GO TO 1
   25 EA=SUMM
      HA=A
      G38=2.0
      IF(G37-1.0)26,30,30
   26 A=A*1.001
      GO TO 1
   30 A=A+(1.0-SUMM)*((DA-HA)/(CA-EA))
      G37 = 0.0
      G38=0.0
      GO TO 1
   35 XMOLB=(6.55/453.)*(YSTOA+YFL*PHE)/(YSTOA*(XH2O+XOH+XNO+XCO+
     12.0*XCO2+2.0*XO2+XO))
      SMH2=XH2  /A
      SMH2O=XH2O/A
      SMN2=XN2/A
      SMOH=XOH/A
      SMH=XH/A
      SMNO=XNO/A
      SMN=XN/A
      SMO2=XO2/A
      SMO=XO/A
      SMCO2=XCO2/A
      SMCO=XCO/A
      RETURN
  100 K=3
      RETURN
      END
      SUBROUTINE SPECY2(PEQ)
      COMMON/ALFA/PHI
      COMMON/JANE/W,X,YFL,ZFL,YSTOA,ZSTOA,PHE
      COMMON/EQ/TEQ,PJK,K,XH2,XH2O,XCO,XCO2,XN2,XNO,XOH,XH,XO,XN,XO2
      COMMON/SOME/SMH,SMOH,SMH2,SMH2O,SMN,SMNO,SMN2,SMO,SMO2,SMCO,SMCO2
      PHE=PHI
      YS=(YFL+YSTOA/PHE)
      ZS=(ZFL+ZSTOA/PHE)
      R=1.987
      P=PEQ/14.7
      IF(TEQ.LE.2800.)TEQ=2800.
      IF(TEQ.GE.5700.)TEQ=5600.
      T=TEQ
C     EQUILIBRIUM CONSTANT EVALUATION FULLOWA
      XK1=10.0**(1.11059-205.213*(100./T)+0.21953*ALOG(T))
      XK2=10.0**(2.38548-235.575*(100./T)+0.11962*ALOG(T))
      XK3=10.0**(3.46218-449.382*(100./T))
      XK4=10.0**(3.0455-460.976*(100./T)+0.32653*ALOG(T))
      XK5=10.0**(2.98031-267.867*(100./T)+0.08329*ALOG(T))
      XK6=10.0**(6.69695-42.5732*(100./T)-0.60636*ALOG(T)+(2.9687E-03)*(
     1T/100.))
      XK7=10.0**(2.24799-315.992*(100./T)+0.15632*ALOG(T))
    1 G1=SQRT(P)
    5 N=0
      A=0.0
      B=0.0
      C=0.0
      D=0.0
      E=0.0
      F=0.0
      G=0.0
      H=0.0
      ZJ=0.0
      ZK=0.0
    2 ALFA=(YS-F-2.0*G-H-ZJ-W)
      BETA=((X-E-F)/2.0)
      THETA=BETA-ALFA
      N=N+1
      GAMA=((XK6*THETA)+ALFA+W)
      A=((SQRT(GAMA**2+4.0*(XK6-1.0)*ALFA*W))-GAMA)/(2.0*(XK6-1.0))
      B=W-A
      C=ALFA-A
      D=THETA+A
      ZI=(ZS/2.0-ZJ-ZK)
      SUM=A+B+C+D+E+F+G+H+ZI+ZK+ZJ
      XN2=ZI/SUM
      XCO2=A/SUM
      XCO=B/SUM
      XH2O=C/SUM
      XH2=D/SUM
      XH=XK1*SQRT(XH2)/G1
      XOH=(XK5*XH2O)/(SQRT(XH2)*G1)
      XO2=(XK4*XH2O**2)/(XH2**2*P)
      XO=(XK2*SQRT(XO2))/G1
      XNO=(XK7*XH2O*SQRT(XN2))/(XH2*G1)
      XN=(XK3*SQRT(XN2))/G1
      IF(N-10)3,3,4
    3 E=SUM*XH
      F=SUM*XOH
      G=SUM*XO2
      H=SUM*XO
      XJ=SUM*XNO
      ZK=SUM*XN
      GO TO 2
    4 SUMX=XH+XH2+XOH+XH2O+XCO+XCO2+XN2+XN+XNO+XO2+XO
      IF(XH2O)100,200,200
  200 XMOLB=(6.55/453.)*(YSTOA+YFL*PHE)/(YSTOA*(XH2O+XOH+XNO+2.*XCO2+
     1XCO+2.*XO2+XO))
      SMH=XH*SUM
      SMH2=XH2*SUM
      SMOH=XOH*SUM
      SMH2O=XH2O*SUM
      SMN=XN*SUM
      SMNO=XNO*SUM
      SMN2=XN2*SUM
      SMO=XO*SUM
      SMO2=XO2*SUM
      SMCO=XCO*SUM
      SMCO2=XCO2*SUM
      RETURN
  100 K=3
      RETURN
      END
```

```
      FUNCTION VOL(THETA)
      CR=7.
      EL1=10.
      EL2=2.25
      BORE=3.25
      AP=(3.14/4.)*BORE**2
      ARC=ABS(THETA*0.01745)
      A=(2/(CR-1.))+(1.-COS(ARC))
      B=1.-SQRT(1.-(((EL2/EL1)*SIN(ARC))**2))
      VOL=AP*((EL2*A)+(EL1*B))/1728
      RETURN
      END
```